CONFIDENTIAL

Impact of Processing Methods on Bovine Pericardial Tissue Integrity

Lezelle Botes

Thesis submitted in fulfilment of the requirements of the degree

PHILOSOPHIAE DOCTOR IN CARDIOTHORACIC SURGERY

(Ph.D.)

Department of Cardiothoracic Surgery

University of the Free State

Faculty of Health Sciences

Bloemfontein, South Africa

Promotor: Prof FE Smit (PhD)

Co-promotor: Prof PM Dohmen (PhD)

Co-promotor: Dr L Laker (PhD)

January 2020

Table of Contents

Declaration of Independent Work

I, Lezelle Botes, do hereby declare that this thesis:

Impact of Processing Methods on Bovine Pericardial Tissue Integrity

submitted to the University of the Free State for the degree Philosophiae Doctor is my own independent work and that it has not been submitted to any institution by me or any other person in fulfillment of the requirements for the attainment of any qualification.

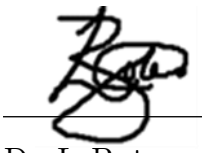

Dr L Botes

Principle Investigator

28/01/2020

Date

Statement of Compliance

The study was conducted in accordance with the International Conference on Harmonization guidelines for Good Clinical Practice (ICH E6), the Code of Federal Regulations on the Protection of Human Subjects (45 CFR Part 46), and the World Medical Association Declaration of Helsinki (64th WMA General Assembly, Fortaleza, Brazil, October 2013). All personnel involved in the conduct of this study have completed Good Clinical Practice (GCP) training or will be under direct supervision of such an accredited researcher.

All animal experiments and surgical procedures were performed in compliance with the Guide for the Care and Use of Laboratory Animals as published by the US National Institutes of Health (NIH Publication 85-23, revised 1996).

List of Figures

List of Tables

Acknowledgements

I would like to express my heartfelt gratitude to the following people:

My promotor, Professor Francis E Smit, for his academic contribution, inspiration and guidance to complete this second doctorate degree. He played a vital role and was the main driving force behind this PhD study and my academic career. Thank you for allowing me to share in your scientific vision, meaningful experiences and invaluable knowledge, to you I will forever be in debt.

Doctor Leana Laker, for the countless hours she dedicated to guide and assist me towards the completion of this study. Your work ethic is truly inspirational.

Prof PM Dohmen, for his input and academic guidance.

For all the dedicated personal in the animal laboratory, specifically Doctor Johan Jordaan, Mr Hans van den Heever and Mr Dreyer Bester. Your high level of expertise and dedication made this research study possible.

Doctor Robert W Frater one of the pioneers of Cardiac Surgery, for your generous financial contributions towards the Department of Cardiothoracic Surgery Research Program. Prof, your commitment and support led to the RWM Frater Cardiovascular Research Centre at the University of the Free State, providing us young academics with a platform to engage in Cardiothoracic research and to enjoy international recognition.

Doctor Linda Potgieter for the statistical analysis and scientific contribution. The Centre for Confocal and Electron Microscopy at the University of the Free State,

specifically, Nonkululeko Phili and Hanlie Grobler. Professor Jackie Goedhals at Anatomical Pathology, University of the Free State for all your expertise and willingness to help.

In conclusion and most notably, I extend a sincere token of my appreciation to my husband Danny Botes Snr and son Danny Botes Jnr for your unwavering support and encouragement during my academic endeavors. Finally, to my parents Gerrie and Hannetjie Jooste for all the sacrifices you made to support and encourage me to fulfil my dreams.

Soli Deo Gloria.....

Important Abbreviations

%	Percentage
≤	Less or equal to
>	More than
°	Degrees
α	Alpha
β	Beta
µg	Microgram
Arg	Arginine
Asp	Aspartic acid
ATE	Tridecyl alcohol ethoxylate
ATP	Adenosine triphosphate
AVIC	Aortic valve interstitial cells
BM	Basement membrane
BP	Bovine pericardium
BPS	Bovine pericardial scaffold
Ca	Calcium
CE	European Conformity
CHAPS	3-((3-Cholaminopropyl)dimethylammonio)-1-propanesulfonate
CHO	Carbohydrate
cm	Centimeter
DAPI	4',6-diamidino-2-phenylindole
DCA	Deoxycholic acid
D-GAD	Decellularized glutaraldehyde fixed and detoxified
DNA	Deoxyribonucleic acid
DNase	Deoxyribonuclease

ECM	Extracellular matrix
EDTA	Ethylenediamine tetraacetic acid
EGTA	Ethylene glycol tetraacetic acid
etc	Et cetera
EVG	Modified Verhoeff Van Gieson
FGF-2	Fibroblast growth factor 2
GA	Glutaraldehyde
GAG	Glycosaminoglycan
GAD	Glutaraldehyde-fixated and detoxified
GF	Growth factor
Gly	Glycine
h	Hour
H&E	Hematoxylin and eosin
HSREC	Animal Ethics Committee of the UFS
IU	International units
IV	Intravenous
KW	Kruskal Wallis
L	Liter
LVRS	Lung volume reduction surgery
Lys	Lysin
MHC I	Major histocompatibility complex I
ml	Milliliter
mm	Millimeters
MMP	Metalloproteinases
Mpa	Megapascal
n.d.	No date
ng	Nanogram
NHLS	National Health Laboratory Service

nm	Nanometer
RAS	Reversible alkaline swelling
RGD	Arginine-Glycine-Aspartate sequence
Rnase	Ribonuclease
RVOT	Right ventricular outflow tract
SDC	Sodium deoxycholate
SDS	Sodium dodecyl sulfate
SEM	Scanning electron microscopy
SJM	St Jude Medical
T_d	Denaturation temperature
TEM	Transmission electron microscopy
TS	Tensile strength
TX	Triton X-100
UFS	University of the Free State
USA	United States of America
YM	Young modulus

Abstract

Introduction: The use of cardiac patches remains one of the main therapeutic solutions for surgical treatment. Cardiovascular patches are either synthetic or biological. Synthetic materials have become less popular over the years because they are rigid, have poor flexibility, are surgically difficult to handle, are prone to endocarditis and local inflammatory reactions that contributes to fibrosis and calcification, and have no regeneration potential. Autologous pericardium tends to retract, thicken, become aneurysmal and develop fibrosis once implanted. Therefore, xenogeneic transplanted tissue dominated by bovine pericardium has become an attractive alternative.

Glutaraldehyde (GA)-fixation was introduced to overcome the aggressive recipient graft-specific rejection response, ensure sterility and to increase durability and mechanical stability. However, the residual GA toxicity and host immune responses seen in GA-preserved bovine pericardium causes degenerative processes that involves structural changes causing rigidity, shrinkage, calcium deposition and subsequent failure of the pericardial patch. Furthermore, GA limits host cell infiltration, remodeling and fails to remove or mask all animal specific antigens that contributes to chronic rejection.

This resulted in several strategies to reduce the side-effects of GA-fixation and to provide alternatives to GA as a crosslinking agent but with mixed results. Therefore, nowadays basic research is focused to produce a scaffold with reduced antigenicity while maintaining structural integrity and create recellularization potential. Attempts to reduce antigenicity included decellularization (e.g., sodium dodecyl sulphate (SDS), Triton X-100 (TX), trypsin), enzymatic or gene knockout removal of epitopes, and solubilization-based antigen removal.

The Frater Cardiovascular Research Centre developed a proprietary decellularization protocol. The aim of the study was to evaluate the potential application of this technology by comparing the structural and morphological performance of decellularized scaffolds with and without GA-fixation and detoxification with two (2) commercially available patches, the Glycar® and Cardiocel® bovine pericardial patches after being implanted in a juvenile ovine model for 180-days.

Methodology: A prospective analytical cohort design was followed. Four (4) groups of bovine pericardial patches were evaluated in vitro and in vivo namely; (i) Glycar® bovine pericardial patches (GA-fixated and detoxified), (ii) CardioCel® bovine pericardial patches (decellularized, GA-fixed and detoxified), (iii) a proprietary decellularized bovine pericardial scaffold (BPS) and (iv) a proprietary decellularized GA-fixed and detoxified (D-GAD) bovine pericardial patch. The patches/scaffolds of each group were implanted in the descending aorta and main pulmonary artery of six (6) juvenile whether sheep per group for a minimum of 180-days. The clinical and mechanical integrity, tissue morphology and pericardial thickness were evaluated and compared between the four (4) bovine pericardial groups prior to implantation and after explantation.

Results: The impact of glutaraldehyde-fixation and detoxification (GAD) technology on tissue seems to be constant, irrespective whether the tissue was decellularized or not. The Glycar®, CardioCel® and D-GAD tissues handled well, had excellent clinical outcomes and did not calcify. The tensile strength (TS) decreased from pre-implantation to explantation in all three (3) groups but still exceeded the strength of the native human aorta (1.8 ± 0.24 MPa). The pericardial tissue was more pliable in all three groups after explantation compared to their pre-implantation counterparts. A fibrous encapsulation developed on all these explants, explaining the thickening of

the pericardial patches. The collagen of the GAD groups was compact and dense which reduces the pore sizes to promote host cell infiltration. Host cell infiltration of fibroblast-like cells was insignificant in the explanted aorta and pulmonary Glycar® patches and limited in the CardioCel® and D-GAD patches. None of the patches in the three (3) groups remodelled after implantation. Only the Glycar® patches demonstrated endothelial cells prior to implantation although severely dehydrated. However, at explantation all three (3) groups demonstrated a monolayer of endothelial cells on the pericardial surface. The fibrous encapsulation caused thickening of both the aortic and pulmonary patches in the Glycar® and CardioCel® groups but in the D-GAD group only the pulmonary patch increased in thickness.

The surgical handling of the decellularized BPS was satisfactory however, surgeons did comment that it was slippery. Furthermore, it had excellent clinical outcomes and did not calcify, disintegrate or developed aneurysms. The TS decreased from pre-implantation to explantation but still exceeded the strength of the native human aorta (1.8 ± 0.24 MPa). The pericardial tissue was more pliable at explantation compared to its pre-implantation counterpart. No fibrous encapsulation developed, and the pericardial patches did not thicken over time. The collagen of the BGS groups was wavy and well-separated providing large pore sizes to promote host cell infiltration. Significant host cell infiltration of fibroblast-like cells was demonstrated in both the explanted aorta and pulmonary scaffolds. The scaffold completely remodelled after implantation. Endothelial cells were absent prior to implantation but at explantation a monolayer of endothelial cells were visible on the pericardial surface.

Conclusion:

All four (4) pericardial groups demonstrated excellent clinical, structural and morphological results when implanted in a juvenile ovine model for 180-days. Adding decellularization to the processing process benefits the collagen matrix, by making the

collagen less dense/compact thus allowing for larger pore sizes. This may allow for better recellularization, especially in the absence of cells or cellular debris, invoking an immunological reaction. The long-term benefit of the limited recellularization seen in both D-GAD products remains to be clearly demonstrated. However, the decellularized BPS should be considered as an alternative to GA-fixed pericardial patches for it demonstrated excellent remodeling and growth potential. The importance of remodelling may be beneficial to the long-term outcomes especially in the younger age group recipients.

Chapter 1- Introduction

Thousands of surgical procedures are performed every day to replace, repair or regenerate tissue that has been damaged through disease, trauma or injury. Cardiovascular diseases (CVD) are one of the leading causes of mortality and morbidity worldwide. In 2015 approximately 17.8 million people died from CVD and it is estimated to reach 22.2 million by 2030 (Di Franco et al., 2018).

The use of cardiac patches remains among the main therapeutic solutions of surgical treatment. Cardiovascular patches are either synthetic or biological in origin (Iop et al., 2018). Synthetic patches like Dacron® has poor biocompatibility, are rigid and stiff disallowing them to simultaneously contract with the beating heart tissue. In the recipient they tend to induce local inflammatory reactions and endocarditis resulting in tissue thickening, fibrosis, calcification and the lack of regeneration (Vaideeswar et al., 2011; Robinson et al., 2005). Therefore, greater clinical interest has been devoted to biologically derived patches.

Biological patches can be transplanted from one site to another in the same individual (autogenic), between same specie donors (allogenic) or from animal origin to human (xenogeneic)(Lam & Wu, 2012). Although these treatments are revolutionary and lifesaving problems still exist. Harvesting of autogenic tissue is painful, expensive, have anatomical limitations and is associated with donor site morbidity due to infection and hematoma formation. Allogenic tissue harvesting is limited by chronic shortage, risk of rejection and the possibility of infection or disease transfer from donor to recipient (Jaganathan et al., 2014; O'Brien, 2011). Therefore, the use of xenogeneic transplanted tissue has become an attractive alternative to expand treatment options. This nonhuman biomaterial is harvested from animals

usually but not limited to cows, pigs and equine (Remi et al., 2011; Kubota et al., 2012).

A biological patch used as treatment option should be biocompatible, with properties favorable for implantation while eliciting minimal adverse effects. Whether the material is used for cardiovascular reconstruction or tissue replacement it must be durable, strong and flexible and must be able to withstand approximately two (2) billion cardiac cycles (amount of cycles in an average lifetime)(Lam & Wu, 2012). The biological properties of the implanted tissue are equally important, and the most desirable characteristics include; anti-thrombogenicity, non-calcification, hemostasis, non-immunogenicity and reendothelialization capability (Muto et al., 2009).

This sparked interest in the use of collagen and collagen-containing tissues from xenogeneic origin. Nowadays, industry offers a broad range of bovine derived biomaterials subjected to different chemical treatments (Iop et al., 2018). To overcome the aggressive recipient graft-specific rejection responses and to increase durability and mechanical stability, glutaraldehyde (GA)-fixation was introduced in 1971 by Ionescu et al. but not without consequences (Ionescu et al., 1977). GA-preserved pericardium is subjected to degenerative processes that involves structural changes causing rigidity, shrinkage, calcium deposition and subsequent failure due to GA residue toxicity and host immune responses (Neethling et al., 2013; Vinci et al., 2013) The GA fails to remove animal specific antigens such as α1, 3-Gal epitope that contribute to the chronic rejection of the implanted prosthesis (Liu et al., 2016).

To overcome these limitations, basic research actively pursued fixation-free protocols to produce a scaffold with reduced antigenicity while maintaining structural integrity and create recellularization potential. Attempts to reduce antigenicity included decellularization (e.g., sodium dodecyl sulphate (SDS), Triton X-100 (TX),

trypsin etc.), enzymatic removal of α-Gal (i.e. α-galactosidase), and solubilization-based antigen removal. Various decellularization methods have been explored through the years (Remi et al., 2011) with mixed results. Complete acellularity achieved by SDS-decellularization made this approach the gold standard (Liu et al., 2016). Decellularization rendered the tissue less antigenic, reduced the inflammatory response and reduced tissue degeneration (Costa et al., 2005). However, the structural and mechanical properties of decellularized tissue can be altered by harsh chemical reagents used during the decellularization process (Liu et al., 2016). Evidence exists that the use of SDS, Trypsin and TX can result in collagen disruption, varied extracellular matrix (ECM) pore sizes, irreversible denaturation, swelling and a decrease in tensile strength (Mendoza-Novelo & Cauich-Rodríguez, 2009; García Páez et al., 2000; Courtman et al., 1994).

To date, no optimal decellularization protocol has been identified, and protocols are continuously adjusted to provide the best decellularization efficacy and functional characteristics ratio. In addition, treatment methods after decellularization can also be applied to improve mechanical and biological features of the decellularized biomaterial.

The aim of the study was to evaluate a proprietary decellularization protocol in a juvenile ovine model. The primary goal was to achieve adequate decellularization while maintaining tissue integrity, restrict calcification and to provide recellularization potential once implanted in an ovine sheep model. The clinical, mechanical and morphological properties of the decellularized pericardium with and without GA-fixation and detoxification was compared with two (2) commercially available bovine pericardial patches (Glycar® and CardioCel®) to demonstrate non-inferiority.

Chapter 2 - Literature Review

2.1 Pericardium: function, structure and composition

More than just a tissue, pericardium is a double layered flask-like sac which encloses the heart through its attachments to the great vessels, namely the vena cava, aorta and pulmonary artery and vein (Ramasamy et al., 2018). Mainly composed of connective tissue, pericardium is derived from somatic mesoderm but is not essential for life and normal cardiac function can be maintained in its absence however, diseased pericardium can be life-threatening (Khandaker et al., 2010). Pericardial thickness varies by region, pericardial thickness $\leq$ 2mm is considered normal, with 2-3 mm equivocal, and $>$ 4mm at any point abnormal (Czum et al., 2014).

2.1.1 Function

The main functions of the pericardium include; anchoring of the heart to the mediastinum, minimizing the friction of cardiac motion and provides a natural barrier to infection and injury (Jaworska-Wilczynska et al., 2016). Recently, the pericardium also fulfills a mechanical role by acting as an intracardiac pressure modulator, limits acute distension of any one cardiac chamber and preserves myofibril function by preventing sarcomere over-distention (Czum et al., 2014).

2.1.2 Structure

The native structure of pericardium consists of an outer sac referred to as the fibrous pericardium and an inner double-layer sac the serous pericardium (Jaworska-Wilczynska et al., 2016).

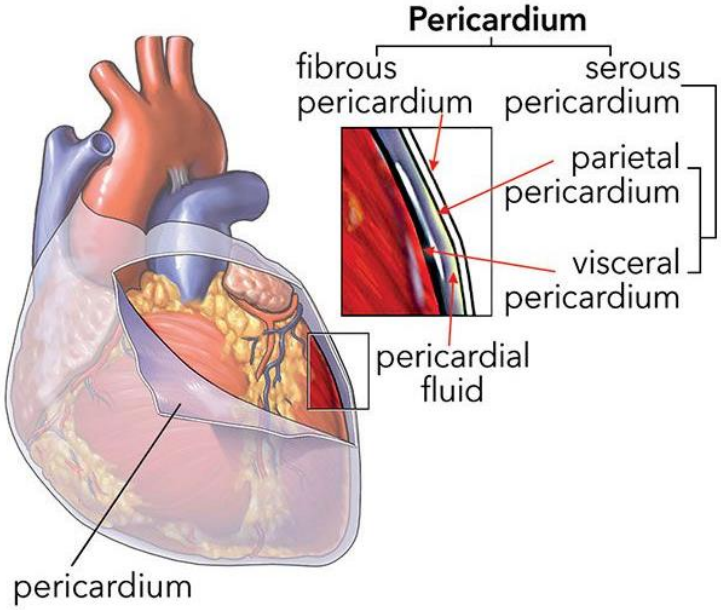

Figure 2.1 The layers of native pericardium (reproduced from McGraw-Hill education, n.d.)

The fibrous pericardium provides mechanical properties to the tissue and is composed of multiple layers of multidirectional collagen bundles with interwoven elastin (Li et al., 2011). The serous pericardium includes the epicardium (visceral layer) that consists of a thin layer of mesothelial cells that covers the heart and great proximal vessels (Figure 2.2) and the parietal layer (Figure 2.3) which lines the fibrous pericardium (Jaworska-Wilczynska et al., 2016).

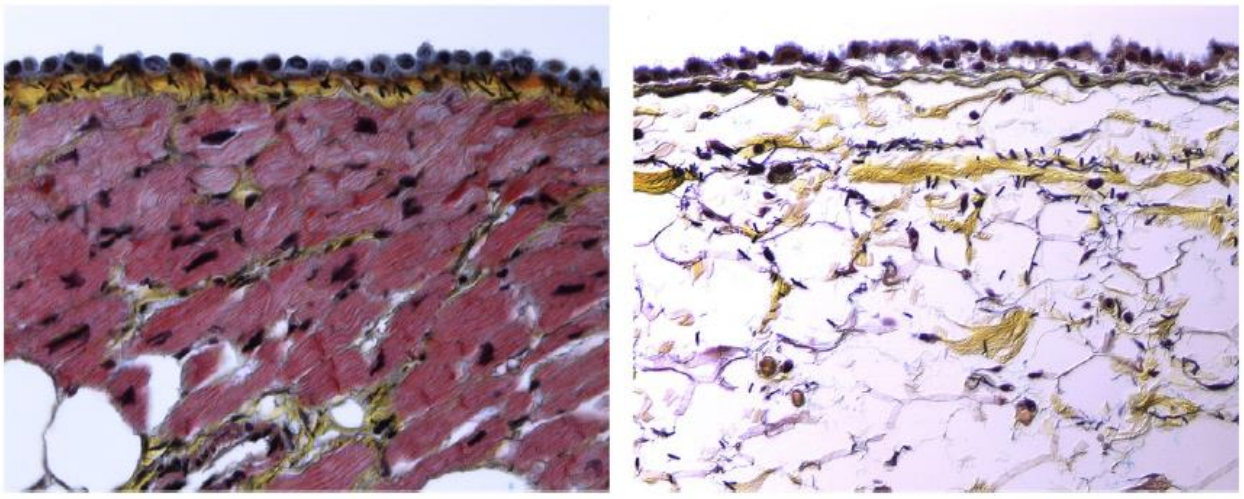

Figure 2.2 **Visceral pericardium.** These two microscopic images show the serosal (mesothelial cell) component of the visceral pericardium that invests the heart. The image on the left represents an area where the visceral pericardium is in direct contact with the myocardium. Only a thin layer of fibrous tissue (yellow) separates the mesothelial cells (gray blue cytoplasm) from the cardiac myocytes (red sarcoplasm). Note the scant amount of elastic lamellae shown as black straight lines in the middle of the yellow fibrous tissue just underneath the mesothelium (x200, Movat pentachrome). The image on the right shows the visceral pericardium as it covers an area of the heart with abundant adipose tissue in the epicardium (such as the interventricular and atrioventricular grooves or around the coronary vessels). These is a small amount of fibrous tissue (yellow) as well as scant elastic lamellae (black). The mesothelial cells forming the serosal layer play an important role in the production and reabsorption of fluid in the pericardial space (x200, Movat pentachrome) (reproduced from Rodriguez & Tan, 2017)

The parietal pericardium is attached to the diaphragm by loose fibrous tissue and to the sternum by sterno-pericardial ligaments. The parietal pericardium can be easily removed from the heart and is used in bioprosthetic devices. The parietal pericardial layer is several times thicker than the visceral pericardial layer (Czum et al., 2014).

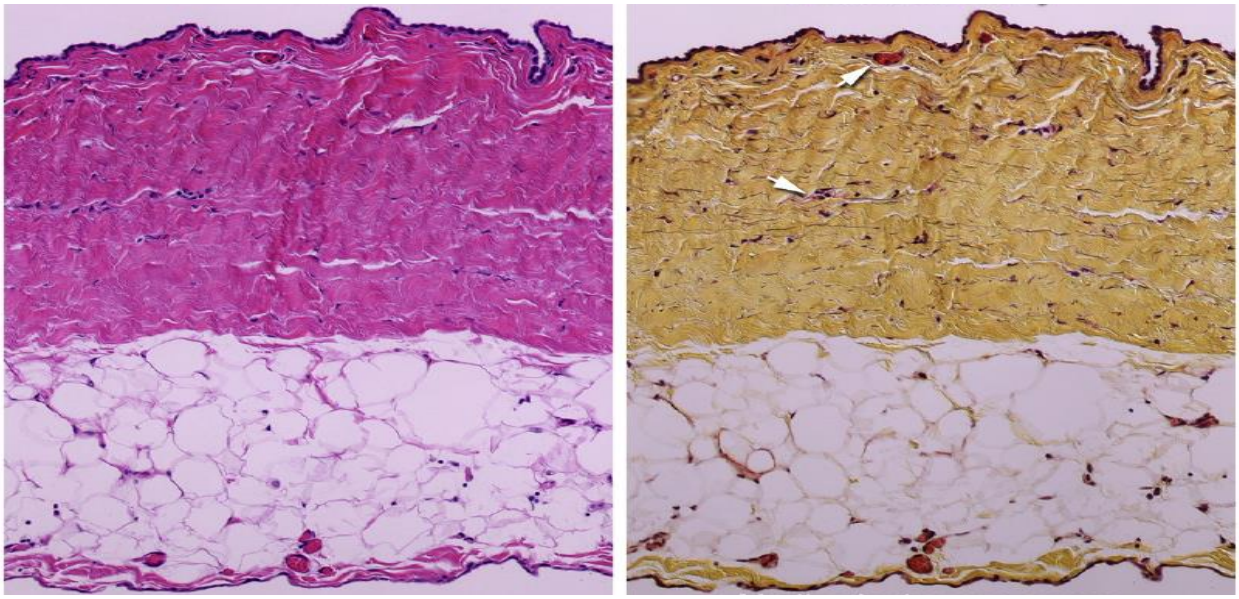

Figure 2.3 **Parietal pericardium.** These microscopic images of the lateral wall of the parietal pericardium shows a serosal layer of the pericardial mesothelial cells lining the pericardial cavity and the fibrous layer. The fibrosa is the thick eosinophilic layer (left image) or yellow layer (right image) made up of dense wavy collagen fibers. Faint black lines represent a minimal amount of elastic lamellae in the fibrosa. The parietal pericardium contains a few small blood vessels (arrows). Between the fibrosa of the parietal pericardium and the mediastinal parietal pleura is a layer of epipericardial fat. Note the serosal layer of the pleura is also made up of a layer of mesothelial cells (x50, H&E and Movat pentachrome)(reproduced from Rodriguez & Tan, 2017)

The visceral and parietal layers are separated by a slit-like pericardial cavity, which contains on average 15 to 50 ml of pericardial fluid (Khandaker et al., 2010). Ultrafiltration from plasma mainly containing globular proteins, phospholipids and surfactant-like prostaglandins give rise to pericardial fluid (Ramasamy et al., 2018).

2.1.3 Composition

Pericardium is mainly composed of simple squamous epithelium and connective tissue which is rich in collagen mostly type I collagen, as well as glycoproteins, glycosaminoglycans (GAGs) and growth factors, cytokines and chemokines (Al-bayati & Hameed, 2018). Type I collagen is arranged hierarchically in different levels of organization with various structures, that differs from fibrils to laminates, fibers and fiber bundles with interwoven elastin and GAGs (Mallis et al., 2017).

Therefore, pericardium can also be referred to as a multi-laminate composite material due to its network of collagen and elastic fibers imbedded in an amorphous matrix, which in turn is mainly composed of free GAGs and proteoglycans GAGs linked to protein cores)(Mendoza-Novelo et al., 2011).

2.2 Sources of pericardial tissue

Autologous tissue still remains the gold standard as biomaterial for its superior functionality and nonimmunogenicity (Lam & Wu, 2012). Besides offering an innate biocompatibility, bodily tissues is uniquely optimized to serve its specific organ system. Human autologous pericardium has several advantages since it is free of donor-derived pathogens and does not provoke any immune response (Mirsadraee et al., 2007), easily handled and low in cost (Neethling et al., 2014; Goetz et al., 2002). Therefore, these characteristics contribute to shorter and less aggressive processing techniques prior to implantation (Remi et al., 2011). These characteristics makes autologous pericardium the most desirable pericardium for cardiovascular application (Neethling et al., 2014).

However, tissue supply, and the patient's health status negatively influence the harvesting of these tissues. The general opinion of homologous pericardium without

fixation is negative due to its tendency to retract, thicken, become aneurysmal and develop fibrosis (Neethling et al., 2014; Remi et al., 2011). This negative results led to the fixation of pericardial tissue with a 0,2% to 0.6% glutaraldehyde solution not only to preserve the tissue but also to stabilize the pericardium, strengthen it and to prevent secondary shrinkage during cusp tissue or valve tissue replacement (Lam & Wu, 2012; Halees et al., 2005; Goetz et al., 2002).

An alternative is to harvest allogeneic tissues or donor tissues from same specie origin but demand still outstrip supply. Therefore, xenogeneic tissues harvested from animals helped to address the need specifically in surgical tissue repairs and valve replacement surgery (Lam & Wu, 2012).

Several pericardial tissues from various species have been assessed or are currently used in clinical practice as biological substitutes, for example; equine (Kubota et al., 2012; Yamamoto et al., 2009), canine (Wiegner & Bing, 1981), ostrich (Maestro et al., 2006), kangaroo (Neethling et al., 2002), bovine, and porcine (Remi et al., 2011). From the list above, bovine and porcine pericardium remains the most frequently used pericardial tissue. However, there is a slight difference between bovine and porcine pericardium. Bovine pericardium has a higher collagen content and tend to obstruct less than porcine valves although, both bovine and porcine pericardial valves show similar hemodynamic performance (Lam & Wu, 2012). Xenogeneic tissues like bovine pericardium is readily available, has excellent biocompatibility and a low rate of infection (Li et al., 2011). Porcine pericardial tissue offers similar biological and mechanical properties as bovine pericardium and can also be used in cardiovascular patching (Tran et al., 2016).

Irrespective of the source, it is still important to note that the ideal pericardial patch material needs to include the following characteristics:

i. Long term stability and durability
ii. Low risk of restenosis
iii. Compliance near that of the host artery
iv. Comfortable handling
v. Easy harvest and ready to use
vi. Anti-coagulation function
vii. Resistance to infection and late degeneration (Muto et al., 2009)

This study will focus on the evaluation of the tissue integrity of bovine pericardium exposed to different processing techniques prior to implantation and explanted from an ovine sheep model after a period of six months.

2.3 Bovine Pericardium

For the past 50-years bovine pericardium has become a well-known biomaterial in clinical use and is used in various fields of medicine and dentistry.

2.3.1 The development of bovine pericardium as a bioprosthetic tissue

After the first xenograft porcine valve implantation in 1965 by Jean-Paul Binet, Jean Langlois and Alain Carpentier followed by the implantation of 61 porcine xenografts in 53 patients in 1968 it became evident from the results that alternative tissues needs to be explored (Carpentier, 1989). In 1965 the porcine valves were preserved in a mercurial solution and despite, initial excellent valvular function upon implantation valves started to deteriorate rapidly after only six months of implantation. The explant results demonstrated extensive inflammatory cell ingrowth with calcification and no morphological evidence of tissue regeneration or fibroblast ingrowth. From the porcine valves implanted in 1969 only 60% were functional after six months and

only 45% at one year (Carpentier et al., 1969). Again, the histological results indicated a host immune response with the ingrowth of inflammatory cells into the graft tissue.

In 1971, Marian Ionescue was the first to introduce bovine pericardium when he constructed prosthetic heart valves from glutaraldehyde treated bovine pericardium. Bovine pericardial tissue possesses to have excellent hemodynamic properties and the "Ionescu-Shiley Pericardial Xenograft" only reported failures 6-10 years postoperatively although a small percentage lasted up to 26 years. Due to long term durability failure the production of these valves were suspended but later Edwards Laboratories manufactured the same valve but sold it as the Carpentier-Edwards Pericardial Bioprosthesis" and better results were recorded for this device in comparison to its predecessor (Athar et al., 2014).

In 1984, Yakirevich et al. reported that glutaraldehyde stabilized xenogeneic bovine pericardial patches were very effective to close the pericardial sacs of 66 patients after open heart surgery. This pericardial tissue showed no hemodynamic problems or any evidence of immunological responses and the lack of adhesion between the material and the pericardium facilitated the reopening of the chest cavities in three patients. These findings led the way and xenogeneic bovine pericardium became the material of choice in cases where the primary closure of the pericardial sac was not feasible.

Since then the application for the use of xenogeneic bovine pericardium expanded dramatically even outside the field of cardiac surgery.

2.3.2 Application of bovine pericardium as a biomaterial

Pericardial patches fabricated from animal tissues have a wide range of applications in various fields of surgery including vascular and general surgery, urology, and cardiac surgery (Table 2.1)(Sobieraj et al., 2016). However, to date pericardium has been mostly used for cardiovascular applications (Remi et al., 2011) i.e. reconstruction of the aorta and pulmonary vessels, closure of interatrial defects, closure of interventricular defects, and reconstruction of atrioventricular valves (Sobieraj et al., 2016).

Other applications of pericardium as medical devices include but are not limited to; soft tissue repair, hernia repair, abdominal & thoracic wall defects, strip reinforcement, orbital repair, dural repair, perivascular patch, heart valve replacement, tendon repair, valvuplasty etc. (Remi et al., 2011; Li et al., 2011). Table 2.1 summarizes the application of bovine pericardium as a graft material.

Table 2.1 Summary of the application of bovine pericardium as a graft material (reproduced from Athar et al., 2014)

	SPECIALTY	RESEARCHER	PROCEDURE
MEDICINE	Cardiac surgery	Marian Ionescue (1971)	Construction of bioprosthetic heart valves
		Yakirevich et al. (1984)	Closure of pericardial sac
		Biasi et al. (1996)	Carotid enderactomy
		David (1998)	Atrial and ventricular septal defects
	General surgery	Hutson (1985)	Abdominal wall and diaphragm defects
		Lopes et al. (2007)	Penile implant
	Ophthalmology	Gupta et al. (2004)	Wrapping of hydroxyapatite orbital implants
		Khanna and Mokhtar (2008)	Corneal ulceration following an alkali injury
	Pulmonary surgery	Allen (1996), Yim et al. (1996)	Treatment of post LVRS emphysema

	Orthopedics	Chvapil et al. (1987), Rossouw and de Villier (2005)	Augmentation of ligaments and tendons
		Gigante et al. (2009)	Rotator cuff surgery
	Neurosurgery	Baharuddin et al. (2002)	Dural graft
DENTISTRY	Oral surgery	Shin and Sohn (2005)	Maxillary sinus perforations
		Steigmann (2006)	Alveolar ridge augmentations
		Stavropoulus et al. (2010), Jepsen et al. (2003)	Deep intrabony defects, periodontal defects

2.3.3 Advantages of bovine pericardium

As a cardiovascular patch bovine pericardium has several advantages but it is important to distinguish between benefits that has been scientifically documented and benefits that are noticed but still lack some scientific evidence (Table 2.2).

Table 2.2 Advantages of bovine pericardium (reproduced from Li et al., 2011)

Benefits	Advantages
Known	Reliable consistency
	Ease of handling
	Durability
	Strength
	Biocompatibility
	Lack of suture line bleeding
	Off the self-availability
	Immediate insonation
Possible	Anticalcification
	Reduced restenosis
	Reduced infections
	Supports cellular ingrowth

Bovine pericardium, mainly composed of type I collagen has a native extracellular matrix (ECM) architecture, creating an environment ideal for host cell migration and proliferation (Gates et al., 2017). Pericardium is known to have a non-thrombogenic inner surface and is extremely pliable thus, adjustable to several shapes

which include tridimensional shapes (Miyamotto et al., 2009). When used in the fabrication of tissue valves Schoen & Levy (2005) stated that tissue valves demonstrates a low rate of thromboembolism without coagulation. This could be attributed to the central pattern flow that mimics that of the natural heart valve and cusps.

Bovine pericardium can be manufactured and processed to a consistent nominal thickness of 0.5mm (Li et al., 2011) therefore providing dependable uniform suture retention (Lam & Wu, 2012). As with autologous vein patches, they display minimal suture line bleeding after implantation and significantly less when compared to other prosthetic patch materials (Li et al., 2011).

The pericardial patches are available in different sizes allowing for custom configurations to a variety of cardiovascular applications. Because bovine pericardium is fixed tissue it offers the benefit of off-the-self availability and is lower in cost when compared to other synthetic patches.

2.3.4 Disadvantages of bovine pericardium

Despite recent advances, biological matrix deterioration and tissue degeneration due to mineralization are complications frequently associated with pericardium (Mendoza-Novelo et al., 2011; Remi et al., 2011). Li et al. (2011) reported that restenosis, pseudoaneurysm formation, thrombosis, calcification, infection and fibrosis has all been associated with the use of bovine pericardium patches although some of them appear less frequent than others.

When used during cardiac surgery some of the major disadvantages include the development of secondary stenosis at the suture site (resulting from fibrosis and

calcification), the possibility of aneurysm development, and, the high cost of these products (Li et al., 2011).

Bovine pericardium is mainly used for the construction of bioprosthetic tissue valves therefore most disadvantages are based on the use of bovine pericardium as a tissue valve bioprosthesis.

In xenogeneic heart valves manufactured from bovine pericardium the major disadvantage remains gradual degeneration and limited durability (Ciubotaru et al., 2013). There are multiple factors that can influence the durability of biological tissues implanted in the human cardiovascular system such as the nature of the tissue, the process of chemical fixation, preservation method, age and medical condition of the patient, the immunological relationship between donor and recipient tissue and the hemodynamic stress exerted by the cardiac cycle (Ciubotaru et al., 2013; Singhal et al., 2013; Jorge-Herrero et al., 2005).

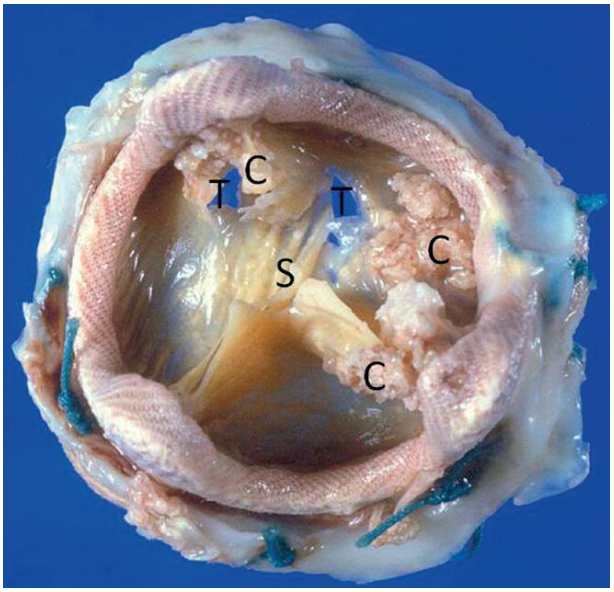

Figure 2.4 Porcine bioprosthetic heart valve. (C) calcification, (T) cusp tears, (S) valve stenosis (reproduced from Manji et al., 2012)

Calcification, a time-related process that matures with time still remains one of the leading causes of bioprosthetic valve failure (Mosier et al., 2018). However, to date the exact mechanism of tissue degeneration that contributes to calcification is still not fully understood. According to Mosier et al. (2018) three mechanism that leads to tissue degeneration can be implicated in the development of calcification namely; i) the degenerative process, ii) the atherosclerotic process and the immune rejection process (Figure 2.5).

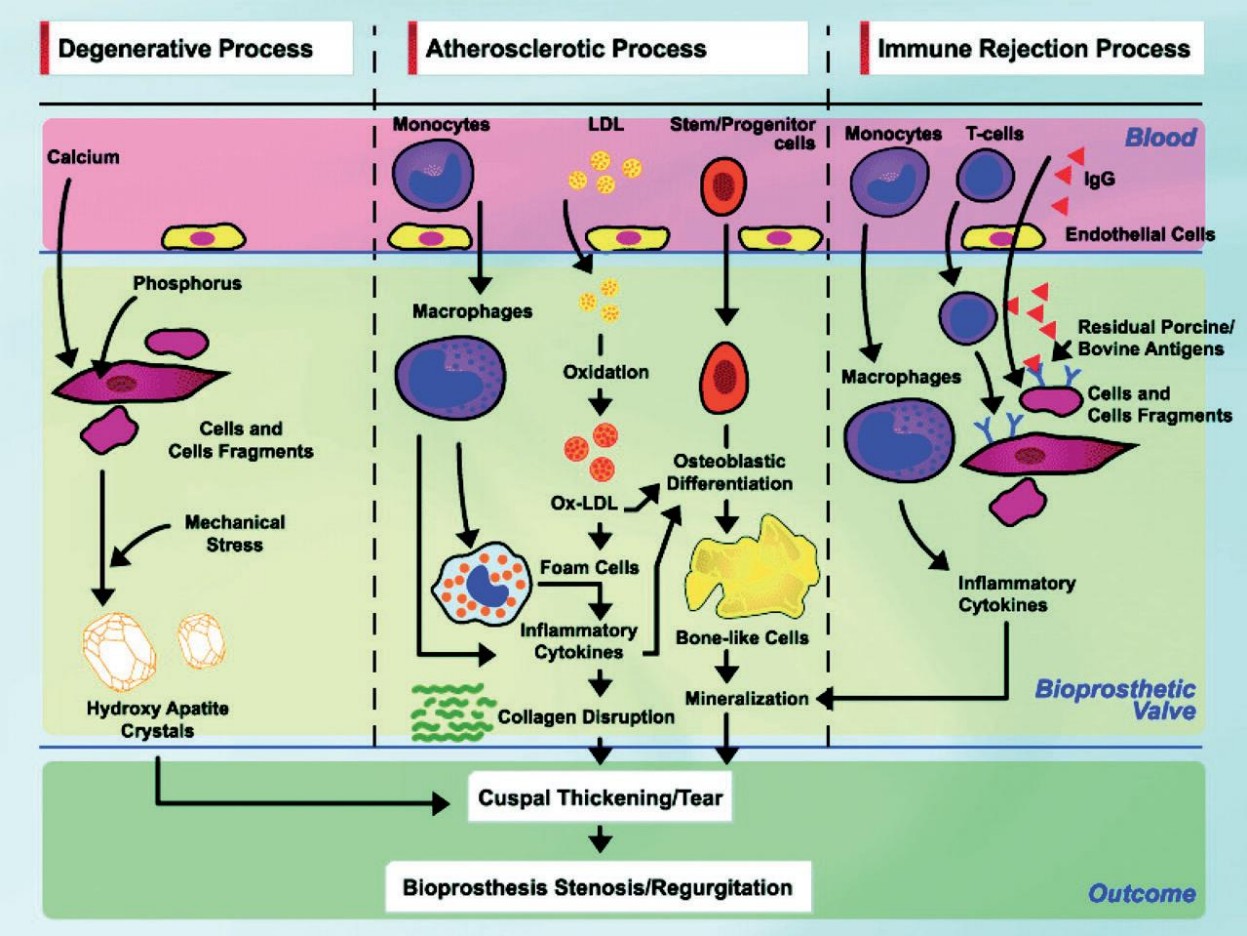

Figure 2.5 A theoretical model showing the degenerative, atherosclerotic, and immune rejection processes involved in the structural degradation of bioprosthetic heart valves (reproduced from Pibarot and Dumesnil, 2009)

Although the exact mechanism of calcification is still unclear the following is suggested. The initial and predominant calcification of connective tissue cells in the bioprosthetic matrix is likely to be the result of the unique calcium binding properties of cells and their compartments (Schoen et al., 1986).

In short, the mineralization process in bioprosthetic valves initiates within nonviable connective tissue cells that has been devitalized but not removed by glutaraldehyde pretreatment procedures (Schoen & Levy, 1999). Calcification of the cells is initiated when the dystrophic calcification mechanism causes calcium-containing extracellular fluid to react with membrane-associated phosphorous. This likely transpire because glutaraldehyde fixation rendered the cells to become nonviable therefore disrupting the normal extrusion of calcium ions. Because healthy cell membranes pump calcium out, the concentration of calcium in cytoplasm is 1,000 to 10,000 times lower ($\pm$ 10^{-7} M) if one keeps in mind that normal plasma-extracellular calcium concentration is 1mg/mL ($\pm$ 10^{-3} M). Low cellular calcium levels are maintained by plasma membrane-bound Ca^{2+}-ATPase, which utilizes energy from ATP hydrolysis to pump Ca^{2+} out of the cell, together with intracellular binding by soluble cytosolic or membrane-bound proteins (Schoen et al., 1986). However, in pretreated glutaraldehyde tissue these physiological mechanisms to eliminate calcium is not available and increase calcium influx (by not restricting calcium flow to specific channels) and decreased efflux (impairment of calcium exclusion mechanisms) (Levy et al., 1991). Therefore, these cell membranes and other intercellular structures which is high in phosphorous (phospholipids, especially phosphatidyl serine and phosphate as the backbone of nucleic acids) can bind calcium and act as nucleators and initiates calcification. Over time these calcification deposits enlarge and coalesce which cause the bioprosthetic valves to malfunction due to gross mineralization that stiffen and weaken the tissue (Schoen & Levy, 2005).

Although the calcification mechanism of elastin and collagen is still not clear it seems that calcification in both ECM proteins occur independently. Collagen calcification is time related and occur significantly later than cell-orientated mineralization, usually prominent after long-term implantation. Levy and Schoen (1986) demonstrated the presence of calcification in subdermal Type I collagen sponges implanted in rats. Calcification occurred in the absence of cells devitalized by glutaraldehyde suggesting that collagen calcification may occur independently from cell-orientated mineralization. According to Vyavahare et al. (1999) glutaraldehyde crosslinking is also not a prerequisite for elastin calcification. Native elastin is intracellularly crosslinked to form isodesmosine and desmosine residues that contains very few lysine groups that reacts with glutaraldehyde, demonstrating the independent calcification of the biological heart valve's extracellular matrix.

2.4 Tissue engineering of bovine pericardium

In today's biotechnological research, tissue engineering is regarded as the holy grail and can be defined as the fabrication of a living replacement tissue indistinguishable from the patient's native tissue. Therefore, the tissue engineered product needs to have the characteristic of self-repair and the potential to growth especially when used in children (Simon et al., 2006). The quest for tissue engineered biological scaffolds is on for the current available biological scaffold materials are less than ideal.

Collagenous tissue harvested from animals used as biological material immediately begins to degrade after harvesting. To exploit this tissue as a biological substitute the deterioration of the tissue needs to be arrested and deferred. However, in doing so the aim is to prolong its original structure and mechanical integrity and to remove or at least neutralize its antigenic properties.

Through the years, various processing techniques have been used to produce tissue that will ensure optimal behavior once implanted. Remi et al., 2011 summarized these processing techniques which include cross-linking treatment (reagents: GA, genipin, epoxy compound, carbodiimides, dye mediated photo-oxidation process, reuterin, tannic acid etc.) coating treatment (reagents: chitosan, silk fibroin, tripeptide Arg-Gly-Asp polypeptides, heparin sodium etc.) and post-fixative treatment (reagent: amino acids, glycine, heparin, hyaluronic acid etc.). Decellularization (physical, enzymatic or chemical) in combination with one of the methods mentioned above can also be performed to improve the mechanical and biological behavior of tissue (Crapo et al., 2011; Gilbert et al., 2006).

2.4.1 Fixation (crosslinking)

Prior to implantation, xenogeneic pericardium needs to be treated with cross-linking chemical agents to stabilize the extracellular matrix components and to mask xenogeneic epitopes (Aguiari et al., 2017). This is accomplished by chemically modifying the collagen to render tissue that is immunogenetically acceptable in the human host (Remi et al., 2011).

In 1969, Carpentier introduced the use of glutaraldehyde (GA) as a fixation solution and since then xenogeneic pericardial tissue is widely used in clinical practice (Carpentier et al., 1969) and are even preferred to autologous pericardium (Remi et al., 2011).

To date, GA still remains the most employed and studied cross-linking reagent for collagen-based biomaterials (Parenteau-Bareil et al., 2010) for it decreases biodegradation, maintains anatomical structure, improves strength and endurance of collagen fibers, reduce immunogenicity, ensure tissue biocompatibility and non-thrombogenicity and also contributes to sterilization (Selçuk Kapisiz et al., 2008;

Webb et al., 1989). Jayakrishnan & Jameela, (1996) reported that tissues fixed with GA also retains most of the viscoelastic characteristics of the collagen fibrillary network.

However, beside the positive attributes GA fixation initiates in biological tissue it also contributes to negative characteristics that complement the fixed tissue once implanted. GA fixation has been linked to the acceleration of calcification and is the main cause of long-term fatigue and failure of GA-fixed pericardial tissue (Remi et al., 2011; Jayakrishnan & Jameela, 1996). The tissue fatigue and failure are mostly attributed to the inflammatory and cytotoxic changes (Huang-Lee et al., 1990), causing continuous wear and tear leading to collagen fiber fragmentation. Once GA-fixed the tissue also has a poor ability to regenerate in vivo (Wong et al., 2016). The GA residues prevents host cell attachment, migration and proliferation of endothelial cells due to its cytotoxic effects (Jayakrishnan & Jameela, 1996). Furthermore, Thubrikar et al. (1983) reported an increase in pericardial tissue stiffness with the possibility of tissue buckling.

2.4.1.1 Chemistry of glutaraldehyde crosslinking

GA, [1, 5-pentanedialdehyde; HCO-$(CH_2)_3$-CHO] an organic compound consists of fairly small molecules, each with two aldehyde groups, separated by a flexible chain of 3 methylene bridges (Kiernan, 2000). Both the -CHO groups provides the potential for cross-linking however, the specific chemistry of collagen fixation with GA remains unclear and not fully understood. It is hypothesized that the amino groups of proteins are involved in the cross-linking reaction, because their nucleophilic nature makes them highly reactive (Migneault et al., 2004; Jayakrishnan & Jameela, 1996).

The large amount of collagen in pericardium offers the amine functionality that allows cross-linking due to the reaction of an aldehyde group with an amino group of

lysine or hydroxylysine, while other extracellular matrix components lack the amine functionalities required for crosslinking (Schoen and Levy, 1999; Cheung et al., 1985). GA exists as large polymers of variable sizes in aqueous solution. On each unit and at the end of each unit of the polymer molecule a free aldehyde group is present (Kiernan, 2000)(Figure 2.6).

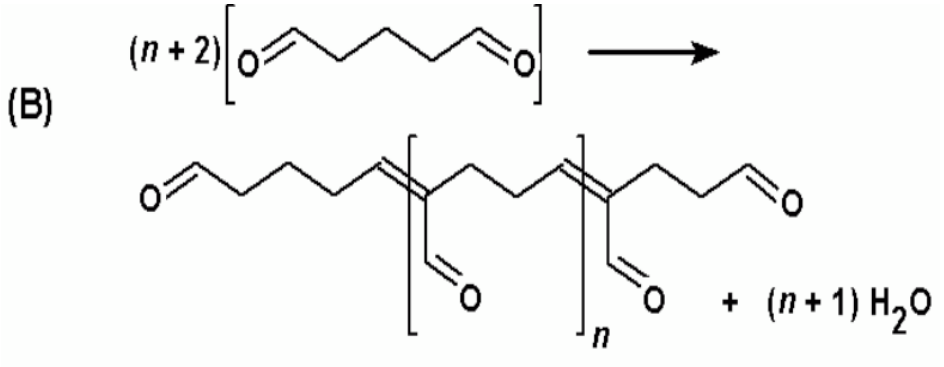

Figure 2.6 Polymerization reaction of glutaraldehyde, showing an aldehyde side-chain on each unit of the polymer (reproduced from Kiernan, 2000)

The -CHO groups will bind to any protein nitrogens to create the potential for cross-linking (Figure 2.7). Besides interacting with amino groups, GA can also react with carboxy, amido and other groups of proteins. Aqueous GA, an unsaturated polymer reacts with the amino group to form a stable imino bond (Schiff base bond). These Schiff base bonds are regarded as the intermediate from which several reactions may occur prior to the formation of a cross-link (Olde Damink et al., 1995). The imino bonds also offers tissue stability against mechanical loading because of the formation of a more tightly crosslinked network between many protein molecules (Ma et al., 2014). However, because GA can be present in various aqueous forms it is plausible that multiple reactions could simultaneously contribute to the crosslinking of tissue (Migneault et al., 2004).

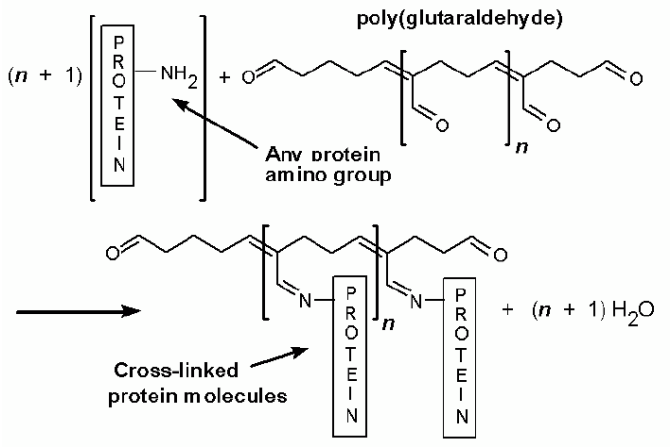

Figure 2.7 Reaction of poly(glutaraldehyde) with amino groups of proteins (reproduced from Kiernan, 2000)

The GA concentration used to cross-link tissue varies from 0.2 to 0.6% (Jayakrishnan & Jameela, 1996). The aldehyde contributes to tissue stiffness at higher concentration while at lower concentrations the aldehyde is ineffective as a sterilant, especially against certain types of mycobacteria. Furthermore, conditions such as concentration, temperature, purity, pH and the extend of exposure to GA determines the extend of cross-linking and the final tissue properties.

2.4.2 Decellularization

To overcome the current limitations of GA-treated scaffolds the successful development of bioprosthetic tissue that is resistant to structural deterioration by the development of GA-free biological materials seems paramount. The decellularization of biological tissue is an emerging alternative to overcome the limitations linked to GA-treated scaffolds.

Decellularization or removal of endothelial and fibroblast cells and nuclear material from biological materials which creates a biological scaffold with decreased immunogenicity/antigenicity and reduced risk of calcification has gained much

interest in recent years. The ultimate goal of a decellularization protocol is to maximize the removal of all cellular and nuclear material while minimizing the adverse effects on the composition, biological activity, and mechanical integrity of the remaining ECM (Gilbert et al., 2006). The effective removal of all cellular remnants during the decellularization process clears donor antigens, reduce the possibility of in vitro cytocompatibility and in vivo adverse host responses, therefore preventing a potential pro-inflammatory response and subsequent immune rejection in the host (Yi et al., 2017).

Through the process of decellularization a biological mesh (ECM) is created which is mainly constituted of pure collagen that act as a regenerative framework that support tissue remodeling and the deposition of newly formed collagen. The ideal biomesh will gradually integrate into the host tissue once implanted and will promote both cellular and vascular regeneration and will eventually produce tissue similar to native tissue (Bielli et al., 2018). However, it is important to remember that any processing step intended to remove cellular and nuclear material will alter the three-dimensional architecture of the ECM (Gilbert et al., 2006).

2.4.2.1 The extracellular matrix (ECM)

Badylak (2007) stated that nature's ideal biological scaffold is an extracellular matrix (ECM). The ECM constitutes a three-dimensional mechanical support structure. Furthermore, it is important for the physical maintenance of all cells and can be defined as a non-cellular component of tissues which act as a glue to bind cells together to form tissues and organs (Kular et al., 2014). Therefore, the ECM acts as a physical barrier between different tissues (Gumbiner, 1996).

Tissues from which the ECM is harvested, the specie of origin, the decellularization method and the terminal sterilization method affects the composition

and ultrastructure of the ECM and ultimately the host tissue response to the ECM scaffold once implanted. One advantage is that the ECM components is generally well conserved and tolerated among species even by xenogeneic recipients (Gilbert et al., 2006).

Therefore, the ECM presents the secreted products of the resident cells within the tissue which functions in a state of dynamic reciprocity with these cells during changes in the microenvironment and provides cues that influence cell migration, proliferation, and differentiation (Crapo et al., 2011).

2.4.2.2 The function of the ECM

Through decades of research our current understanding of the ECM is that it influences cellular activity and responses (Kular et al., 2014). It is very difficult to exactly mimic the ECM in native tissues due to their multiple functions, complex composition and dynamic nature. Therefore, the goal in tissue engineering is to create an ECM that mimics as much of these functions without compromising the integrity of the ECM. Table 2.3 summarizes the function of the extracellular matrix in native and tissue engineered scaffolds.

Table 2.3 Functions of extracellular matrix (ECM) in native tissues and of scaffolds in engineered tissues (reproduced from Chan & Leong, 2008)

Functions of ECM in native tissues	Analogous functions of scaffolds in engineered tissues	Architectural, biological, and mechanical features of scaffolds
i) Provides structural support for cells to reside	Provides structural support for exogenously applied cells to attach, grow, migrate and differentiate in vitro and in vivo	Biomaterials with binding sites for cells; porous structure with interconnectivity for cell migration and for nutrients diffusion; temporary resistance to biodegradation upon implantation
ii) Contributes to the mechanical properties of tissues	Provides the shape and mechanical stability to the tissue defect and gives the rigidity and stiffness to the engineered tissues	Biomaterials with sufficient mechanical properties filling up the void space of the defect and simulating that of the native tissue
iii) Provides bioactive cues for cells to respond to their microenvironment	Interacts with cells actively to facilitate activities such as proliferation and differentiation	Biological cues such as cell-adhesive binding sites; physical cues such as surface topography
iv) Acts as the reservoirs of growth factors and potentiates their actions	Serves as delivery vehicle and reservoir for exogenously applied growth-stimulating factors	Microstructures and other matrix factors retaining bioactive agents in scaffold
v) Provides a flexible physical environment to allow remodeling in response to tissue dynamic processes such as wound healing	Provides a void volume for vascularization and new tissue formation during remodeling	Porous microstructures for nutrients and metabolites diffusion; matrix design with controllable degradation mechanisms and rates; biomaterials and their degraded products with acceptable tissue compatibility

2.4.2.3 Major components of the ECM

The composition of the ECM includes a large collection of biochemically distinct components which includes proteins, glycoproteins, proteoglycans, and polysaccharides displaying different physical and chemical characteristics. These proteins provide the structure and support to cells and tissues and can be categorized as fibrous proteins (e.g. collagen, elastin, fibrillin, and fibulin), adhesive glycoproteins (e.g. laminin, fibronectin, tenasin, thrombospondin, and integrin), and glycosaminoglycans (Yi et al., 2017). Other important components of the ECM includes growth factors and a group of matrix metalloproteinases (MMPs)(Kular et al., 2014)(Figure 2.8).

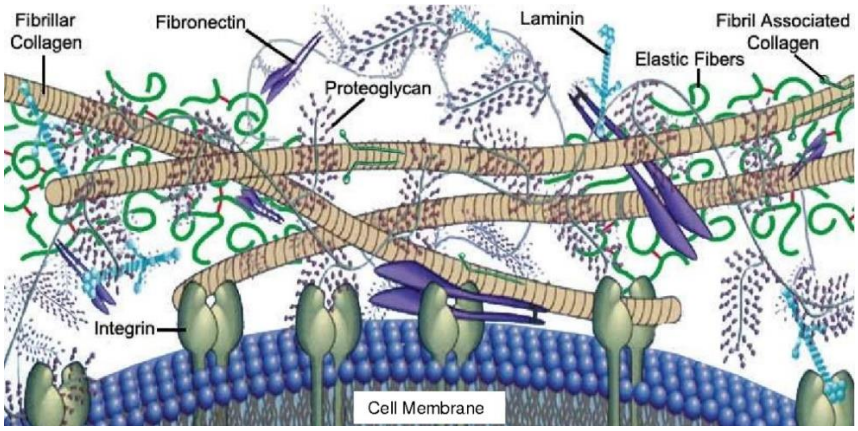

Figure 2.8 Representative cartoon of ECM compositional layout indicating cellular engagement with ECM biomolecules and primary components of general ECM space (reproduced from Aamodt and Grainger, 2016)

Structurally these components make up both the basement membrane (BM) and the interstitial matrix (Lu et al., 2012). The basement membrane is a thin non-cellular tissue that is more dense and less porous than the interstitial matrix (Kular et al., 2014) and separates the underlying connective tissue from the outer (epithelial, mesothelial, or endothelial) tissue. On the other hand the interstitial matrix is highly charged, hydrated, and contributes greatly to the mechanical strength of the tissue and is rich in fibrillar collagens, proteoglycans, and various glycoproteins like tenascin C and fibronectin (Lu et al., 2012). Although the protein components vary between tissues the majority of functional and structural molecules remain common amongst most scaffolds (Costa et al., 2017):

i) Collagen

Collagen, specifically Type I collagen is the most abundant protein in the body and account for approximately 85% of the dry weight of the ECM (Di Lullo et al., 2002; Costa et al., 2017). Due to collagen's highly hydrophilic nature it can support and improve the interaction of cells with the scaffold (Al-bayati & Hameed, 2018). More

than 20 different types of collagen has been described all with specific functional attributes (Costa et al., 2017).

The fibril-forming collagens (types I, II, III, V and XI), but specifically Type I collagen provides the mechanical integrity (strength and load-bearing) and is therefore regarded as a major structural protein (Costa et al., 2017; Yue, 2014)(Figure 2.9).

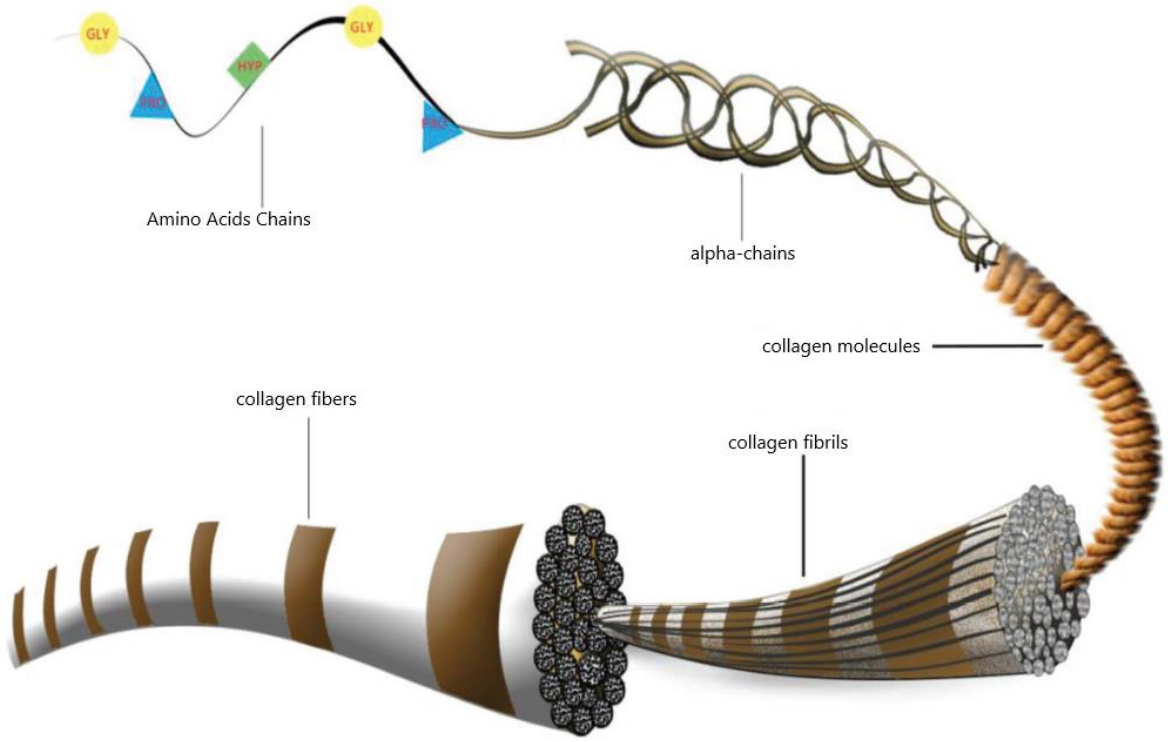

Figure 2.9 Structure of collagen (reproduced from Lin et al., 2018)

Type I collagen is also often used on gel scaffolds as a coating to promote cell adhesion. Type IV collagen, most abundant in the basement membrane together with laminin plays and important role in cell adhesion, migration, differentiation and growth (Tanjore & Kalluri, 2006). Type IV collagen link matrix macromolecules and cells interact with collagen Type V and fibronectin to contribute to the structural integrity of tissue scaffolds (Galla et al., 2010).

ii) Elastin

Elastin with a similar role as collagen is composed of single tropoelastin subunits cross-linked with an outer layer of fibrillin microfibrils (Kular et al., 2014). The main function of elastin is to provide tissue with the ability to recover after continued stretching (Figure 2.10). Crucial to the proper function of the elastic fiber is the extensive cross-linking of tropoelastin mediated by the extracellular enzyme lysyl oxidases which is responsible to oxidize selective lysine residues in peptide linkage to allysine (Yue, 2014).

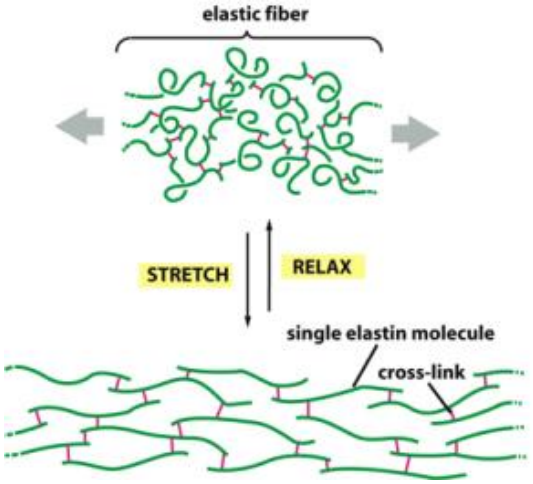

Figure 2.10 The stretch and recoil of an elastic fiber (reproduced from Lahir, 2015)

iii) Proteoglycans and glycosaminoglycan's

Proteoglycans also referred to as mucopolysaccharides (e.g. aggrecan, brevican, decorin, keratocan, lumican, neurocan, perlecan, syndecan, and versican) are formed when core proteins covalently link with GAGs (Yi et al., 2017). Proteoglycans and glycosaminoglycans dominates the physical properties of the ECM and participates in cell-to-cell and cell-to-matrix interactions, cell proliferation, migration, wound healing and tissue remodeling (Ghatak et al., 2015).

GAGs are linear, anionic polysaccharides fabricated from repeating disaccharide units and plays an important role in the binding of growth factors and cytokines, water retention and ensuring extraordinary mechanical loading by distributing the forces within the tissue (Badylak, 2002). There are four (4) groups of GAGs; i) hyaluronic acid, ii) keratan sulfate, iii) chondroitin/dermatan sulfate; iv) and heparan sulfate which include heparin, all sulfated except hyaluronic acid (Yue, 2014)(Figure 2.11).

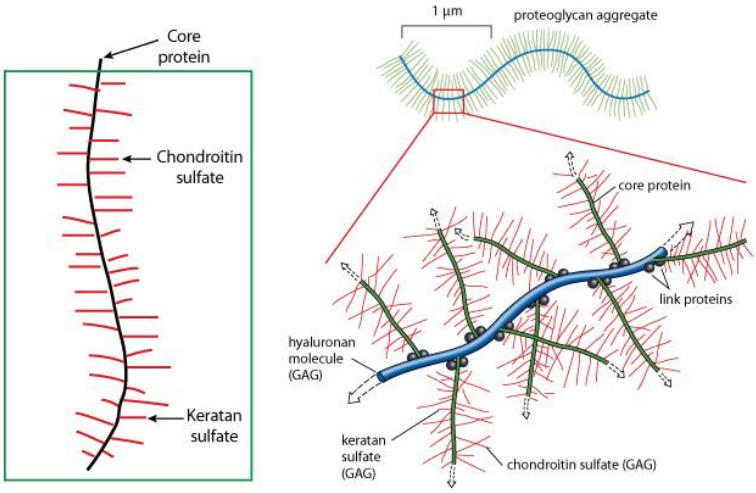

Figure 2.11 Structure of proteoglycan (reproduced from Med Info Education, n.d.)

Due to the high concentration of negative charges and their hydrophilicity GAGs can absorb large amounts of water. Because of this characteristic GAGs are considered fundamental components for the mechanical behavior of tissue (Cigliano et al., 2012). Heparin-rich GAGs are extremely desirable components of scaffolds for tissue repair because of the heparin-binding properties of numerous cell surface receptors and of many growth factors (Badylak, 2002).

GAGs can support regions subjected to large compressive loads. Removal of GAGs from a scaffold can negatively influence the viscoelastic behavior of a scaffold, since water retention is one of the major functional characteristics of GAGs within

tissue (Galla et al., 2010). According to Grande-Allen et al. (2007) the loss of GAGs in bioprosthetic heart valves might dramatically compromise the mechanical function, structure, and/or onset of dystrophic calcification.

iv) Fibronectin

Fibronectin the second most abundant protein in the ECM is a dimeric molecule that contains binding domains for many other ECM proteins like collagen (Yue, 2014). The fibronectin act as a biological glue and is crucial for the attachment and migration of cells. The reason for this is because fibronectin contains RGD (Arginine-Glycine-Aspartate) domains which interact with the cell membrane integrin α5β1 which is the principal receptor involved in the process of fibronectin matrix assembly (Costa et al., 2017). The fibronectin matrix is associated with the actin cytoskeleton of cells via integrin activity which is key to successful matrix formation. Once formed the fibronectin develop into fibrils that varies in thickness between 10 and 1000 nm (Kular et al., 2014).

Fibronectin are primarily located in both the submucosal and basement membrane structures of the ECM (Badylak, 2002). The protein exists in two (2) forms either as plasma that circulates in blood or as a cellular protein produced by fibroblasts (Kular et al., 2014).

v) Laminin

Laminin, a trimeric-cross linked polypeptide is a complex adhesion protein mainly found in the basement membrane of the ECM. The laminin family consists of about 20 glycoproteins assembled in a cross-linked web, interwoven with the type IV collagen network (Yue, 2014).

Laminin provides attachment substrate for tissue homeostasis and during organ development and wound healing they actively modulate cell behavior, regulate cell proliferation, differentiation, adhesion, and migration, promote re-epithelialization and angiogenesis and play and active role in tissue morphogenesis (Yi et al., 2017). The prominent role of laminin in the formation and maintenance of vascular structures makes the ECM very attractive as a scaffold for tissue repair (Badylak, 2002).

vi) Growth factors (GF)

GF are polypeptides that are responsible for a wide variety of biological processes that includes cell proliferation, cell differentiation, cell migration and ion transport. The ECM control the biological activities of GF's and has also been referred to as a reservoir for GFs (Kular et al., 2014; Kanwar et al., 1997). The ECM can store GFs that can be made available when needed. The GFs diffuse freely through the tissue and bind when in contact with its cognate growth factor receptor (Wilgus, 2012).

The interaction between the ECM and GFs controls the surrounding cells. During the direct interaction of GFs with the ECM components they dictate cellular responses. In doing so they protect GFs from degradation and assist with the formation of concentration gradients which is necessary to direct the migration of cells to certain sites within the tissue. For fibroblast growth factor 2 (FGF-2) signaling growth factor-ECM binding is necessary (Wilgus, 2012).

vii) Matrix Metalloproteinases (MMPs)

MMP's are a family of multigenic proteins involved in both normal and pathological tissue remodeling which remains inactive until activated. The majority of MMPs are secreted though membrane type MMPs are also present (Yue, 2014). During tissue repair, MMPs are triggered into action when there is an increase in cytokine and GF activity.

They function as enzymes and play an important role in cleaving ECM proteins, cytokines and GFs to produce fragments with new bioactivities, that can activate GF receptors (Schultz & Wysocki, 2009; Corda et al., 2000).

MMPs can breakdown the ECM matrix. However, this breakdown of the matrix is important because it is necessary for the on-going remodeling process of the ECM and occurs during neovascularization and bone remodeling (Kular et al., 2014).

viii) Integrin

Integrin, a heterodimeric glycoprotein adheres to the extracellular matrix ligands through its cytoplasmic tail and act as a transmembrane connection between the intracellular cytoskeleton and the ECM. The ß1 integrin's are the major binding-integrin's which has an affinity for fibronectin, collagens and laminins (Yue, 2014)(Figure 2.12).

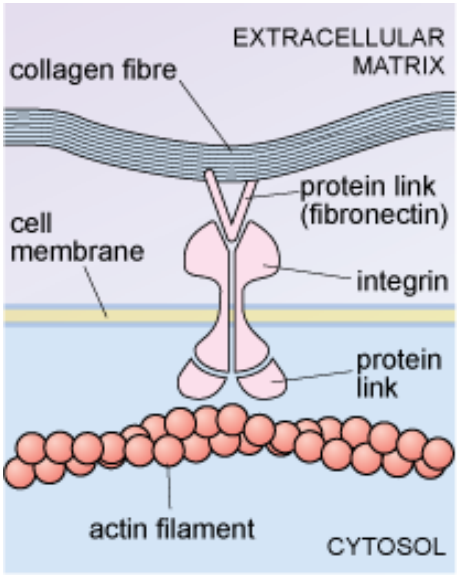

Figure 2.12 Schematic diagram showing how the extracellular matrix is linked to some cells, via integrin molecules (reproduced from the OpenLearn University, n.d.)

Besides the adhesive role that integrin's play it also act as a signal transduction receptor which mediates cell signaling pathways of transmembrane protein kinases by transmitting the signals between the ECM and the cell. Integrin's also participates in various biological interactions such as tissue development, hemostasis, angiogenesis, inflammation and tissue repair by playing an active role in cell growth, division, differentiation, survival, and apoptosis (Yi et al., 2017).

2.4.2.4 Decellularization methods

Decellularization can be achieved by a combination of chemical and enzymatic compounds together with physical/mechanical agitation to destroy the cell membranes and to remove all the nuclear material, cell debris and residual chemicals, leaving an acellular extracellular matrix (ECM) with a retained three-dimensional architecture (Crapo et al., 2011; Mendoza-Novelo et al., 2011). The most popular decellularization methods involve a combination of physical, chemical and enzymatic approaches.

The majority of decellularization protocols start with physical treatments or ionic solutions to lyse the cell membranes, followed by enzymatic treatments to separate cellular components from the ECM. Detergents are used for the solubilization of the cytoplasm and nuclear components and the final step of the decellularization process is to remove cellular debris from the tissue (Gilbert et al., 2006). The effectiveness of these methods can be improved by mechanical agitation. Prior to implantation it is important to remove all residual chemicals by incorporating a washing step, thus avoiding any host tissue response (Remi et al., 2011). Table 2.4 summarize the most commonly used decellularization methods and chaotropic agents.

Table 2.4 Commonly used decellularization methods and chaotropic agents (reproduced from Gilbert et al., 2006)

Method	Mode of action	Effects on ECM
Physical		
i) Snap freezing	Intracellular ice crystals disrupt cell membrane	ECM can be disrupted or fractured during rapid freezing
ii) Mechanical force	Pressure can burst cells and tissue removal eliminates cells	Mechanical force can cause damage to ECM
iii) Mechanical agitation	Can cause cell lysis, but more commonly used to facilitate chemical exposure and cellular material removal	Aggressive agitation or sonication can disrupt ECM as the cellular material is removed
Chemical		
i) Alkaline; acid	Solubilizes cytoplasmic components of cells; disrupts nucleic acids	Removes GAGs
Non-ionic detergents		
i) Triton X-100	Disrupts lipid-lipid and lipid-protein interactions, while leaving protein-protein interactions intact	Mixed results, efficiency dependent on tissue, removes GAGs
Ionic detergents		
i) Sodium dodecyl sulfate (SDS)	Solubilize cytoplasmic and nuclear cellular membranes; tend to denature proteins	Removes nuclear remnants and cytoplasmic proteins; tends to disrupt native tissue structure, remove GAGs and damage collagen
ii) Sodium deoxycholate		More disruptive to tissue structure than SDS
iii) Triton X-200		Yielded efficient cell removal when used with zwitterionic detergents
Zwitterionic detergents		
i) CHAPS	Exhibit properties of non-ionic and ionic detergents	Efficient cell removal with ECM disruption similar to that of Triton X-100
ii) Sulfobetaine-10 and-16 (SB-10, SB-16)		Yielded cell removal and mild ECM disruption with Triton X-200
iii) Tri(n-butyl) phosphate	Organic solvent that disrupts protein-protein interactions	Variable cell removal; loss of collagen content, although effect on mechanical properties was minimal
iv) Hypotonic and hypertonic solutions	Cell lysis by osmotic shock	Efficient for cell lysis, but does not effectively remove cellular remnants
v) EDTA, EGTA	Chelating agents that bind divalent metallic ions, thereby disrupting cell adhesion to ECM	No isolated exposure typically used with enzymatic methods (e.g. trypsin)
Enzymatic		
i) Trypsin	Cleaves peptide bonds on the C-side of Arg and Lys	Prolonged exposure can disrupt ECM structure, removes laminin, fibronectin, elastin, and GAGs
ii) Endonucleases	Catalyze the hydrolysis of the interior bonds of ribonucleotide and deoxy ribonucleotide chains	Difficult to remove from the tissue and could invoke an immune response

2.4.2.5 Pericardial decellularization protocols

The first attempt to decellularized bovine pericardium was conducted in 1994 by Courtman et al. They used a four-step extraction process which included; (i) immersing the tissue in a hypotonic tris buffer (pH 8.0) containing a protease inhibitor (phenylmethyl-sulfonyl fluoride, 0.35 ml/L) for 24 hours at 4°C followed by (ii) 1% Triton X-100 (octylphenoxypolyethoxyethanol) in tris-buffer with protease inhibitor for 24 hours at 4°C, (iii) digestion with DNase and RNase at 37°C for 1 hour and (iv) extraction with Triton-X 100 for 24 hours in tris buffer. They concluded that the tissue was acellular consisting mainly of elastin and insoluble collagen, and tightly bound glycosaminoglycans with mechanical integrity comparable to that off fresh tissue.

Goncalves et al. (2005) decellularization protocol included standard decellularization practices consisting of hypotonic lysis and treatment with DNAse/RNAse followed by either 0.5% Triton X-100, 0.5% sodium deoxycholate (SD), 0.1% sodium dodecyl sulfate (SDS) for 24 hours. Histology revealed only partial removal of cells but persistence of xenogeneic antigens. Only after adding SDS acellularity was obtained and xenogeneic antigens were removed.

Mendoza-Novelo et al. (2011) compared the surfactant tridecyl alcohol ethoxylate (ATE) and the reversible alkaline swelling (RAS) treatments to Triton-X 100. Based on histology the results of all three decellularization processes revealed a substantial decrease in cellular antigens. However, the GAG content varied significantly between the three groups; 88.6 ± 0.2% (RAS), 62.7 ± 1.1% (ATE) and 61.6 ± 0.6% (TX).

Sajith, 2017 conducted a comparative study comparing two different decellularization protocols. In protocol I, 0.25% Trypsin-EDTA solution at 21°C for 2 hours, 3% Triton-X 100 at 21°C for 2 hours and 4% Deoxycholic acid (DCA) at 21°C for 2 hours were used. Protocol II included 1% DCA for 24 hours at 37°C, 100 µg/ml DNase and 150 IU/ml RNase for 12 hours at 37°C. The tissue decellularized according to protocol I showed complete decellularization, but the ECM was significantly distorted. Considerable amounts of collagen fibers were lost which resulted in decreased collagen density with widening of interfibrillar spaces. However, the bovine pericardium treated with protocol II resulted in completely decellularized bovine pericardium with an intact ECM.

Li et al. (2018) compared seven different bovine pericardium decellularization protocols; i) native (control), ii) 1% sodium deoxycholate (SD), iii) 1% SDS + 0.5% SD, iv) 1% Triton-X 100, v) 1% Triton-X 100 + 0.5% SD, vi) freeze-thaw cycles + 1% SDS + 0.5% SD and vii) freeze-thaw cycles + 1% Triton-X 100 + 0.5% SD. From the results protocol 6 and 7 were most effective to remove both the DNA material and the galactose-α-1,3-galactose antigen. Protocol 4, 5 and 7 maintained collagen content and had no cytotoxicity to human umbilical vein endothelial cells. Although all protocols showed a loss in elastin and GAG content after decellularization the highest preservation was seen in protocol 4 followed by 5 and 7. Protocol 7 implants displayed minimal infiltration of macrophages and T-lymphocytes, with no evidence of peri-implant necrosis and calcification after 14 days.

From this section it is very clear that numerous decellularization protocols exist in literature all with different degrees of effectiveness. To develop an effective decellularization protocol, optimization regarding specific reagents, concentrations, incubation temperatures, pH, and duration of exposure needs to be conducted and standardized.

Decellularization also aims to remove cells and nuclear material to reduce the cellular and humoral immune responses targeted against the bioprosthesis. However, by just removing cells does not automatically imply adequate removal of xenoantigens, nor mitigation of the immune response and for this reason antigen removal protocols has also been investigated. Cell membrane antigens [oligosaccharides beta-Gal; galactose-alpha1,3-galactose (alpha-gal) and major histocompatibility complex (MHC) I] can initiate an immune response ultimately causing calcification but can be prevented by effective and adjusted decellularization protocols (Badylak & Gilbert, 2009; Gonçalves et al., 2005). Additional treatment options such as pericardial coating and post-fixative treatment after decellularization can improve both the mechanical and biological features of the graft thus contributing to long-term graft durability.

However, the host response to acellular pericardium still remains unclear and a better understanding of this is needed to develop decellularization protocols (for example immunoproteomic approaches) that will improve biological scaffold integration and clinical safety (Gates et al., 2017).

2.4.2.6 The impact of decellularization on tissue properties

Depending on the type of decellularization protocol used, decellularization usually affects the mechanical and structural integrity of the treated tissue as well as the alteration of the ECM histoarchitecture in different ways. Currently, no optimal decellularization protocol has been identified and all protocols are reproduced to provide the best decellularization efficiency and functional characteristic ratio for the targeted tissue.

Decellularization protocols mediates alteration of the structural and mechanical properties of tissue by removing or decreasing the amount of GAGs present after the decellularized process (Badylak et al., 2015). When GAGs are removed from the

tissue it negatively impacts the pericardial viscoelastic properties by limiting the amount of water retention in the tissue necessary to maintain flexibility and ultimately strength (Mendoza-Novelo et al., 2011; Galla et al., 2010). Furthermore, decreasing the amount of GAGs also impair the biological role of cell signaling and communication which ultimately contributes to impaired tissue response and repair (Cigliano et al., 2012). Therefore, by selecting the optimal decellularization protocol one needs to consider not only the tissue type but also the targeted implantation site and application.

For instance, Liao et al. (2008) investigated the effect of decellularization on the mechanical and structural properties of porcine aortic valve leaflets by comparing three (3) decellularization agents; i) anionic detergent (SDS); ii) enzymatic agent (Trypsin) and iii) a non-ionic detergent (Triton X-100). All three (3) agents initiated the disruption of the collagen network after decellularization. Overall, SDS appeared to maintain critical mechanical and microstructural properties the best when compared to the other two (2) agents although scanning electron microscopy suggested that the repopulation of aortic valve interstitial cells (AVIC) may not be optimal due to a dense ECM network and a small pore size.

Using SDS in the decellularization protocol of bovine pericardium is known to cause irreversible denaturation, swelling and decrease tensile strength when compared to native tissue (Lin et al., 2014; Courtman et al., 1994). Therefore, non-ionic detergents present an alternative for decellularization of pericardial tissue but challenges such as toxic and estrogenic effects might still remain (Mendoza-Novelo et al., 2011). On the other hand, Mirsadraee et al. (2006) used SDS in an attempt to produce an acellular human scaffold and reported that successful decellularization was obtained by producing an biocompatible matrix that retained major structural components and strength when compared to native tissue.

2.4.2.7 Evaluation of effective decellularization processes

The goal of successful decellularization is to remove all cells from the tissue or organ leaving a complex mixture of structural and functional proteins that constitute the ECM. Effective cellular removal avoids potential proinflammatory responses and immune rejection in the recipient by the removal of donor antigens, limiting the potential of in vitro cytocompatibility and an in vivo adverse host response (Rana et al., 2017). However, although it is almost impossible to remove all cellular remnants from tissue during decellularization minimal criteria has been set to satisfy the intent of decellularization:

i) < 50 ng double-stranded DNA per mg dry weight of the ECM;
ii) < 200 base pair DNA fragment length and
iii) histological evidence (Yi et al., 2017; Crapo et al., 2011)

With histological stains the first line of inspection to determine if any nuclear structures are present is with the H&E stain. Alternative histological stains to evaluate the presence of various cytoplasmic and extracellular molecules can include; Masson's Trichrome, Movat's Pentachrome, or Safrin O. Specific intracellular proteins can be detected by using immunohistochemical methods such as actin and vimentin. The presence of DNA in the decellularized tissue can be verified by 4',6-diamidino-2-phenylindole (DAPI) or Hoechst staining. Both are fluorescent molecules that bind to the AT clusters in the minor groove of DNA (Yi et al., 2017; Gilbert et al., 2006).

It is also important to note that the minimum number of cells remaining within the extracellular matrix capable of provoking an immune response may vary and is dependent on donor source, composition of the tissue, tissue density, recipient tissue type and host immune function (Crapo et al., 2011).

In addition, to determining what has been removed, it is also important to confirm that the desirable components of the extracellular matrix have been retained though the decellularization process. Any decellularization processing step intended to remove cells can alter the native three-dimensional architecture of the ECM. It is therefore important that the ECM retains its adhesion proteins like fibronectin and laminin, GAG's, growth factors, elastic fibers, and collagens needed for the infiltration of the matrix by cells of choice both in vitro or in vivo (Gilbert et al., 2006).

Effective decellularization can thus be summarized as the successful removal of all cellular and nuclear remnants while limiting the adverse effect on tissue composition, biological activity, and mechanical integrity of the remaining ECM.

2.4.2.8 Decellularized fixed and capped pericardial tissue

Decellularization of biological tissues can induce some alterations in the mechanical properties and structural composition of the extracellular matrix, associated either to the denaturation of the collagen triple helix or to the loss of macromolecular substances such as glycoproteins and glycosaminoglycans. In studies on pericardium it has been demonstrated to cause a reduction in thermal denaturation temperature (T_d) and almost a 50% reduction in tensile strength when compared to native tissue. Therefore, a pre-treatment of collagen-rich biomaterials with different concentrations of ethanol may be advantageous in preventing calcification by removal of phospholipids and cholesterol and additional cross-linking formation (Mendoza-Novelo and Cauich-Rodriguez, 2011).

Additional crosslinking as stabilization of the connective tissue can also be included in the tissue engineering protocol, and several techniques and chemicals have been proposed by researchers, of which GA has been most widely studied and used. Stabilization of the collagen matrix decreases antigenicity (Jana et al., 2014), inhibits

autolysis, gives a prolonged shelf-life and allows surgeons to have products of various sizes readily available. It also maintains thromboresistance and antimicrobial sterility, but results in reduced cellular compatibility because of its toxicity, a reduction in proliferative capacity of cells following repopulation (Mendoza-Novelo and Cauich-Rodriguez, 2011). Despite being highly effective in creating additional cross-links, the presence of residual free aldehyde groups remaining in the tissue has been associated with degeneration and calcification of bio-prostheses (Jorge-Herrero et al., 2010). Cross-linking of artificial scaffolds also resulted in a lower porosity and smaller pore size, and a stiffer ECM in biological scaffolds. This must be countered with additional acidic treatments to allow increased proliferation and migration of cells into the deeper layers (Jana et al., 2014).

Blocking (capping) of these free aldehyde groups through the incorporation of different molecules in the connective tissue to prevent the deleterious effects have been proposed, and the use of propylene glycol and propylene oxide has been shown to be highly effective (Lee et al., 1994).

2.5 Commercially available pericardial patch implants

Cardiovascular patches can either be synthetic or biological in origin. Synthetic materials include but are not limited to GORE-TEX® (W.L. Gore & Associates, Inc., Flagstaff, Arizona, USA), Dacron® (Koch Industries, Inc., Wichita, KS, USA), PTFE (polyutetrafluoroethylene) etc. Synthetic patches became less popular over the years because they are rigid with poor flexibility and biocompatibility. They are known to induce endocarditis and local inflammatory reactions that contributes to fibrotic processes and calcification and have no regeneration potential (Iop et al., 2018; Vaideeswar et al., 2011; Robinson et al., 2005). This led to greater clinical interest in biologically derived patches and substitutes.

Today, the biomedical industry offers a broad range of commercialized xenogeneic pericardia from different species manufactured according to different processing techniques (Table 2.5). The majority of these pericardial patches are GA-treated to induce an immunological barrier, but also to increase durability and chemical stability (Lee et al., 2011). Despite the wide use of GA-fixated tissue over the last 50 years, there are still controversies regarding effective long-term durability and biocompatibility (Iop et al., 2018). Representative problems associated with GA-fixation includes; patch thickening and shrinkage, chronic inflammation, calcification, stiffness after fixation, toxicity and slow release of GA due to the dissociation of the unstable Schiff's base (Iop et al., 2018; Jang et al., 2012; Umashankar et al., 2012).

Table 2.5 Commercialized pericardial patches (reproduced from Iop et al., 2018)

Product Name	Manufacturers	Tissue source	Pre-commercial treatment
CardioCel®	Admedus, Malaga, Western Australia	Bovine pericardium	Decellularized, GA-crosslinked and treated with a proprietary anticalcification treatment (ADAPT®)
Edwards Bovine Pericardial Patches	Edwards Lifesciences Irvine, California, USA	Bovine pericardium	GA-crosslinked and treated with a proprietary anticalcification treatment (XenoLogiX)
Matrix Patch™	Auto Tissue Berlin GmbH	Equine pericardium	Decellularized
No-React®	BioIntegral Surgical Mississauga, Ontario, Canada	Porcine pericardium	Proprietary method, heparin based, to prevent the reduction of aldehyde release of GA crosslinking treatment
Peri-Guard	Baxter International Inc. Deerfield, Illinois, USA	Bovine pericardium	GA-crosslinked
Peripatch-EQ	Neovasc Inc	Equine and bovine	Proprietary method
Peripatch-BV	Richmond, British Columbia, Canada	Equine and bovine pericardium	Proprietary method
PhotoFix®	CryoLife Kennesaw, Georgia, USA	Bovine pericardium	Decellularized and photo oxidized
Vascutek Porcine Pericardial Patch	Vascutek LTD Inchinnan, UK	Porcine pericardium	GA-crosslinked
SJM Biocor™ Patch	St. Jude Medical Saint Paul, Minnesota, USA	Bovine pericardium	GA-crosslinked

SJM Pericardial Patch with EnCap™ AC Technology	St. Jude Medical Saint Paul, Minnesota, USA	Bovine pericardium	GA-crosslinked and treated with a proprietary anticalcification treatment
SURGIFOC	FOC Medical Buenos Aires, Argentina	Bovine and porcine pericardium	GA-crosslinked
dCELL® vascular patch	Tissue Regenix Group PLC	Porcine pericardium	Proprietary decellularization process based on SDS and protease inhibitors
Vascu-Guard	Baxter	Bovine pericardium	GA-crosslinked

Despite countless efforts to reduce calcification potential and cytotoxic aldehyde release from cross-linked biomaterials new strategies are now aimed to improve tissue biocompatibility by means of decellularization. The purpose of decellularization is to deliver a scaffold freed from potentially immunogenic and pro-calcific cell elements, while maintaining the ECM properties through the application of physical, chemical and/or enzymatic treatments (Remi et al., 2011). Several acellular products derived from bovine or porcine origin have since been commercialized; CorMatrix® (CorMatrix Cardiovascular, Inc., Roswell, Atlanta, and Alpharetta, GA, USA), CardioCel® (Admedus, Malaga, Western Australia), Matrix Patch™ (Auto Tissue Berlin GmbH, Goerzallee, Berlin, Germany); PhotoFix® (CryoLife Kennesaw, Georgia, USA); dCELL® vascular patch (Tissue Regenix Group PLC, Walbrook, London, UK)(Table 2.5). However, so far, no optimal decellularization treatment process has been identified and protocols are continuously being reproduced to improve decellularization efficiency and functional characteristics. Moreover, some of the commercial patches mentioned above include additional treatment steps after decellularization to improve mechanical, calcification and biological graft features. Remi et al. (2011) provides a detailed summary on cross-linking, coating and post-fixative treatments developed over the years.

For the purpose of this study two (2) commercially available pericardial patches from bovine origin was included as controls; a GA-crosslinked and decellularized patch. The GA-crosslinked patch with proprietary anticalcification treatment is referred to as the SJM Pericardial Patch with EnCap™ AC Technology, marketed by St Jude Medical, Saint Paul, Minnesota, USA. However, in SA the pericardial patch is marketed by Glycar SA Pty Ltd and for the purpose of this study we will refer to this pericardial patch as the Glycar® patch. We selected this patch because it is most widely used in SA for cardiovascular surgical application. One of the new up and coming commercial decellularized patches, CardioCel® was selected as the decellularized patch of choice to be included in the study. CardioCel® is marketed by Admedus situated in Malaga, Western Australia.

2.5.1 Glycar® bovine pericardial patch

The Glycar pericardium patch is harvested from bovine spongiform encephalopathy (BSE) free, range fed, hormone free cattle that is traceable from birth from a European Conformity (CE) approved abattoir. The pericardium reaches the Glycar plant with a minimal bioburden count. During the processing of the pericardium patch it is glutaraldehyde tanned. The aldehyde tanned bovine pericardial tissue is treated with propylene glycol which cap any residual unlinked aldehyde groups. This changed the tanned pericardium into a biocompatible material with minimal inflammatory reaction and reduced tendency to calcify when implanted into juveniles. The patches are stored in sterile water containing 2% propylene oxide. Only a three-minute rinse is necessary prior to use.

Furthermore, the patches are controlled for strength, thickness and pliability. Strength is measured from a strip contiguous to the selected piece. The thickness of the 5 x 10 cm and 9 x 14 cm patches ranges between 0.2 – 0.4 mm and the 4x5 cm patch, intended for pediatrics range from 0.15 to 0.25 mm.

(http://glycar.co.za/downloads/Glycar_Patch_Brochure.pdf; Glycar 510k:96:3368.; US Patent # 6,174,332. RSA and other worldwide patents).

2.5.2 CardioCel® bovine pericardial patch

The tissue-engineered CardioCel® bovine pericardium patch is manufactured from BSE-free pericardium. The manufacturing process includes several tissue engineering processes (Figure 2.13). Cytotoxicity is reduced to zero by applying the ADAPT TEP® anti-calcification process. ADAPT TEP® limits cytotoxicity by removing lipids, cells and cell remnants, nucleic acids (DNA & RNA) and α-Gal (galactosyl) epitopes. Cross-linking of the collagen fibers is achieved with a low concentration of engineered monomeric glutaraldehyde. Detoxification is accomplished by non-glutaraldehyde sterilization and storage in a glutaraldehyde free solution (Bell et al., 2019; Neethling et al., 2013; Neethling et al., 2010).

The average scaffold thickness of the 5 x 8 cm, 4 x 4 cm and 2 x 2 cm scaffolds are < 0.5 mm https://pdf.medicalexpo.com/pdf/admedus/cardiocel-reproduced-collagen-scaffold/119228-178009.html.

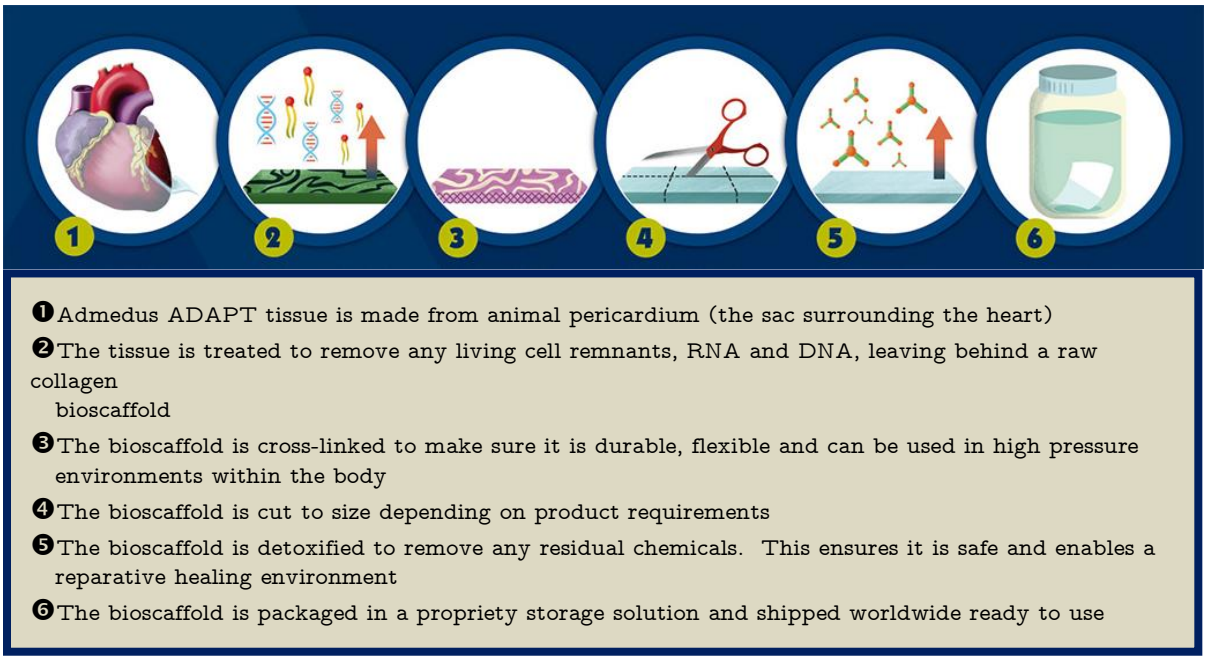

Figure 2.13 Processing of CardioCel® pericardial patch (reproduced from Admedus Innovative Health Solutions, n.d.)

Chapter 3 - Aim

3.1 Aim of study

The aim of the study was to evaluate the impact of different processing techniques (fixed, decellularized, decellularized and fixed) on the tissue integrity of bovine pericardial tissue after implantation in an ovine sheep model.

The aim of the study was addressed in four (4) separate articles and the conceptual framework of the study is summarized in Figure 3.1.

3.2 Aim: Article 1

Advantages of decellularized bovine pericardial scaffolds compared to glutaraldehyde fixed bovine pericardial patches demonstrated in a 180-day implant ovine study

3.3 Aim: Article 2

Comparing the impact of processing techniques between Glycar® and CardioCel® bovine pericardial patches after 180-days implantation in a juvenile ovine model

3.4 Aim: Article 3

The impact of pericardial patch processing techniques after 180-days implantation in an ovine model: Glycar® versus a tissue engineered decellularized, glutaraldehyde-fixed and detoxified bovine pericardium

3.5 Aim: Article 4

Comparison of the tissue integrity and morphology between decellularized bovine pericardial scaffolds with and without glutaraldehyde fixation in a 180-day implant study in the juvenile ovine model

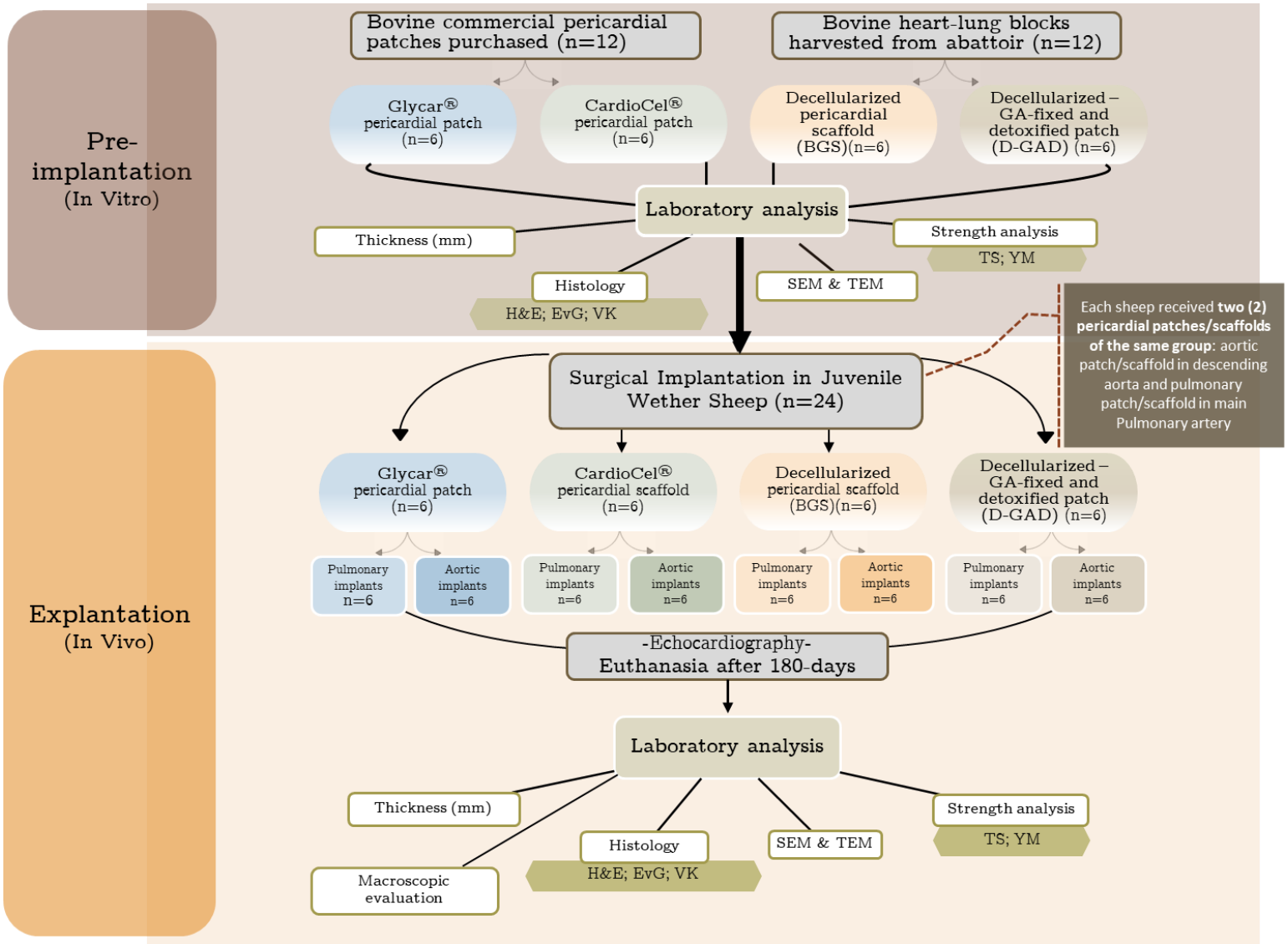

Figure 3.1 Conceptual framework of the study

Chapter 4 - Article 1

Advantages of decellularized bovine pericardial scaffolds compared to glutaraldehyde fixed bovine pericardial patches demonstrated in a 180-day implant ovine study

Botes L[1], Laker L[2], Dohmen PM[2&3], van den Heever JJ[2], Jordaan CJ[2], Goedhals J[4], Smit FE[2]

[1]*Department of Health Sciences, Central University of Technology, Free State, Bloemfontein, South Africa*

[2]*Department of Cardiothoracic Surgery, University of the Free State, Bloemfontein, South Africa*

[3]*Department of Cardiac Surgery, Heart Centre Rostock, University of Rostock, Germany*

[4]*Department of Anatomical Pathology, University of the Free State, Bloemfontein, South Africa*

Abstract

Introduction: Glutaraldehyde (GA)-fixed bovine pericardial patches remain the cardiovascular industry standard despite reports of degradation, thickening, inflammation, calcification and lack of tissue remodeling. Decellularization provides the opportunity to attenuate some of these immune mediated processes. The aim of the study was to compare the mechanical and morphological integrity of bovine pericardium that is GA-fixated with a proprietary decellularization protocol. Methods: The impact of the processing methods on tissue strength and morphology was assessed prior to implantation. Glycar® patches (Group 1: control) were implanted in the descending aorta and main pulmonary artery of six (6) juvenile sheep and decellularized bovine scaffolds (BPS) (Group 2) were implanted in six (6) juvenile sheep at the same anatomical locations. The pericardial implants were clinically evaluated during implantation using echocardiography. Patches were explanted after 180-days and evaluated for strength, calcification and biological interaction. Results: The pre-implanted pulmonary patches of Group 1 were significantly stronger (tensile strength (TS), $p = 0.0238$) and less pliable (Youngs Modulus (YM), $p = 0.0001$) compared to the scaffolds in Group 2. Group 1 demonstrated devitalized cells after processing and acellularity was confirmed in Group 2. The collagen in Group 1 was densely compacted while Group 2 demonstrated wavier collagen bundles. The clinical performance of both groups was excellent, and echocardiography confirmed the absence of aneurysm formation, calcification and degeneration. The explanted pulmonary TS of Group 1 were significantly higher than Group 2 ($p = 0.0144$) but above the minimum native human ascending aorta strength (1.8 ± 0.24 MPa). The YM of both groups improved from pre-implantation to explantation but did not differ statistically at explantation ($p=0.0604$). Collagen was preserved in both groups, but Group 1 demonstrated compact and dense collagen with minimal host cell infiltration. Group 1 developed a fibrous encapsulation that contributed to patch thickening. The explanted scaffolds in Group 2 did not thicken and collagen was well preserved with a wavelike appearance and adequate pore size that promoted infiltration of fibroblast-like cells. Secretory vacuoles visible within these cells can promote procollagen secretion. No evidence of calcification was observed in the explanted pericardium of both groups. Conclusion: The decellularized pericardial scaffolds demonstrated recellularization, resistance to calcification, reendothelialization and adequate strength after 180-day implantation. The proprietary decellularization protocol produced pericardial scaffolds that could be considered as an alternative to GA-fixed pericardial patches.

Keywords: Pericardium, Bovine, Glutaraldehyde, Fixation, Decellularization, Re-cellularization, Calcification

4.1 Introduction

Since 1971 extracellular matrix biomaterial of xenogeneic origin, such as bovine pericardium, had been used extensively in the field of cardiovascular surgery. Ionescu et al. (1977) constructed the first prosthetic heart valve using glutaraldehyde (GA)-preserved pericardium (Carpentier et al., 1969). GA success as a fixative and sterilant can be attributed to its mixed hydrophobic and hydrophilic character, thus allowing rapid molecule penetration of both aqueous media and cell membranes (Schmidt & Baier, 2000). However, GA treatment does not eliminate the immune response and elicit a cytotoxic T cell and humoral response once implanted (Dahm et al., 1990). Both residual cellular debris and extracellular matrix (ECM) proteins in GA-fixated tissue can contribute to an immune response (Coito and Kupiec-Weglinski, 1996). Therefore, immunogenicity can only be partially attenuated by GA-crosslinking and the use of GA to minimize antigenicity comes at an expense of other undesirable effects such as structural changes and calcium deposition thus compromising longevity (Salameh et al., 2018; Baucia et al., 2006). GA crosslinking also increase resistance to enzymatic degradation that is essential for tissue remodeling and healing in vivo (Cohen et al., 2018).

Different processing techniques have been investigated in attempts to reduce calcific degeneration caused by GA preservation. Some of these methods include; alternative crosslinking agents like genipin, epoxy compound, carbodiimides etc.; coating treatments, post-fixative treatments and decellularization (physically, enzymatic or chemical) (Remi et al., 2011; Crapo et al., 2011; Oswal et al., 2007; Gilbert et al., 2006). Decellularization is known to reduce xenograft immunogenicity and is therefore considered an emerging alternative to GA treatment (Umashankar et al., 2012). Ideally, the aim of decellularization procedures is to produce a scaffold freed from potentially immunogenic and pro-calcific cell elements, while preserving the properties of an intact ECM through the use of physical, enzymatic or chemical

treatments (Iop et al., 2018). The most commonly used decellularization solutions include sodium dodecyl sulfate (SDS), sodium deoxycolate (SDC), TritonX-100 (TX), trypsin and DNase (Collatusso et al., 2011). Besides the advantages of these chemical reagents several disadvantages also accompany the use of each of the treatments used. Finding the correct balance between reagent combination at optimal concentration while simultaneously considering the tissue type and application still eludes us in finding the optimal decellularization protocol for biomaterial implants.

The aim of this study was to demonstrate that bovine pericardial tissue processed according to a proprietary decellularization protocol was not inferior to GA treated commercial pericardial patches. Therefore, to characterize the Frater Cardiovascular Centre's decellularized bovine pericardial scaffold (BPS) we analyzed its structural and morphological properties and compared it to a commercial fixated patch, the Glycar® bovine pericardial patch after 180-days implantation in an ovine model.

4.2 Materials and Methods

The study was conducted at the RWM Frater Cardiovascular Research Centre, Department of Cardiothoracic Surgery, University of the Free State (UFS), South Africa. The Animal Ethics Committee of the UFS (HSREC) granted ethical approval for the study (ETOVS Number: UFS-AED2015/0081, Appendix A1).

Glycar® bovine pericardial patch with Aldecap

The SJM (St Jude Medical, Saint Paul, Minnesota, USA) pericardial patch with EnCap™ AC Technology is marketed in South Africa as the Glycar® bovine pericardial patch (Glycar Pty Ltd, Irene, South Africa (SA) and will be referred to as the Glycar® patch. The pericardium is harvested from range fed cattle, certified disease free at slaughter and destined for the European market (Food and Drug

Administration, USA Patent #6,174,332 and European Conformity (CE) approved. Pericardium selection is based on tissue thickness and strength. The pericardium is sterilized with formaldehyde (4%) and propylene oxide and cleared for bovine spongiform encephalopathy. The tissue is crosslinked with GA (0.625%) followed by the removal of residual aldehyde toxicity by the Aldecap process. The aldehyde tanned tissue is treated with propylene glycol (2%) which cap any residual unlinked aldehyde groups limiting host inflammatory response and calcification http://glycar.co.za/downloads/Glycar_Patch_Brochure.pdf).

Decellularized bovine pericardial scaffolds (BPS)

Bovine pericardial sacs from freshly slaughtered young animals (n=6) were collected from a local abattoir and transported on ice to the RWM Frater laboratory and processed using a proprietary decellularization process (Bester et al., 2017). Pericardial patches were cut from a homogenous part of the pericardium and submerged in an antibiotic cocktail (2.5 mg Amphotericin B, 50mg Piperacillin, 50 mg Vancomycin and 25 mg Amikacin sulphate), washed and decellularized using a mixture of 0.5% SDS, 1% SDC and 1% TX. The pericardium was sterilized with 40 µg/ml IturinA (Sigma-Aldrich, Johannesburg, SA) and 70% ethanol. After processing, samples of the decellularized scaffolds were tested for sterility and stored in antibiotic solution at 4°C till implantation. The decellularization protocol took 16-days to complete.

4.2.1 Study design and layout

A prospective analytical cohort design was followed. The mechanical integrity [tensile strength (TS) and Young's Modulus (YM)] tissue morphology [hematoxylin and eosin (H&E), modified Verhoeff's von Gieson (EvG), Von Kossa (VK) histological stains, scanning electron microscopy (SEM) and transmission electron microscopy (TEM)]

and thickness were evaluated in both groups prior to implantation and after explantation. (Figure 4.1).

The Glycar® patches and the BPS were implanted into twelve (12) juvenile Dorper Wether sheep. In the control group (Group 1) six (6) sheep received two Glycar® pericardial patches, the first implanted in the descending aortic arch and the second in the main pulmonary artery. In Group 2, six (6) sheep received two (2) BPS in the same surgical locations as mentioned above (Figure 4.1).

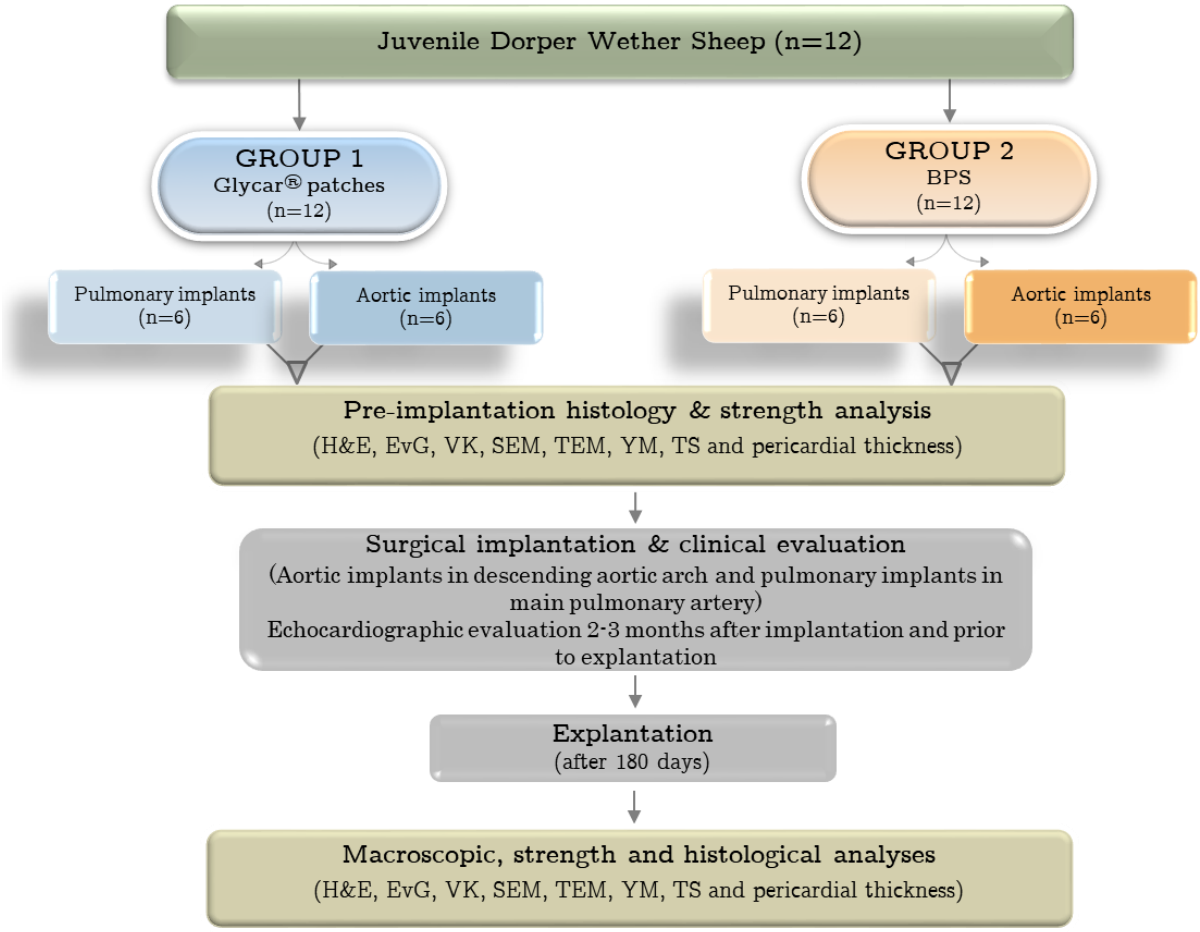

Figure 4.1 Study layout: Glycar® patches and decellularized bovine pericardial scaffold (BPS) (H&E = hematoxylin and eosin; EvG = modified Verhoeff's von Gieson; VK = Von Kossa; YM = Young's Modulus; TM = transmission electron microscopy; SEM = scanning electron microscopy; TEM = transmission electron microscopy)

4.2.2 Surgical protocol

The twelve (12) recipient sheep (age, 6 - 12 months; mean weight 25.75 ± 2.20kg) were premedicated intramuscularly with 0.175 mg/kg Neurotranq (VirbacRSA (Pty) Ltd, Halfway House, South Africa) and 0.2 mg/kg Atropine (Bayer (Pty) Ltd, Animal Health Division, Isando, South Africa), followed by anesthesia induced intravenously with Bomathal (12 mg/kg IV, Merial SA (Pty) Ltd, Halfway House, Johannesburg, South Africa). The sheep was positioned in the lateral decubitus position, intubated and ventilated.

A mini thoracotomy was performed on the left side of the sheep and the fourth rib removed. Patches were implanted by creating surgical defects in the descending thoracic aorta (2 x 2 cm) and the main pulmonary artery (2 x 4 cm). The Glycar® patches and BPS were sutured into the defects using 5/0 continuous polypropylene sutures and the mini thoracotomy closed in layers. Systemic pain medication (2 mg Morphine Sulphate, Bodene (Pty) Ltd, trading as Intramed, Port Elizabeth, South Africa) was administered intramuscularly twice a day and 5 mg Depomycin (Intervet SA (Pty) Ltd, Johannesburg, South Africa) was administered as antibiotic daily for five (5) days post-operatively.

The sheep were extubated between 2 and 4 hours post-operatively and transported to an overnight holding facility with a companion sheep to alleviate stress experienced by the recipient sheep. After a minimum of one hundred and eighty (180)-days the sheep was euthanized, and the pericardial patches and scaffolds explanted.

4.2.3 Laboratory analysis

Samples of the twelve (12) implanted Glycar® patches and BPS were taken prior to implantation and after explantation surgery. Analysis were performed on both the

aorta and pulmonary explants, but strength analysis was only performed on the pulmonary explants due to limited tissue available.

4.2.3.1 Clinical evaluation

Six (6) sheep received Glycar® pericardial patches and six (6) sheep received BPS. Echocardiographic examinations were performed 2-3 months after implantation and just before explantation to evaluate the patches for calcification, infective endocarditis and aneurysm formation.

4.2.3.2 Validation of acellularity

4', 6-Diamidino-2-Phenylindole (DAPI) staining

Efficacy of the decellularization process was confirmed by the DAPI histological stain for it stains and detect cell nuclei, membrane residues, and cytoskeletal actin. This fluorescent stain binds strongly to the adenine-thymine regions of DNA making it visible under a fluorescent microscope (Bancroft and Cook, 1994). The DAPI stains was done by the Cardiovascular Research Unit of the University of Cape Town according to their standard operating procedure.

4.2.3.3 Strength evaluation

Tensile strength (TS) and Young's Modulus (YM)

The mechanical properties of the pulmonary pericardial patches and scaffolds were uniaxially assessed at room temperature by an automated and computerized TS testing apparatus (Lloyds LS100 Plus, IMP, Johannesburg, South Africa). Both ends of the patches and scaffolds were fixed between two grips (Mark-10 Corporation, USA) and gradually stretched at 0.1 mm/s by applying constant tension to both ends (Thubrikar, 1983). Force was calculated by using a 500 N load cell. If the breakage did not occur in the center of the sample the test run was discarded to account for slippage and jaw-breaks. The TS (Mpa) were calculated from the stress-strain curves

as described by Sasaki & Odajima, 1996. The YM (Mpa) or modulus of elasticity was calculated from the stress-strain curved using Nexygen Plus 3 software (Lloyd Instruments, IMP, SA).

The explanted aortic patches and scaffolds were too small to provide accurate strength (TS and YM) results and only the pulmonary patches and scaffolds were analyzed.

4.2.3.4 Structural evaluation

Light microscopy and electron microscopy

Pre-implanted and explanted tissue samples were fixated in 10% phosphate buffered formalin (pH = 7.4) for 12 to 24 hours. The fixed samples were embedded in paraffin wax (Siemens, Johannesburg, south Africa) and two (2) micrometer thick longitudinal sections were prepared and stained; (i) H&E to visualize nuclear material and extracellular matrix structures, (ii) EvG to evaluate collagen and elastin, and (iii) VK histological stain to evaluate calcification (Bancroft and Cook, 1994). The samples were processed and stained by the Department of Anatomical Pathology of the National Health Laboratory Services (NHLS) in Bloemfontein using standard operational procedures. An anatomical pathologist evaluated and reported on the different histological stains.

Electron microscopy

All SEM pericardial samples were immediately fixed in 0.1 M (pH 7.0) sodium phosphate-buffered glutaraldehyde (3%) (Merck, Johannesburg, South Africa) for at least three (3) hours, followed by one (1) hour fixation in buffered osmium tetroxide (1%). The tissue was then dehydrated in a graded ethanol series (50%, 70% and 95%) for 20 minutes (each phase) followed by two changes in 100% ethanol for one (1) hour. The tissue samples were dried using a critical point dreyer (Tousimis critical point

dryer, Rockville, Maryland, USA). After drying, the samples were mounted on aluminium pin stubs (Cambridge pin type 10mm) using epoxy glue and gold sputter coated (± 60nm) by a Bio-Rad sputter coater (Bio-Rad, United Kingdom). The samples were visually assessed using a Shimadzu SSX 550 scanning electron microscope (Kyoto, Japan, with integral imaging [SDF, TIF and JPG format]). A representative image (1200x magnification) of the implant surface was selected for inclusion in the results. The SEM analysis was done by the Centre for Microscopy at the University of the Free Sate, Bloemfontein.

A second sample of each pericardial patch and scaffold was immediately fixed in 3.0% GA for TEM analysis. Thereafter all samples were post fixated in Palade's Osmium Tetroxide. The tissue samples were washed and dehydrated in a graded series of acetone and embedded in an epoxy resin for ultrathin sectioning using the Leica Ultracut UC7 (Leica Microsystems, Johannesburg, SA). The samples were stained with uranyl acetate and lead citrate and photographed with the Soft Imaging System Megaview III digital camera (Olympus, Johannesburg, SA) while samples were visualized using a Philips CM100 Transmission Electron Microscope (FEI, Netherlands).

4.2.3.5 Pericardial thickness

Pericardial thickness was determined prior to surgical implantation and repeated on both the aortic and pulmonary explants. Thickness was measured microscopically using a LeicaDM500 binocular microscope (Leica microsystems, Wetzlar, Germany). The H&E pre-implantation and explant tissue sections (100x magnification) were used to determine patch and scaffold thickness.

Thickness vary significantly within the same group making accurate comparisons very difficult if not impossible. To provide data that could be analyzed,

the thinnest part of each pre-implanted and explanted pericardial scaffold or patch was measured. The fibrous encapsulation was measured separately using the same methodology as above. The median and standard deviation (SD) were calculated for the six (6) pre-implanted patches and scaffolds and for the six (6) explanted aorta and pulmonary patches and scaffolds.

4.3 Statistical analysis

The data was analyzed using SAS 9.4 statistical software (Cary, North Carolina, USA). Descriptive statistics were used to present continuous results and categorical data was summarized as frequency tables and percentages. Due to the limited sample size (not possible to test whether data are normal distributed), all statistical analyses were done using non-parametric methods. The continues results were subjected to a Kruskal Wallis (KW) multiple comparison analysis and the Dunn's method was used to do individual comparisons between groups. A p-value of less than 0.05 were considered statistically significant.

4.4 Results

4.4.1 Clinical evaluation

The handling quality of both patches were satisfactory with the BPS patches being a bit more slippery than the Glycar® patches. All twelve (12) sheep survived till they were euthanized after a minimum of 180-days. The echocardiographic (2-3 months after implantation and prior to explantation) and macroscopic (after explantation) evaluations of the Glycar® and PBS groups demonstrated no evidence of aneurysm formation, infective endocarditis or calcification. One (1) sheep developed a false aneurysm (3 x 4 mm) on the suture line of the explanted aortic BPS.

4.4.2 Validation of acellularity: 4', 6-Diamidino-2-Phenylindole (DAPI) staining

The DAPI stain demonstrated the absence of intact cells and nuclear material in the Glycar® patches and BPS (100x magnification)(Figure 4.2). However, when overexposed at 400x magnification DNA remnants were visible. The DAPI stain confirmed acellularity in all decellularized scaffolds prior to implantation.

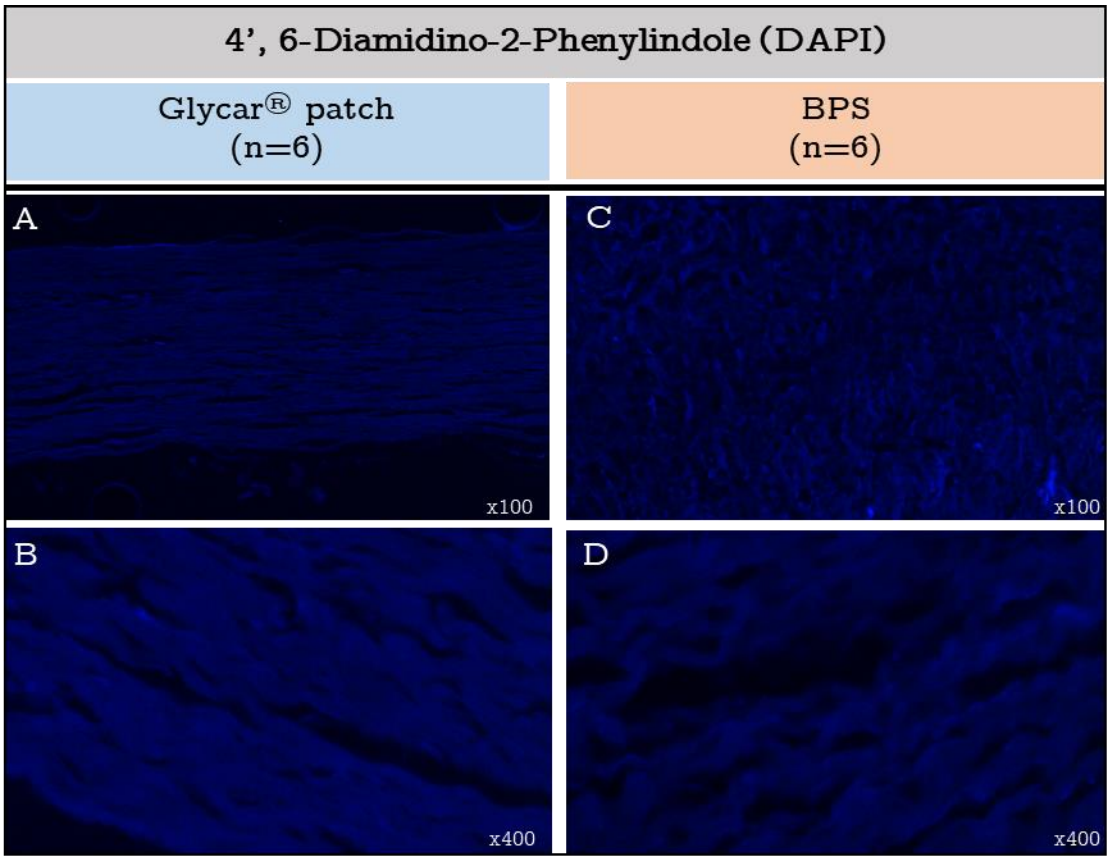

Figure 4.2 DAPI pre-implantation histological stain: Glycar® patches (A, B) and BPS (C, D). (A, C = 100x magnification and B, D = 400x magnification)

4.4.3 Strength evaluation

The TS and YM results are summarized in Table 4.1. The Glycar® group showed a significant decrease in tissue elasticity (YM) form pre-implantation to explantation (p

= 0.0027) but the BPS not (p=0.2228). Therefore, the explanted Glycar® tissue was more elastic and flexible than the pre-implanted tissue. Between groups the YM of the pre-implanted samples of the Glycar® patches were significantly less pliable compared to the BPS (p = 0.001) but the pliability did not differ significantly between groups at explantation (p = 0.0604).

Both the Glycar® patches and decellularized scaffolds demonstrated a significant decrease in tissue strength from pre-implantation to explantation (p = 0.0004 and p = 0.0004, respectively). The pre-implanted as well as the explanted TS of the BPS were significantly less than the Glycar® patches (p = 0.0238; p = 0.0144, respectively).

Table 4.1 Strength analysis of the pre-implanted and explanted pulmonary pericardium: Glycar® patches and BPS

Variable	Glycar® patches (n=6) (Median ± SD)			BPS (n=6) (Median ± SD)		
	Pre-implantation patch	Explant (Pu)	Pre-implant vs. Explant	Pre-implantation scaffold	Explant (Pu)	Pre-implant vs. Explant
YM (MPa)	114.50±40.41	19.58±17.18	p=0.0027*	16.69±9.87	9.81±3.55	p=0.2228
Glycar® vs. BPS				p=0.0001*	p=0.0604	
TS (MPa)	23.02±4.72	6.02±0.96	p=0.0004*	15.02±3.25	3.60±1.28	p=0.0004*
Glycar® vs. BPS				p=0.0238*	p=0.0144*	

*- Significant (p<0.05)(SD = Standard Deviation; Pu = Pulmonary; YM = Youngs modulus; TS = tensile strength)

4.4.4 Structural evaluation

4.4.4.1 Light and electron microscopy

Hematoxylin and eosin (H&E)

The H&E stain demonstrated the presence of cells in the pre-implanted Glycar® patches (Figure 4.3 B) but were absent in the BPS (H). A fibrous encapsulation

developed on the interior and posterior side of the aorta and pulmonary Glycar® explanted patches (C, E). The cellular ingrowth into the Glycar® patch itself were insignificant but within the fibrous encapsulation fibroblast-like cells were present in abundance (D, F). The explanted BPS did not develop this fibrous encapsulation and fibroblast-like cells within the aortic and pulmonary scaffolds were significant (J, L). The collagen of the BPS had a wavier structure of interwoven collagen bundles that were well separated (H) while the collagen of the Glycar® patches demonstrated densely compacted collagen bundles with loss of collagen fiber integrity (B). At 180-day explantation both the aorta and pulmonary BPS were resorbed by the native surrounding tissue but the Glycar® patches not.

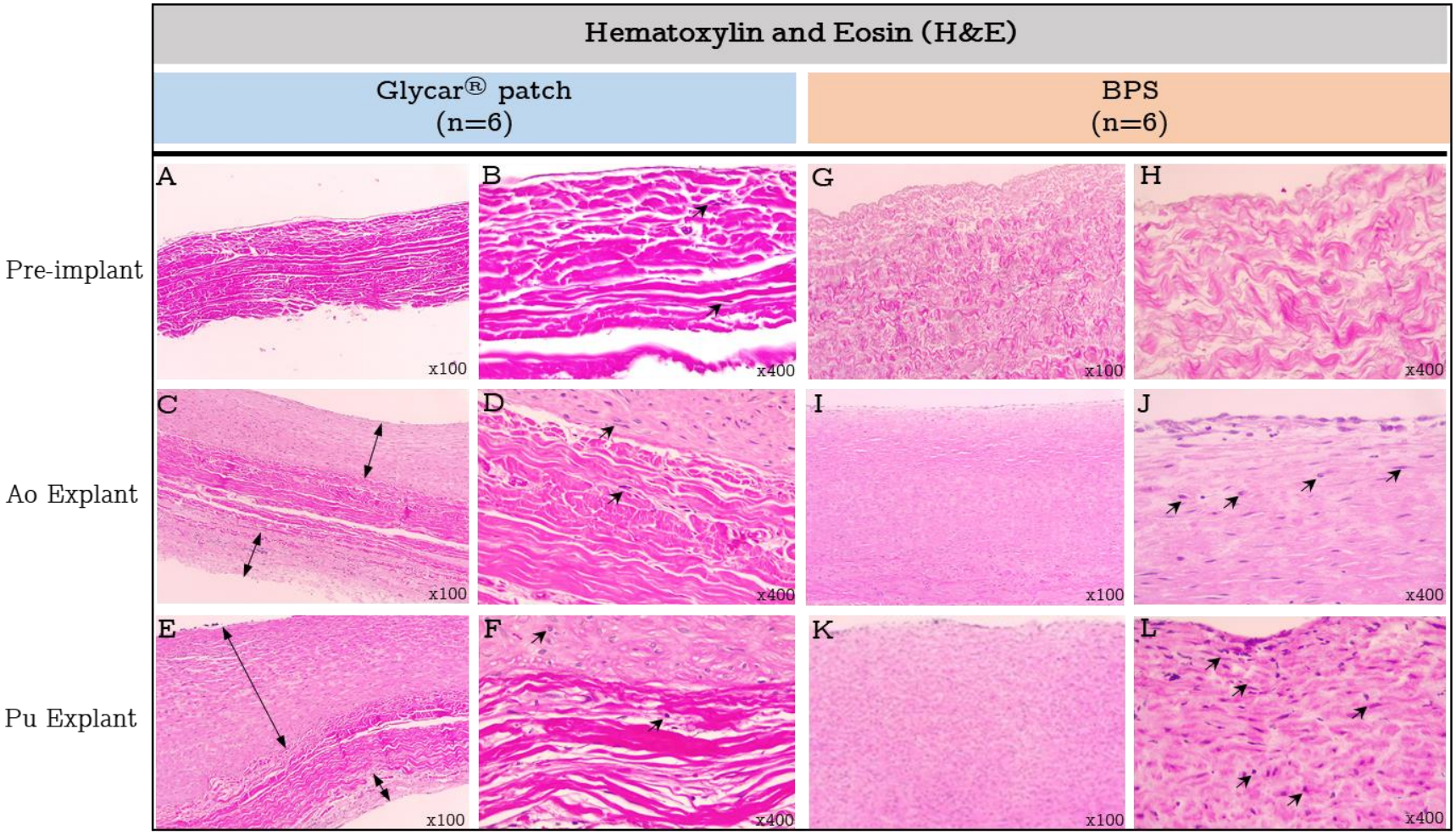

Figure 4.3 H&E of pre-implanted and explanted aortic and pulmonary pericardium: Glycar® patches and BPS. (↑) fibroblast-like cells; (↕) fibrous encapsulation. (A, C, E, G, I, K = 100x magnification and B, D, F, H, J, L = 400x magnification)

Modified Verhoeff von Gieson (EvG)

The EVG histological stain demonstrated elastin (visualized as black fiber strains) in the pre-implanted (Figure 4.4A) and explanted Glycar® pericardial patches (B, C). Elastin were present in the pre-implanted decellularized scaffolds (D) but were not well preserved in both the explanted aorta (E) and pulmonary (F) BPS. Elastin was present in the fibrous encapsulation of the Glycar® patches.

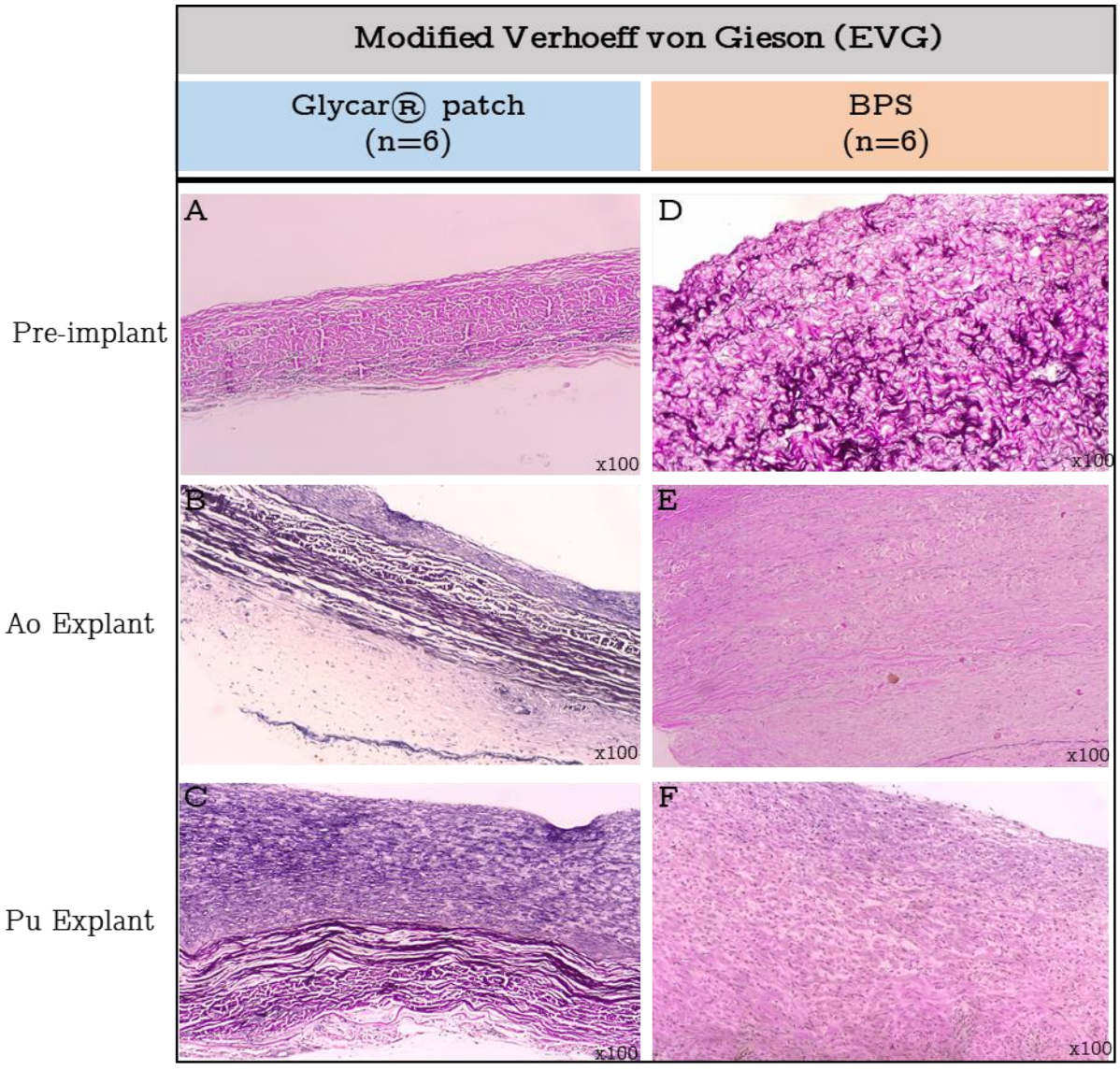

Figure 4.4 EvG histological stain of the pre-implanted and explanted aortic and pulmonary pericardium: Glycar® patches and BPS. (A-F = 100x magnification)

Von Kossa (VK)

The VK stain confirmed the absence of calcification (black calcification deposits) in both the Glycar® and BPS (Figure 4.5).

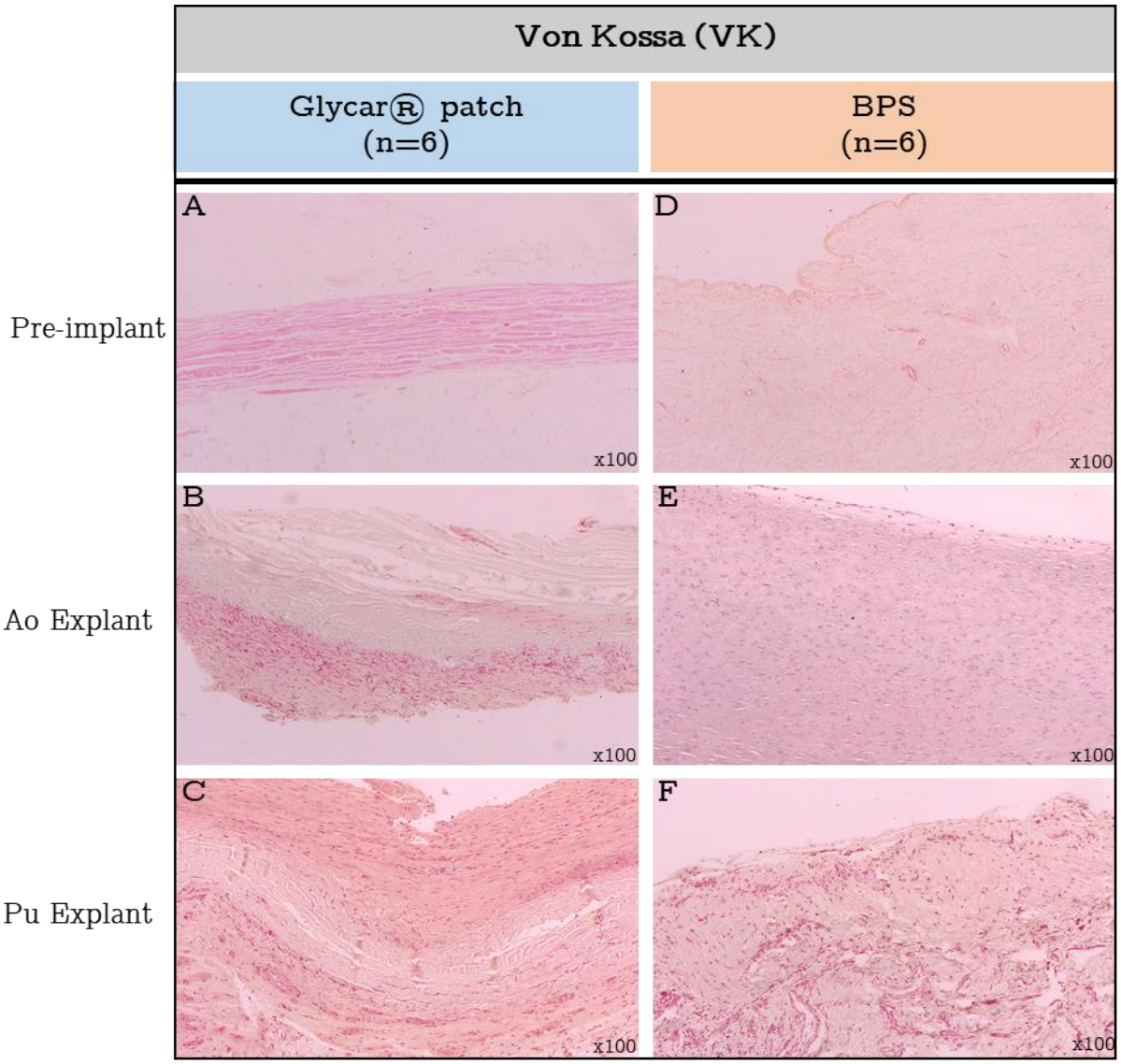

Figure 4.5 VK histological stain of the pre-implanted and explanted aortic and pulmonary pericardium: Glycar® patches and BPS. (A-F = 100x magnification)

Scanning electron microscopy (SEM)

The pre-implant Glycar® micrographs demonstrated scattered endothelial cells in various amounts on the pericardial serosa, some with collapsed extranuclear areas and areas of dehiscence from the basal membrane but with minimal loss of fiber architecture (Figure 4.6A). However, the pre-implanted BPS demonstrated no endothelial cells or basal membrane leaving only the collagen scaffold to remain (D). The explanted pulmonary and aortic Glycar® patches (B, C) and BPS showed a confluent monolayer of endothelial cells (E, F).

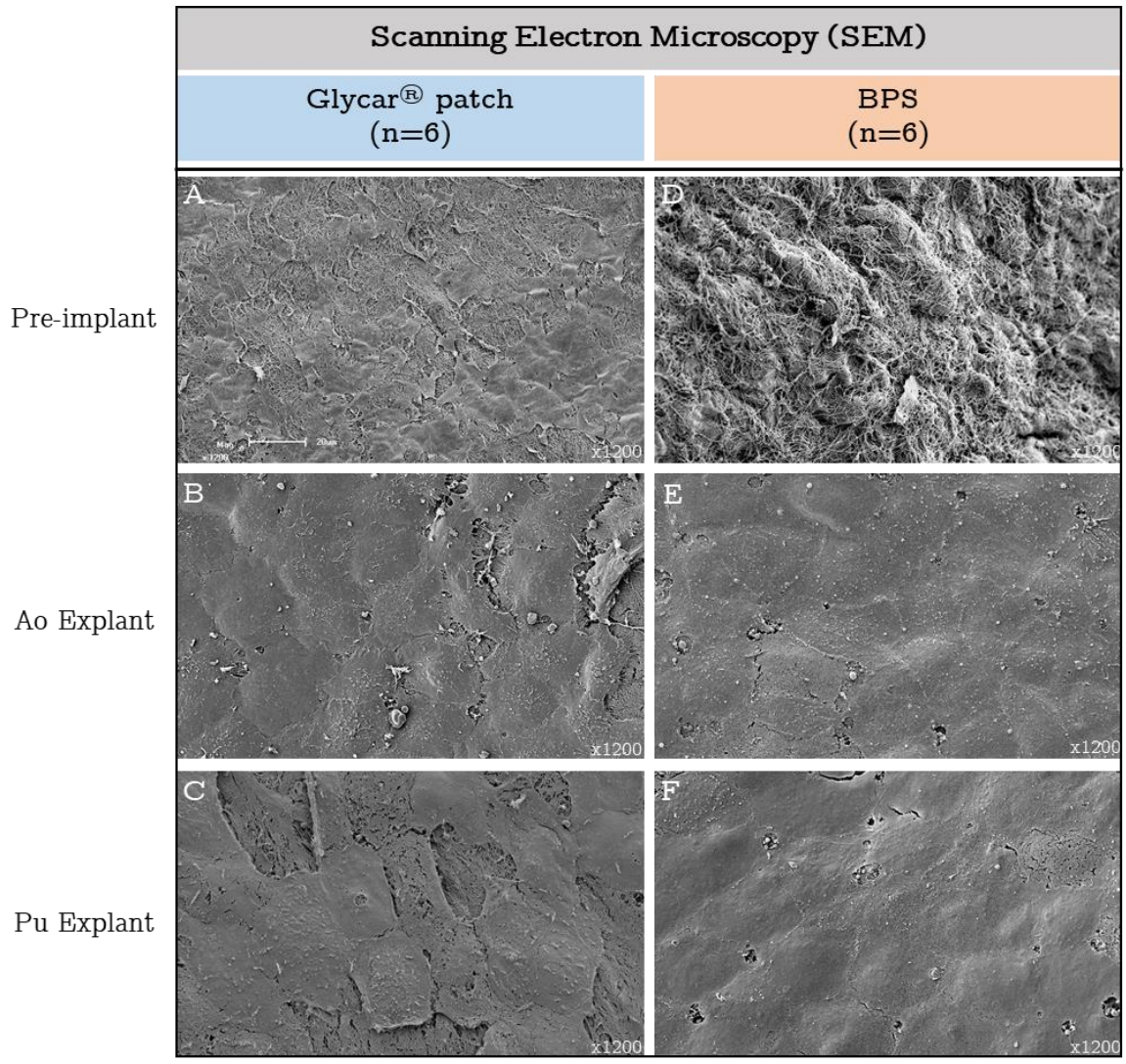

Figure 4.6 SEM of pre-implanted and explanted aorta and pulmonary pericardium: Glycar® patches and BPS. (A-F = 1200x magnification)

Transmission electron microscopy (TEM)

The Glycar® patches and BPS displayed well-defined collagen fibers (Figure 4.7A, B, G, H). Transverse (a) and longitudinal (b) cut fibrils were visible on both the Glycar® patches and BPS (A, G). However, the collagen of the Glycar® patches were densely compacted while the collagen of the BPS was wavier and well-separated (pre-implants and explants). The explanted BPS demonstrated fibroblast-like cells (d) in the aorta and pulmonary explants. However, the explanted Glycar® patches showed pyknotic fibroblast-like cells (e) with loss of membrane integrity (C) and edema (D). The fibroblast-like cells in the BPS demonstrated secretory vacuoles (▲) in which the procollagen is packaged from the Golgi complex (J, K, L). Elastin fibers (↑) were visible in the pre-implantation micrographs of both groups (A, G) but were more abundant in the Glycar® patches.

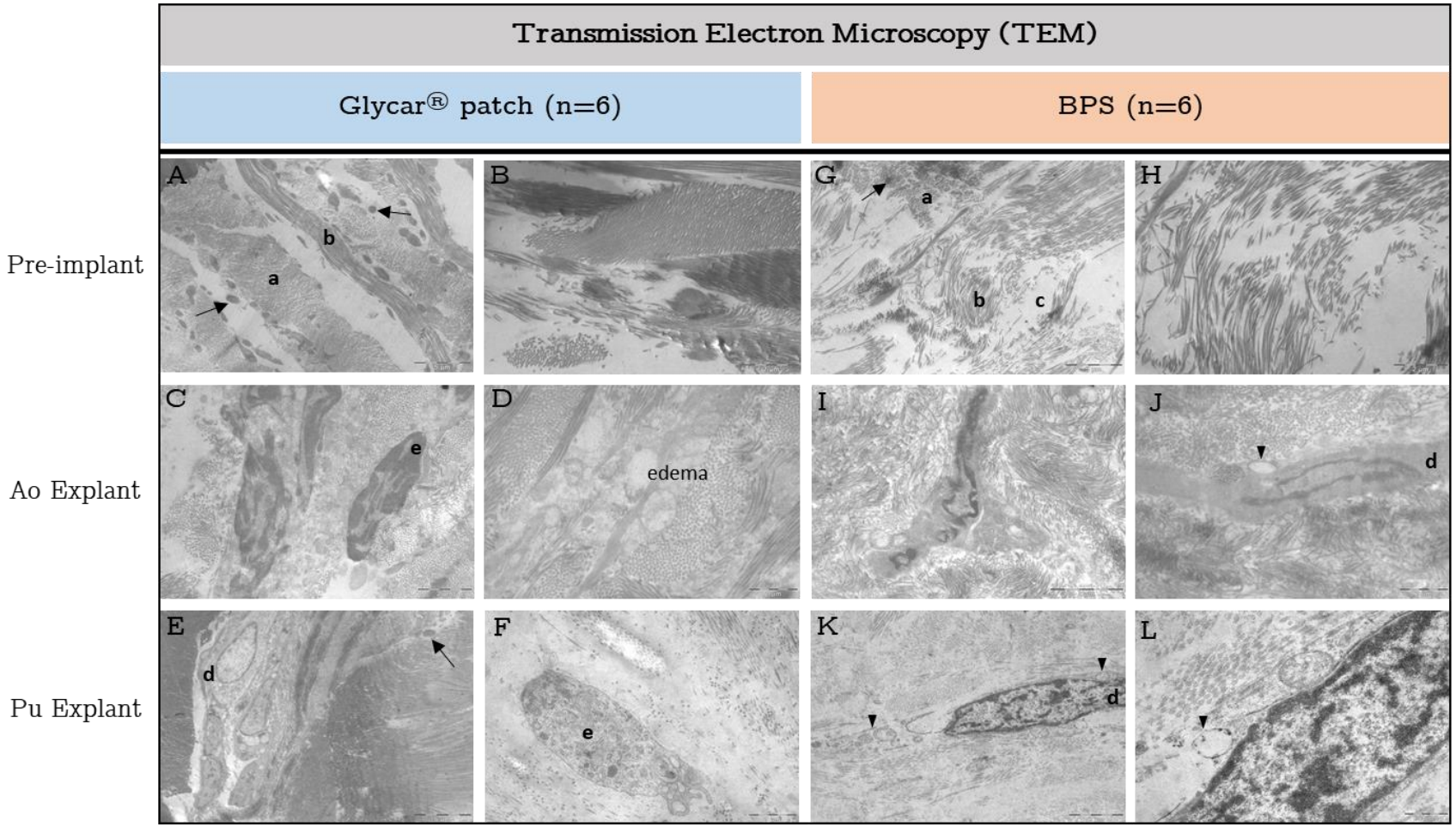

Figure 4.7 TEM of pre-implanted and explanted aorta and pulmonary pericardium: Glycar® patches and BPS. (a) transverse cut fibrils, (b) longitudinal cut fibrils (c) removed cells, (d) cells displaying fibroblast-like properties, (e) devitalized fibroblast-like cells with loss of membrane integrity (↑) elastin fiber and (▲) secretory vacuoles (A, E, G = 3400x; B, C, I, K = 7900x; D, F, H, J =13500x; F = 25000x magnification)

4.4.5 Pericardial thickness

Glycar® patches are selected based on strength and pericardial thickness however, this was not done for the BPS and only a homogenous part of the pericardium was selected and processed. Therefore, when evaluating pericardial thickness each group served as its own control and the groups were not compared.

The total explanted Glycar® patch thickness (patch plus fibrous encapsulation) increased from pre-implantation (0.278 ± 0.074) to explantation (aorta, 0.403 ± 0.085; pulmonary, 0.951±0.116). This could be attributed to the formation of a fibrous encapsulation during implantation. The explanted BPS did not develop this fibrous encapsulation and both the explanted aorta (1.416 ± 0.456 mm) and pulmonary (1.054 ± 0.533 mm) scaffolds did not thicken over time when compared to the pre-implantation thickness (1.452 ± 0.129 mm)(Figure 4.8).

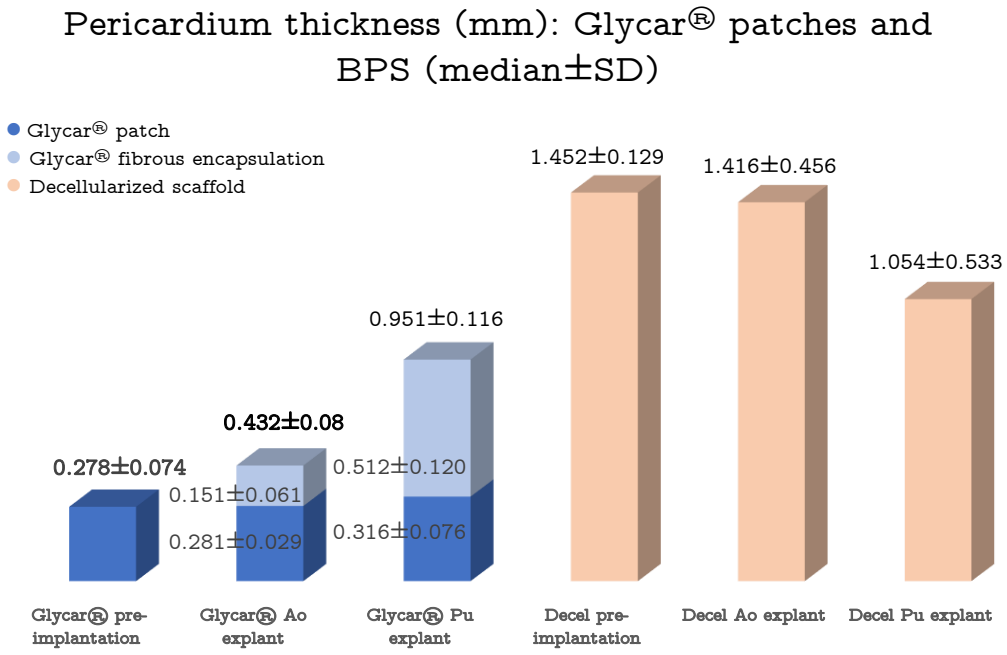

Figure 4.8 Pericardial thickness: Glycar® patches and BPS

4.5 Discussion

This study demonstrated that the structure and tissue integrity of our BPS were well preserved and importantly, is not inferior to the commercially available Glycar® GA-fixed and detoxified bovine pericardium.

This was demonstrated in both the clinical, structural and morphological evaluations of the explanted aorta and pulmonary scaffolds after being implanted in a juvenile ovine model for 180-days. Using our proprietary decellularization process with evidence of synergy as described by Dr Laker, PhD (2019), tissue strength in the BPS were retained, and both the pre-implanted and explanted aorta and pulmonary scaffolds exceeded the minimum strength of the native human ascending aorta (Sommer et al., 2008). Furthermore, no clinical failures, or evidence of aneurysm formation, infective endocarditis or calcification were observed in any of the BPS scaffolds except for the false aneurysm that developed on the suture line of an aortic explant in one (1) sheep. The BPS were not only well preserved but clearly demonstrated recipient cell infiltration with remodeling and reendothelialization.

Different combinations and concentrations of decellularization detergents have different effects on the ECM of a biological scaffold (Bielli et al., 2018). We demonstrated synergy in the decellularization/sterilization process developed at our institution with well retained strength and structure (Dr L Laker, PhD, 2019; Bester et al., 2017) using a combination of 0.5% SDS, 1% SDC and 1% TX.

The DAPI and H&E stain confirmed effective decellularization by detecting no traces of cells or cellular remnants in the pre-implanted aortic and pulmonary patches. Dr L Laker, PhD (2019) confirmed the absence of DNA with a quantitative DNA analysis.

In most commercially available biological scaffolds residual DNA fragments still remains after decellularization with minimal impact on their clinical efficacy (Bielli et al., 2018) but might contribute to calcification and tissue rejection (Mallis et al., 2017).

The mechanical integrity of both the pulmonary Glycar® patches and BPS decreased from baseline to explantation. Importantly, in both groups the strength of the explanted pulmonary patches/scaffolds were still well above the minimum strength of the native human ascending aorta (1.8 ± 0.24 MPa)(Sommer et al., 2008).

As expected, the Glycar® patches were significantly stronger compared to the BPS prior to implantation ($p = 0.0238$). This was also demonstrated in explants ($p = 0.0144$). GA-crosslinking involves a heterogenous crosslinking distribution occurring only on the surface of fibrils and fibers, leading to predominant intermolecular crosslinks that connects collagen molecules (Delgado et al., 2015). On the other hand, decellularization detergents like SDS is known to weaken and change the elastic properties of biological scaffolds. SDS is also an ionic detergent capable of promoting swelling in tissue (Li et al., 2018; Mallis et al., 2017). Mendoza-Novelo and Cauich-Rodriguez, (2009) reported that irreversible swelling in decellularized bovine pericardium was associated with a 50% reduction in tissue strength when compared to native tissue and tissue treated with TX.

At explantation the pericardial patches in both groups were more elastic than their pre-implantation counterparts. The elastic modulus of the BPS was significantly lower compared to the Glycar® patches at implantation ($p = 0.0001$) but did not statistically differ between groups at explantation ($p = 0.0604$). Similar results were reported by Hülsmann et al. (2012) stating that decellularization has allowed for decreases in the elastic modulus relative to GA treatment of bovine pericardium. If

pliability is negatively affected by the processing method it might have a negative effect on patch performance in vivo, as stiffness can affect compliance and can initiate unwanted hemodynamic effects that can contribute to graft failure (Neethling et al., 2018).

The H&E demonstrated that the BPS were resorbed by the native surrounding tissue after 180-days for no remnants of the scaffold was visible at explantation. On the other hand, the Glycar® patches were not resorbed and were clearly visible at explantation. This was also previously described by Badylak & Gilbert, (2009) who stated that 60% of the mass of the ECM is degraded and resorbed between one to three months after in vivo grafting. The fibroblast-like cells (Dohmen et al., 2014) demonstrated numerous secretory vacuoles within the cytoplasm, which are normally associated with the transport of protein complexes synthesized within the rough endoplasmic reticulum, to the Golgi apparatus (Cross and Mercer, 1993). Moreover, many of these vacuoles might play an integral role in the secretion of procollagen from the cell (Canty & Kadler, 2005). These collagen-containing vacuoles might be an important indicator of young fibroblast-like cells actively involved in the production of new collagen fibrils and bundles.

Vast differences were demonstrated between the collagen of the pre-implanted and explanted Glycar® patches and BPS. The collagen of the BPS had a wave-like pattern of interwoven collagen bundles that were well-separated. On the other hand, the collagen of the Glycar® patches demonstrated loss of collagen fiber integrity, making the collagen densely compacted (Wong et al, 2016). The collagen bundles of the Glycar® patches did not reorganize from pre-implantation to explantation after 180-days.

Despite advantages in strength GA-treated pericardium has a poor regenerative ability in vivo as a result of tissue crosslinking and the cytotoxic effects that prevents host cell infiltration, migration and proliferation (Remi et al., 2011; Huang-Lee et al., 1990). Recipient cell infiltration was insignificant in the Glycar® patch. This could be contributed to the dense/compact collagen structure. If the pores within the patch are too small cell migration is limited, resulting in a cellular capsule formation around the edges of the scaffold. Maintaining the balance between optimal pore size for cell migration and specific surface area for cell attachment is essential (Murphy & O'Brien, 2010). The collagen structure of the BPS was less dense/compact with a much wavier and well-separated appearance which provided a pore size optimal for host cell infiltration. Furthermore, compared to GA-treated pericardium, BPS are non-toxic and therefore promotes cellular ingrowth. Elastin was better preserved from pre-implantation to explantation in the Glycar® patches compared to the BPS. The amount of elastin decreased from pre-implantation to explantation in both the aorta and pulmonary BPS.

SEM of the BPS demonstrated a well-preserved collagen fiber network prior to implantation and at explantation both the Glycar® and BPS demonstrated a confluent monolayer of endothelial cell coverage. In contrast, the pre-implanted aortic and pulmonary Glycar® patches demonstrated large areas of partial endothelial coverage, some with collapsed extranuclear areas and areas of dehiscence from the basal membrane but with minimal loss of fiber architecture. These cells were severely dehydrated.

TEM demonstrated fibroblast-like cells with loss of membrane integrity and the presence of edema on the explanted Glycar® patches. In contrast, the BPS showed recellularization with large numbers of infiltrating fibroblast-like cells throughout the ECM. Umashankar et al., 2012 reported the total lack of host tissue

incorporation in GA-treated bovine pericardium compared to excellent host fibroblast incorporation within the implanted decellularized bovine pericardium. This could be attributed to GA-treated bovine pericardium being resistant to collagenase, a major enzyme in the body responsible for ECM remodeling.

Of concern is that the Glycar® patches demonstrated cells in abundance within the fibrous encapsulation that separated the implant from the host tissue. Although the residual aldehydes of GA crosslinking reduces bacterial contamination it also limits host cell infiltration (Jayakrishnan & Jameela, 1996). A fibrous encapsulation developed on both the explanted aortic and pulmonary Glycar® patches. This encapsulation can be the result of a chronic inflammatory response as evidenced by the early dense accumulation of mononuclear cells and the prolonged presence of macrophages, predominant M1 macrophages and increased proinflammatory cytokine release which typically represents a foreign body response seen in surgical implants of many types (Ketchedjian et al., 2005; Delgado et al., 2015). However, this mononuclear response was not seen in the explanted aorta or pulmonary Glycar® patches. Although the VK showed no signs of calcification this fibrous encapsulation might act as the precursor for calcification formation.

More importantly the fibrous encapsulation also contributed to patch thickening of both the explanted aorta and pulmonary patches. The increase in patch thickness could be detrimental when this Glycar® tissue is used for the construction of heart valve leaflets. The pre-implanted Glycar® patch thickness (0.281 ± 0.029 mm) compared well with the manufacturer's description of 0.2 - 0.4 mm but thickened when implanted. Similar results were reported by (Neethling et al., 2014). The pre-implantation BPS (1,452 ± 0.129 mm) were thicker than the pre-implanted Glycar® patch (0.278 ± 0.074). The SDS used during the decellularization process can bind to collagen fibers and glycosaminoglycans (GAGs) and by removing the GAGs it can

promote swelling of the tissue, caused by the potential break in hydrogen bonds of the collagen fibers (Mallis et al., 2017; Remi et al., 2011; Courtman et al., 1994). The explanted BPS did not thicken over time and both the aortic (1.416 ± 0.456 mm) and pulmonary (1.054 ± 0.533 mm) explants were thinner than their pre-implantation counterpart (1.452 ± 0.129 mm).

4.6 Conclusion

GA-fixed bovine pericardial patches remain the industry standard in cardiovascular surgery despite numerous reports of degradation, thickening, inflammation, calcification and the lack of in vivo tissue remodeling. Decellularization provides us the opportunity to attenuate some of these immune mediated processes. As decellularization methods might weaken tissue it is important to demonstrate structural integrity of decellularized scaffolds in large animal models before human implants is undertaken. In this study the impact of our decellularization process was evaluated and compared to the Glycar® patch in a juvenile ovine model, expecting in vivo recellularization and tissue remodeling.

The BPS demonstrated adequate strength prior to implantation. Clinically, all scaffolds performed well with no evidence of aneurysm formation, calcification or disintegration at 180-days. The explanted aortic and pulmonary scaffolds demonstrated recellularization, tissue remodeling, resistance to calcification, reendothelialization and strength in excess of the native human aorta of 1.8 ± 0.24 MPa (Sommer et al., 2008). Histology demonstrated a wave-like appearance of well-separated collagen fibers that provided pore sizes adequate to promote fibroblast infiltration with new collagen formation after an implantation time of 180-days.

Therefore, BPS should be considered as an alternative to GA-fixed pericardial patches for it demonstrated excellent remodeling and growth potential. This could be an ideal scaffold for younger patients.

Limitations

Data provided by the juvenile sheep model cannot be unconditionally applied to human patients. Measuring pericardial thickness prior to processing was not available for the Glycar® patches. Due to technical limitations, tissue implanted in the descending aorta did not allow a large enough tissue sample upon explantation for TS/YM determination.

For future studies we recommend that immunohistochemistry be added to the list of analyses to describe cell types and immunological processes involved.

References

Badylak, S.F., & Gilbert, T.W. 2009. Immune response to biologic scaffold materials. Seminars of Immunology. *Seminars in Immunology*, 20(2): 109–116.

Bankcroft, J.D. and Cook, H.C. 1994. Manual of histological techniques and their diagnostic application. Published by Churchill Livingstone.

Baucia, J.A., Leal Neto, R.M., Rogero, J.R. & do Nascimento, N. 2006. Anti-calcifying treatment of glutaraldehyde fixed bovine pericardium: comparisons and evaluation of possible synergic effects. *Brazilian Journal of Cardiovascular Surgery*, 21(2):180-187.

Bester, D., Smit, F.E., van den Heever, J.J., Botes, L., Dohmen P. M. C. E. Detoxification and stabilization of implantable or transplantable biological material. Patent 16702008.0-1455, EU, 2017.

Bielli, A., Bernardini, R., Varvaras, D., Rossi, P., Di Blasi, G., Petrella, G., Buonomo,

O.C., Mattei, M. & Orlandi, A. 2018. Characterization of a new decellularized bovine pericardial biological mesh: Structural and mechanical properties. *Journal of the Mechanical Behavior of Biomedical Materials*, 78:420–426.

Canty, E.G. & Kadler, K.E. 2005. Procollagen trafficking, processing and fibrillogenesis. *Journal of Cell Science*, 118(7):1341-1353.

Carpentier, A., Lemaigre, G., Robert, L., Carpentier, S. & Dubost, C. 1969. Biological factors affecting long-term results of valvular heterografts. *The Journal of Thoracic and Cardiovascular Surgery*, 58(4): 467–483.

Cohen, S., Magal, S., Yakov, I., Sirabella, E., Bitman, A., Groisman, G. & Lotan, C. 2018. Tissue processing techniques for fabrication of covered stents for small-diameter vascular intervention. *Acta Biomaterialia*, 65: 248–258.

Coito, A.J., Kupiec-Weglinski, J.W. 1996. Extracellular matrix proteins: bystanders or active participants in the allograft rejection cascade? *Annuals of Transplantation* 1:14-18.

Collatusso, C., Roderjan, J.G., Vieira, E.D., Myague, N.I., de Noronha, L. da Costa, F.D.A. 2011. Decellularization as an anticalcification method in stentless bovine pericardium valve prosthesis: a study in sheep. The Brazilian Journal of Cardiovascular Surgery, 26(3): 419–426.

Courtman, D.W., Pereira, C.A., Kashef, V., McComb, D., Lee, J.M. & Wilson, G.J. 1994. Development of a pericardial acellular matrix biomaterial: Biochemical and mechanical effects of cell extraction. *Journal of Biomedical Materials Research*, 28(6): 655–666.

Crapo, P.M., Gilbert, T.W. & Badylak, D.V.M. 2011. An overview of tissue and whole organ decellularization processes. *Biomaterials*, 32(12): 3233–3243.

Cross, P.C, Mercer, K.L. 1993. Cell and Ultrastructure. WH Freeman publishers, 2nd edition. pages 70-75.

Dahm M., Lyman, W.D., Schwell, A.B., Factor, S.M., Frater, R.W. 1990. Immunogenicity of glutaraldehyde-tanned bovine pericardium. *Journal of Thoracic and Cardiovascular Surgery*, 99:1082-1090.

Delgado, L.M., Bayon, Y., Pandit, A. & Zeugolis, D.I. 2015. To crosslink or not to crosslink? Crosslinking associated foreign body response of collagen-based devices. *Tissue Engineering - Part B: Reviews*, 21(3): 298–313.

Dohmen, P.M., da Costa, F.D.A., Lopes, S.V., Vilani, R., Bloch, O. & Konertz, W. 2014. Successful implantation of a decellularized equine pericardial patch into the systemic circulation. *Medical Science Monitor Basic Research*, 20: 1–8.

Gilbert, T.W., Sellaro, T.L. & Badylak, S.F. 2006. Decellularization of tissues and organs. *Biomaterials*, 27(19): 3675–3683.

Glycar South Africa. n.d. Glycar pericardial patch with Aldecap. Retreived from http://glycar.co.za/downloads/Glycar_Patch_Brochure.pdf [accessed 30 March 2019].

Hülsmann, J., Grün, K., El Amouri, S., Barth, M., Hornung, K., Holzfuß, C., Lichtenberg, A., Akhyari, P. 2012. Transplantation material bovine pericardium: biomechanical and immunogenic characteristics after decellularization vs. glutaraldehyde-fixing. *Xenotransplantation*, 19(5): 286-297.

Huang-Lee, L.L., Cheung, D.T., Nimni, M.E. 1990. Biochemical changes and cytotoxicity associated with the degradation of polymeric glutaraldehyde derived crosslinks. *Journal of Biomaterials Research*, 24(9): 1185-1201.

Ionescu, M.I., Tandon, A.P., Mary, D.A. & Abid, A. 1977. Heart valve replacement with the Ionescu-Shiley pericardial xenograft. *The Journal of Thoracic and Cardiovascular Surgery*, 73(1): 31–42.

Iop, L., Palmosi, T., Sasso, E.D. & Gerosa, G. 2018. Bioengineered tissue solutions for repair, correction and reconstruction in cardiovascular surgery. *Journal of Thoracic Disease*, 10(Suppl 20): S2390–S2411.

Jayakrishnan, A. & Jameela, S.R. 1996. Glutaraldehyde as a fixative in bioprostheses

and drug delivery matrices. *Biomaterials*, 17(5): 471–484.

Ketchedjian, A., Jones, A.L., Krueger, P., Robinson, E., Crouch, K., Wolfinbarger, L. & Hopkins, R. 2005. Recellularization of decellularized allograft scaffolds in ovine great vessel reconstructions. *Annals of Thoracic Surgery*, 79(3): 888–896.

Laker L. The evaluation of a novel decellularization and sterilization process on bovine pericardial tissue. PhD Thesis, University of the Free State, South Africa, 2019.

Li, N., Li, Y., Gong, D., Xia, C., Liu, X. & Xu, Z. 2018. Efficient decellularization for bovine pericardium with extracellular matrix preservation and good biocompatibility. *Interactive CardioVascular and Thoracic Surgery*, 26(January): 768–776.

Mallis, P., Michalopoulos, E., Dimitriou, C., Kostomitsopoulos, N. & Stavropoulos-Giokas, C. 2017. Histological and biomechanical characterization of decellularized porcine pericardium as a potential scaffold for tissue engineering applications. *Bio-Medical Materials and Engineering*, 28(5): 477–488.

Mendoza-Novelo, B. & Cauich-Rodríguez, J. V. 2009. The effect of surfactants, crosslinking agents and L-cysteine on the stabilization and mechanical properties of bovine pericardium. *Journal of Applied Biomaterials and Biomechanics*, 7(2): 123–131.

Murphy, C.M. & O'Brien, F.J. 2010. Understanding the effect of mean pore size on cell activity in collagen-glycosaminoglycan scaffolds. *Cell Adhesion and Migration*, 4(3): 377–381.

Neethling, W.M.L., Brizard, C., Firth, L. & Glancy, R. 2014. Biostability, durability and calcification of cryopreserved human pericardium after rapid glutaraldehyde-stabilization versus multistep ADAPT® treatment in a subcutaneous rat model. *European Journal of Cardiothoracic Surgery*, 45(4): 110–117.

Neethling, W.M.L., Puls, K. & Rea, A. 2018. Comparison of physical and biological properties of CardioCel® with commonly used bioscaffolds. *Interactive Cardiovascular and Thoracic Surgery*, 26(6): 985–992.

Oswal, D., Korossis, S., Mirsadraee, S., Wilcox, H.E., Watterson, K., Fisher, J. & Ingham, E. 2007. Biomechanical characterization of decellularized and crosslinked bovine pericardium. *Journal of Heart Valve Disease*, 16(2): 165–174.

Remi, E., Khelil, N., Di, I., Roques, C., Ba, M., Medjahed-Hamidi, F., Chaubet, F., Letourneur, D., Lansac, E. & Meddahi-Pelle, A. 2011. Pericardial Processing: Challenges, Outcomes and Future Prospects. *Biomaterials Science and Engineering*. Retrieved from: vailable online: http://www.intechopen.com/books/biomaterials-science-and-engineering/pericardial-processing-challenges-outcomes-and-future-prospects. [accessed 20 November 2018].

Salameh, A., Greimann, W., Vondrys, D. & Kostelka, M. 2018. Calcification or Not. This Is the Question. A 1-year study of bovine pericardial vascular patches (CardioCel) in minipigs. *Seminars in Thoracic and Cardiovascular Surgery*, 30(1): 54–59.

Sasaki, N. & Odajima, S. 1996. Stress-strain curve and Young's modulus of a collagen molecule as determined by the X-ray diffraction technique. *Journal of Biomechanics*, 29(5): 655–658.

Schmidt, C.E. & Baier, J.M. 2000. Acellular vascular tissues: natural biomaterials for tissue repair and tissue engineering. *Biomaterials*, 21(22): 2215–31.

Sommer, G., Gasser, T.C., Regitnig, P., Auer, M. & Holzapfel, G.A. 2008. Dissection properties of the human aortic media: An experimental study. *Journal of Biomechanical Engineering*, 130(2): 1-13.

Thubrikar, M.J., Deck, J.D., Aouad, J., Nolan, S.P. 1983. Role of mechanical stress in calcification of aortic bioprosthetic valves. *Journal of Thoracic Cardiovascular Surgery*, 86:115–125.

Umashankar, P.R., Mohanan, P. V & Kumari, T. V. 2012. Glutaraldehyde treatment elicits toxic response compared to decellularization in bovine pericardium. *Toxicology International*, 19(1): 51–58.

Wong, M.L., Wong, J.L., Vapniarsky, N., Griffiths, L. G. 2016. In vivo xenogeneic scaffold fate is determined by residual antigenicity and extracellular matrix preservation. *Biomaterials*, 92: 1-12.

Chapter 5 - Article 2

Comparing the impact of processing techniques between Glycar® and CardioCel® bovine pericardial patches after 180-days implantation in a juvenile ovine model

Botes L[1], Laker L[2], Dohmen PM[2&3], van den Heever JJ[2], Jordaan CJ[2], Goedhals J[4], Smit FE[2]

[1]*Department of Health Sciences, Central University of Technology, Free State, Bloemfontein, South Africa*

[2]*Department of Cardiothoracic Surgery, University of the Free State, Bloemfontein, South Africa*

[3]*Department of Cardiac Surgery, Heart Centre Rostock, University of Rostock, Germany*

[4]*Department of Anatomical Pathology, University of the Free State, Bloemfontein, South Africa*

Abstract

Introduction: Glutaraldehyde (GA) remains the industry standard to crosslink pericardium but reports of tissue degeneration and calcification motivated tissue engineers to develop alternative processing methods to improve functionality and longevity. Detoxification of GA cytotoxicity can reduce calcification but adding a decellularization process can prevent calcification and offer recellularization with remodeling potential. This study compares the impact of processing prior to implantation and the in vivo performance of a recently commercialized decellularized, GA-fixed bovine pericardial patch with anticalcification treatment, CardioCel®; with an established commercialized GA-fixated, and detoxified bovine patch (Glycar®) in a juvenile ovine model. Methods The impact of the processing methods on tissue strength and morphology was assessed prior to implantation. Glycar® patches (Group 1) were implanted in the descending aorta and main pulmonary artery of six (6) sheep and CardioCel® patches (Group 2) were implanted in six (6) sheep at the same anatomical locations. The pericardial implants were clinically evaluated during implantation using echocardiography. After 180-days the mechanical and morphological integrity of the explanted patches were evaluated and compared. Results: The tensile strength (TS) and Youngs Modulus (YM) of the pre-implanted pulmonary patches were comparable between group 1 and 2 with no statistically significant differences. Group 1 demonstrated devitalized cells after processing and acellularity was confirmed in Group 2. The collagen in Group 1 was densely compacted while Group 2 demonstrated wavier well-separated collagen bundles. The clinical performance of both groups was excellent, and echocardiography confirmed the absence of aneurysms, calcification and degeneration. The TS ($p = 0.4432$) and YM ($p = 0.3720$) of the explanted pulmonary pericardium were comparable between groups and above the minimum native human ascending aorta strength (1.8 ± 0.24 MPa). In both groups, calcification was absent in the explanted aorta and pulmonary arteries. The collagen bundles of Group 1 were compact and dense at explantation and the collagen in Group 2 were less dense with a wavier appearance. Although limited Group 2 demonstrated more fibroblast-like cell infiltration with secretory vacuoles which can promote procollagen secretion. Both groups developed a fibrous encapsulation that contributed to patch thickening. Conclusion: The structural integrity and pliability between the two (2) groups were comparable, both developed a fibrous encapsulation and no evidence of calcification was demonstrated. Host cell infiltration was limited in both groups, but Group 2 showed more potential. Extending the 180-day implantation time might reveal more distinguishing differences between the two (2) groups.

Keywords: Pericardium, Bovine, Glutaraldehyde, Decellularization, Calcification, Tensile Strength, Recellularization

5.1 Introduction

Pericardial tissue is widely used as a biomaterial for cardiovascular implants, such as heart-valve substitutes and patch materials (Lee et al., 2011). Over the years the use of glutaraldehyde (GA) has become the method of choice to crosslink pericardial tissue. GA-fixation increases tissue strength and durability by providing stability to fibers, it reduces antigenicity and also acts as a sterilization agent (Cohen et al., 2018; Prabhu et al., 2017; Collatusso et al., 2011). However, several limitations have been associated with GA-fixed pericardium like degeneration and calcification causing the material to become rigid and shrink and ultimately contributes to long-term failure (Bell et al., 2019; Remi et al., 2011). Failure of these substitutes increases the probability of reoperation and associated risks. Any surgical strategy would want to employ the most compatible and durable tissue available. Therefore, focus shifted to tissue engineering to develop a more suitable bio-patch.

With the use of physical, chemical and enzymatic methods an extracellular matrix patch is produced with lower antigenicity in which the three dimensional structure is adequately preserved to promote remodeling once implanted (Mallis et al., 2017; Tran et al., 2016). CardioCel® (Admedus Regen Pty Ltd, Perth, Western Australia) is a biological patch manufactured from bovine spongiform encephalopathy-free pericardium that obtained Food and Drug Administration (FDA) approval in 2014 (Patent K130872). The patch is subjected to an anitcalcification tissue-engineered process called ADAPT TEP. ADAPT TEP reduces cytotoxicity by removing lipids, cells and cellular remnants, nucleic acids (DNA, RNA) and α-Gal (galactosyl) epitopes making the patch less susceptible to calcification. Crosslinking of collagen fibers is achieved with an ultra-low concentration of monomeric GA (0.05%) and toxicity is eliminated by chemical detoxification. The crosslinking strengthens the patch and preserves the mechanical properties of the extracellular

matrix. The patch is sterilized using propylene oxide (Bell et al., 2019; Prabhu et al., 2017; Neethling et al., 2013).

Current opinion favors the development of tissue engineered decellularized bovine pericardial patches, however, excellent results have been achieved with over 10 000 implants without a single adverse event reported (personal communication Dr RWM Frater) using the Glycar® patch developed with EnCap™ technology. With this study, we evaluated and compared the in vivo performance of a tissue-engineered decellularized patch (CardioCel®) and GA-fixated and detoxified bovine pericardial patch (Glycar®) after 180-days as a cardiovascular substitute in the aortic and pulmonary positions of an ovine model. The mechanical and morphological integrity, calcification, remodeling ability and thickness of the pericardial groups were evaluated and compared prior to implantation and after explantation.

5.2 Materials and Methods

The study was completed at the RWM Frater Cardiovascular Research Centre, University of the Free State (UFS), South Africa and ethical approval was obtained from the Animal Ethics Committee of the UFS (ETOVS Number: UFS-AED2015/0081, Appendix A1).

Bovine Glycar® pericardial patch and CardioCel® bovine pericardial patch

For the detailed processing method of the Glycar® patch refer to section 4.2, Materials and methods, Article 1, Chapter 4.

The CardioCel® patches were purchased from Admedus Innovative Health Solutions, Malaga, Western Australia.

5.2.1 Study design and layout

A prospective analytical cohort study was conducted. The clinical and mechanical integrity [tensile strength (TS) and Young's modulus (YM)] tissue morphology [hematoxylin and eosin (H&E), modified Verhoeff's von Gieson (EvG), Von Kossa (VK) histological stains, scanning electron microscopy (SEM) and transmission electron microscopy (TEM)] and thickness were evaluated in both groups prior to implantation and after explantation (Figure 5.1).

Bovine Glycar® and CardioCel® patches were implanted into twelve (12) juvenile Dorper Wether sheep. After being taken from the preservation container intraoperatively, the patches did not require any additional preparation prior to implantation.

Six (6) sheep received two (2) Glycar® pericardial patches (Group 1), one implanted in the descending aortic arch and the other in the main pulmonary artery. Another six (6) sheep (Group 2) received CardioCel® pericardial patches in the same surgical locations. Samples of each pericardial patch were taken prior to surgical implantation to evaluate processing impact and to establish pre-implantation values. This process was repeated when the patches were explanted after 180-days. Intraoperatively the functionality of the patches was evaluated using echocardiography.

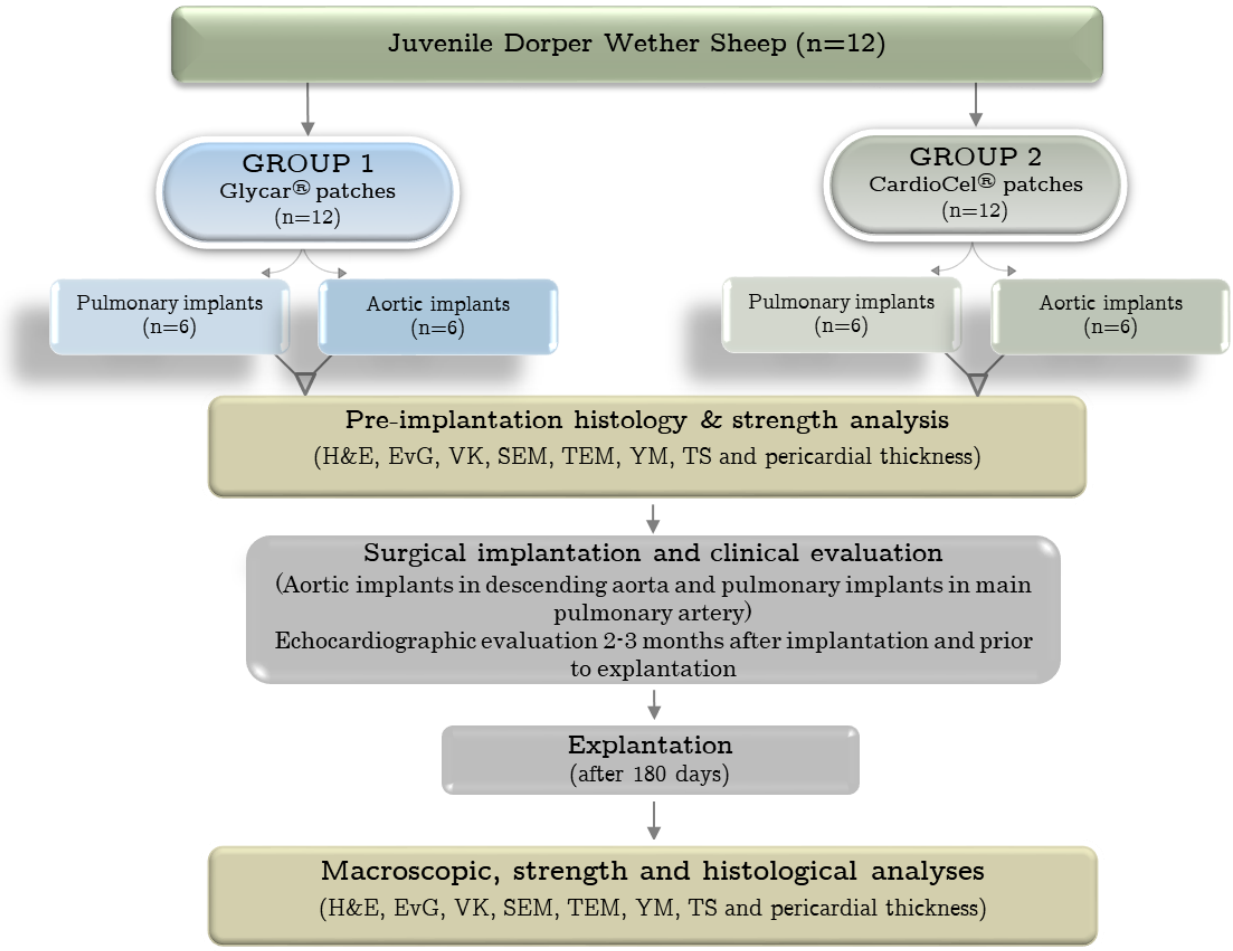

Figure 5.1 Study layout: Glycar® and CardioCel® bovine pericardial patches (H&E = hematoxylin and eosin; EvG = modified Verhoeff's von Gieson; VK = Von Kossa; YM = Young's Modulus; TEM = transmission electron microscopy; SEM = scanning electron microscopy

5.2.2 Surgical protocol

A mini thoracotomy was performed on twelve (12) recipient sheep (age 6-12 months; mean weight 30.25 ± 5.82kg). Refer to section 4.2.2 of Article 1 for a detailed description of the surgical protocol.

5.2.3 Laboratory analysis

Analysis were performed on both the aorta and pulmonary explants of the Glycar® and CardioCel® patches. However, strength analysis (YM and TS) was only performed on the pulmonary explants in both groups due to limited tissue available.

5.2.3.1 Clinical evaluation

Echocardiographic examinations were performed 2-3 months after implantation and prior to explantation to evaluate the patches for calcification, infective endocarditis and aneurysm formation.

5.2.3.2 Validation of acellularity

4', 6-Diamidino-2-Phenylindole (DAPI) staining

The DAPI stains were performed by the Cardiovascular Research Unit of the University of Cape Town according to their standard operating procedure. Refer to section 4.2.3.2, Validation of acellularity, Article 1, Chapter 4 for a detailed description of the DAPI method.

5.2.3.3 Strength Evaluation

Tensile strength (TS) and Young's Modulus (YM)

Refer to section 4.2.3.3, Strength evaluation, Article 1, Chapter 4 for detailed TS and YM methods.

5.2.4.4 Structural Evaluation

Light Microscopy and electron microscopy

Refer to section 4.2.3.4, Structural evaluation, Article 1, Chapter 4 for detailed light and electron microscopy (SEM and TEM) methods.

5.2.4.5 Pericardial thickness

The measurement of pericardial thickness is described in section 4.2.3.5, Pericardial thickness, Article 1, Chapter 4.

5.3 Statistical analysis

Refer to section 4.3, Statistical analysis, Article 1, Chapter 4 for statistical methods used.

5.4 Results

5.4.1 Clinical evaluation

The handling quality of both patches were satisfactory. All twelve (12) sheep survived till they were euthanized after a minimum period of 180-days. The echocardiographic and macroscopic (after explantation) evaluation showed no evidence of calcification, aneurysm formation or infective endocarditis.

5.4.2 Validation of acellularity: 4', 6-Diamidino-2-Phenylindole (DAPI) staining

The DAPI stain demonstrated no evidence of intact cells in both the Glycar® patches or the CardioCel® patches prior to implantation (Figure 5.2).

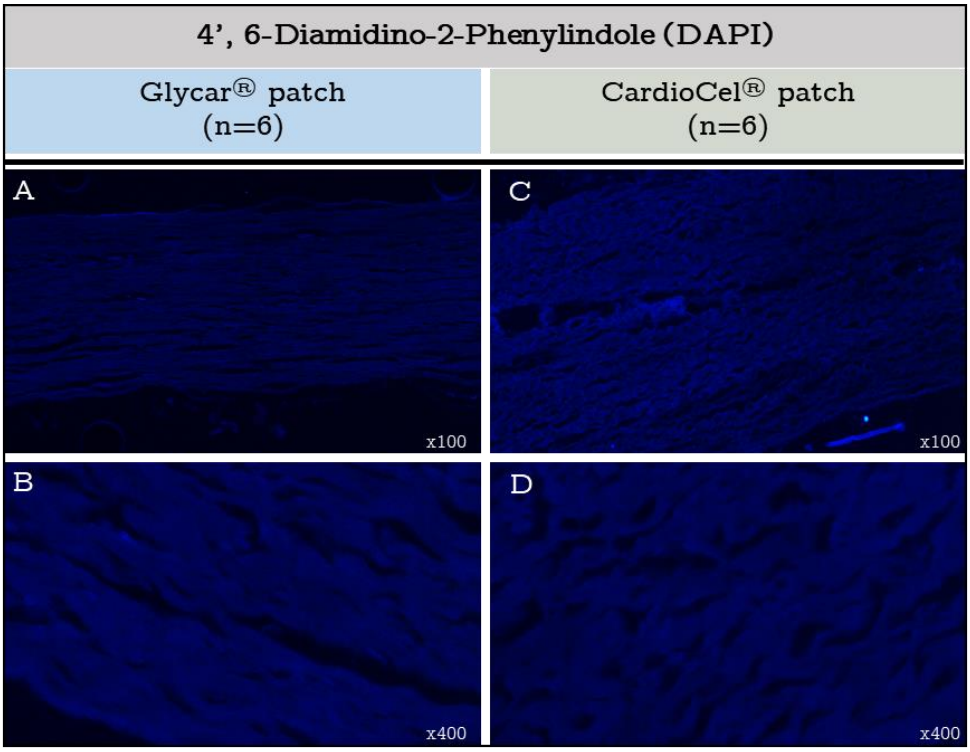

Figure 5.2 DAPI pre-implantation histological stain: Glycar® (A, B) patches and CardioCel® patches (C, D). (A, C = 100x magnification and B, D = 400x magnification)

5.4.3 Strength evaluation

The mechanical properties of the Glycar® patches and CardioCel® patches are summarized in Table 5.1. In both groups, the YM (Glycar®, p=0.0027; CardioCel®, p=0.0040) and TS (Glycar®, p=0.0004; CardioCel®, 0.0059) significantly decreased from pre-implantation to explantation. The decrease in YM implies that the elastic properties of the explanted pericardial tissue increased making the explanted pericardium more flexible and pliable in comparison to their pre-implantation counterparts.

The TS and YM of the pre-implanted and explanted patches were comparable between the Glycar® and CardioCel® groups and did not differ significantly in strength or elasticity (Table 5.1).

Table 5.1 Strength analysis of pre-implanted and explanted pulmonary pericardium: Glycar® and CardioCel® patches

Variable	Glycar® patches (n=6) (Median ± SD)			CardioCel® patches (n=6) (Median ± SD)		
	Pre-implantation patch	Explant (Pu)	Pre-implant vs. Explant	Pre-implantation patch	Explant (Pu)	Pre-implant vs. Explant
YM (MPa)	114.50±40.41	19.58±17.18	p=0.0027*	63.97±18.43	12.22±8.04	p=0.0040*
Glycar® vs CardioCel®				p=0.1167	p=0.3720	
TS (MPa)	23.02±4.72	6.02±0.96	p=0.0004*	16.81±2.58	6.99±3.18	p=0.0059*
Glycar® vs CardioCel®				p=0.1208	p=0.4432	

*- Significant (p<0.05)(SD = Standard Deviation; Pu = Pulmonary; YM = Youngs modulus; TS = tensile strength)

5.4.4 Structural evaluation

5.4.4.1 Light and electron microscopy

Hematoxylin and eosin (H&E)

The H&E stain demonstrated pyknotic cells (↑) in the pre-implanted Glycar® patches (Figure 5.3B) but were absent in the pre-implant CardioCel® patches (H). The absence of cells confirmed that the decellularization step effectively removed all cellular components while preserving the tissue architecture (G, H) (Figure 5.3).

Fibrous encapsulation (↕) developed on the interior and posterior side of both the explanted aorta and pulmonary Glycar® and CardioCel® patches. In both groups' cells were present in abundance in the fibrous encapsulation (D, F & J, L) but within both the Glycar® and CardioCel® pericardial patches the number of host cell infiltration were limited (D, F & J, L). The collagen of the explanted CardioCel® patches had a well-preserved wavelike structure of interwoven collagen bundles (H, J, L) that were well-separated while the collagen of the Glycar® patches remained densely compacted (B, D, F).

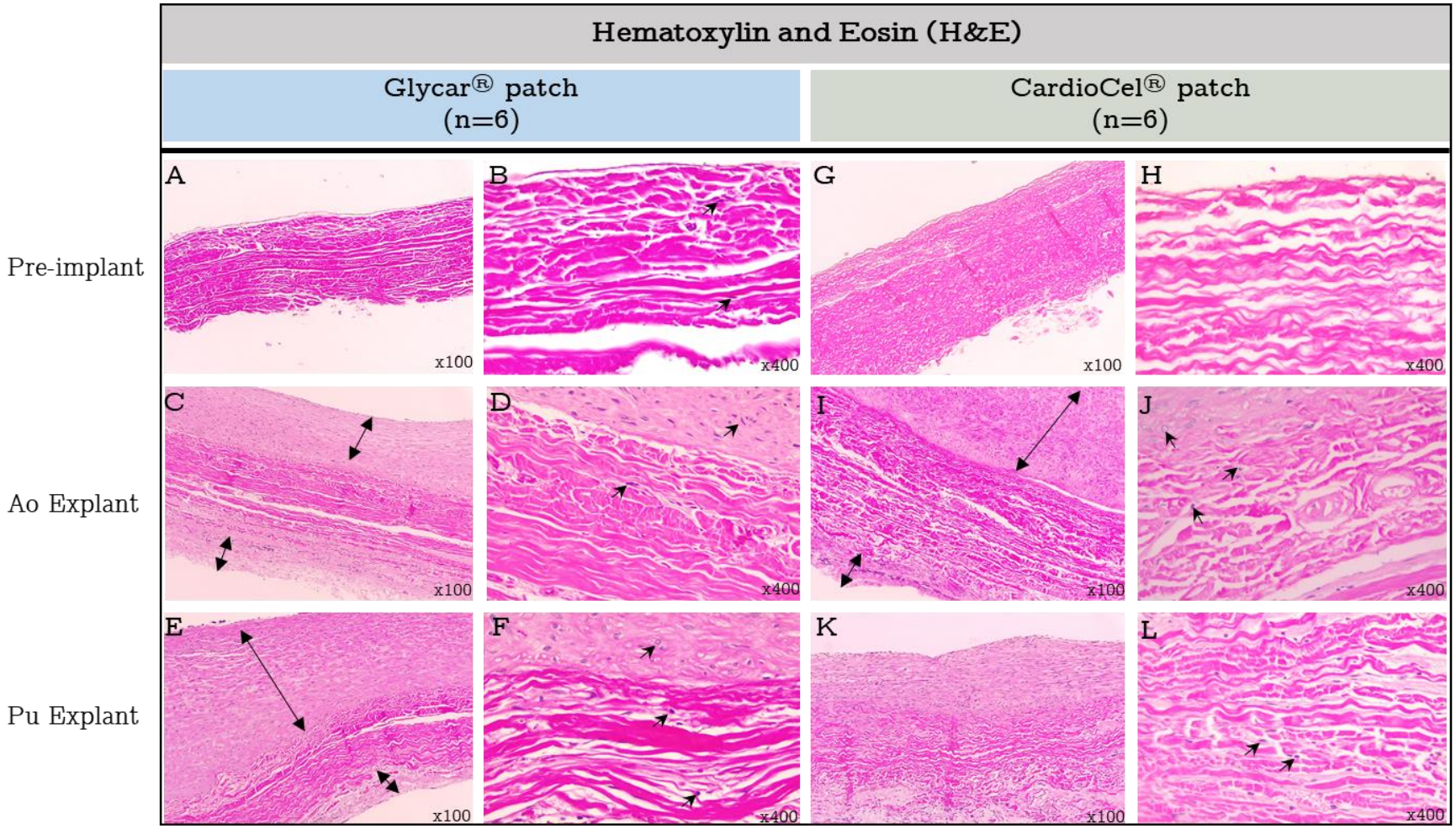

Figure 5.3 H&E of pre-implanted and explanted aortic and pulmonary pericardium: Glycar® patches and CardioCel® patches. (↑) fibroblast-like cells; (↕) fibrous encapsulation. A, C, E, G, I, K = 100x magnification and B, D, F, H, J, L = 400x magnification)

Modified Verhoeff von Gieson (EvG)

Elastin (visualized as black fiber strains on the EvG) was present prior to implantation and after explantation on the Glycar® and CardioCel® patches (Figure 5.4). However, the Glycar® patches retained more elastin from pre-implantation (A) to explantation (B, C). The amount of elastin decreased from pre-implantation (D) to explantation in the CardioCel® patches with more elastin preserved in the pulmonary explants (F) compared to the aortic explants (E). Both groups demonstrated elastin in the fibrous encapsulation (B, C, E, F). The circle demonstrates (F) a possible new blood vessel in the explanted pulmonary CardioCel® patch that could be an indication of neovascularization.

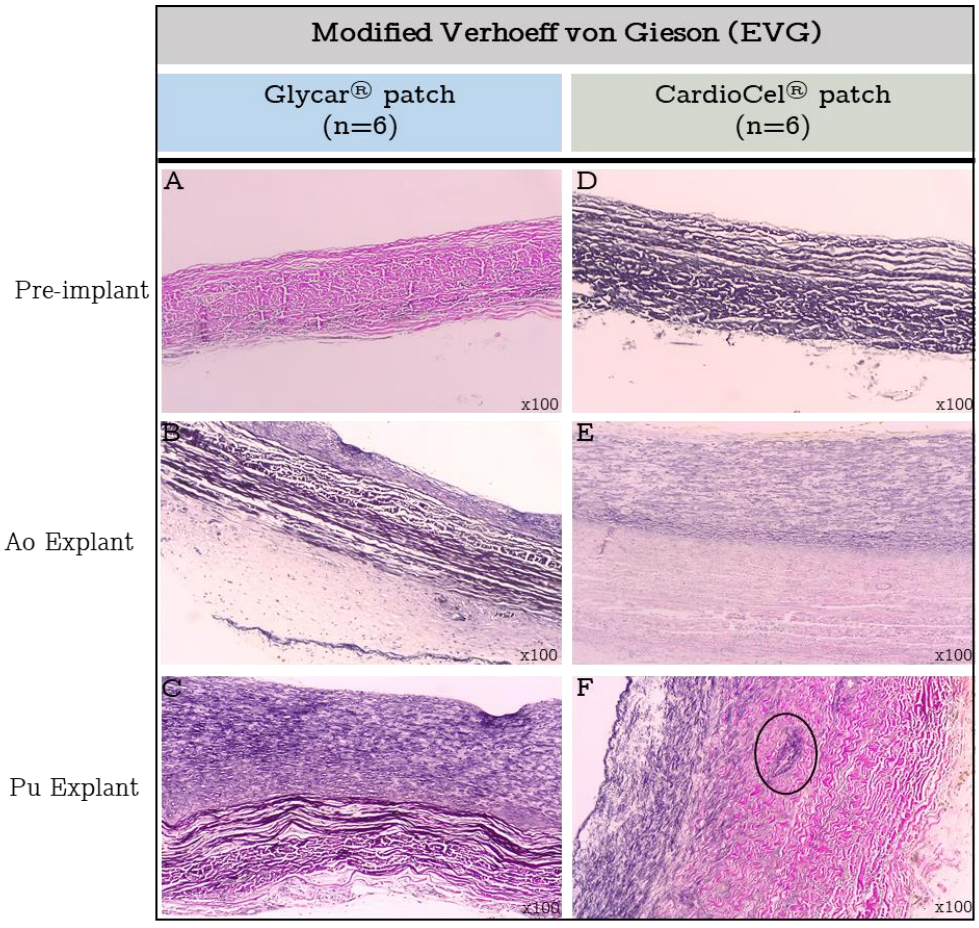

Figure 5.4 EvG histological stain of pre-implanted and explanted aortic and pulmonary pericardium: Glycar® and CardioCel® patches. (A-F = 100x magnification)

Von Kossa (VK)

None of the Glycar® or CardioCel® patches demonstrated calcification (black calcification deposits) prior to implantation or after explantation (Figure 5.5).

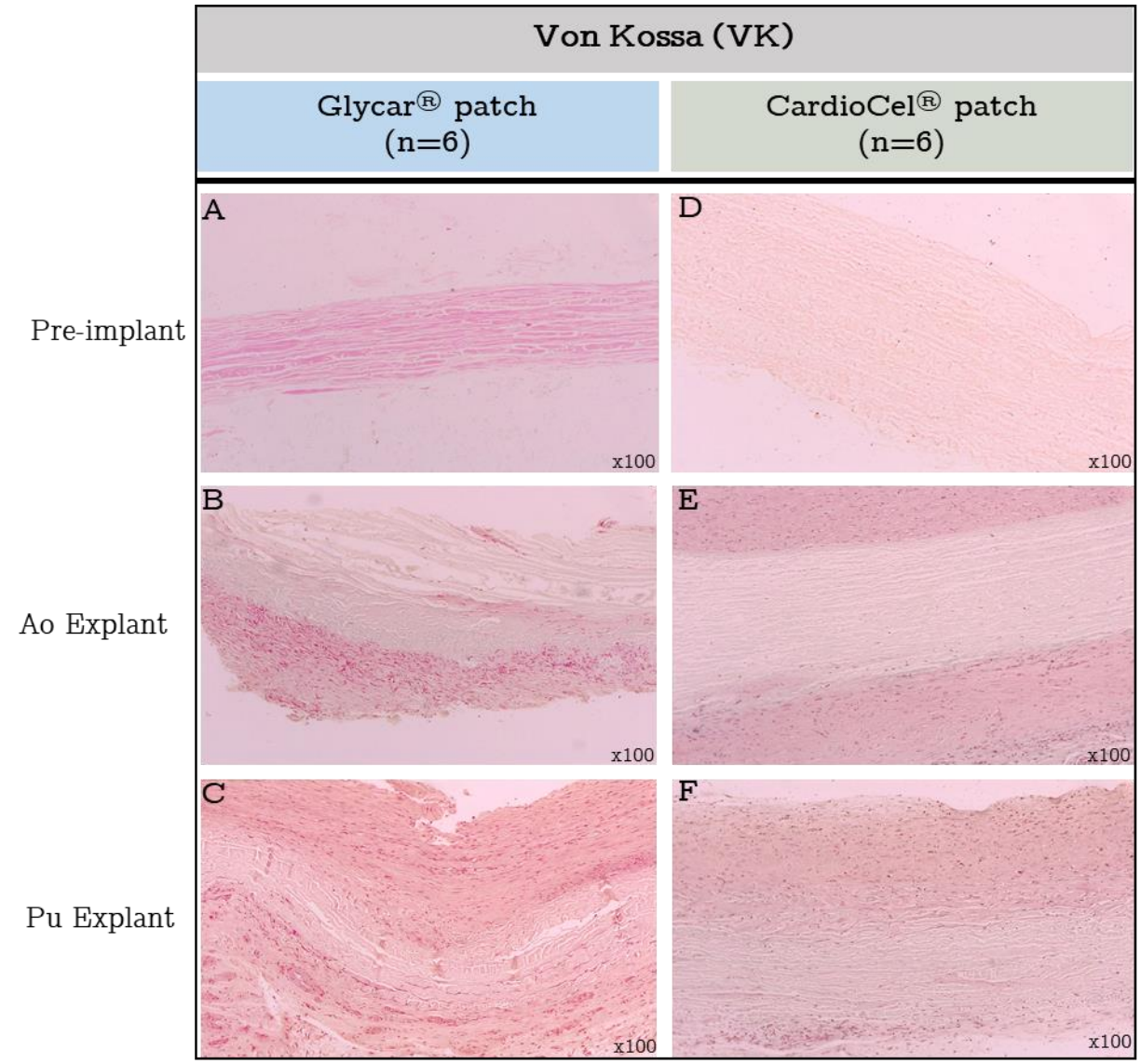

Figure 5.5 VK histological stain of baseline and explanted aortic and pulmonary pericardial patches: Glycar® and CardioCel® patches. (A-F = 100x magnification)

Scanning electron microscopy (SEM)

SEM confirmed that only the collagen patch was retained after decellularization of the CardioCel® pericardial tissue (Figure 5.6D). The pre-implanted Glycar® patches (A) demonstrated endothelial cells that were severely dehydrated with collapsed extra nuclear areas and areas of dehiscence from the basal membrane but with minimal loss of fiber architecture. The explant micrographs of the CardioCel® (E, F) and Glycar® (B, C) patches demonstrated a confluent monolayer of endothelial cells.

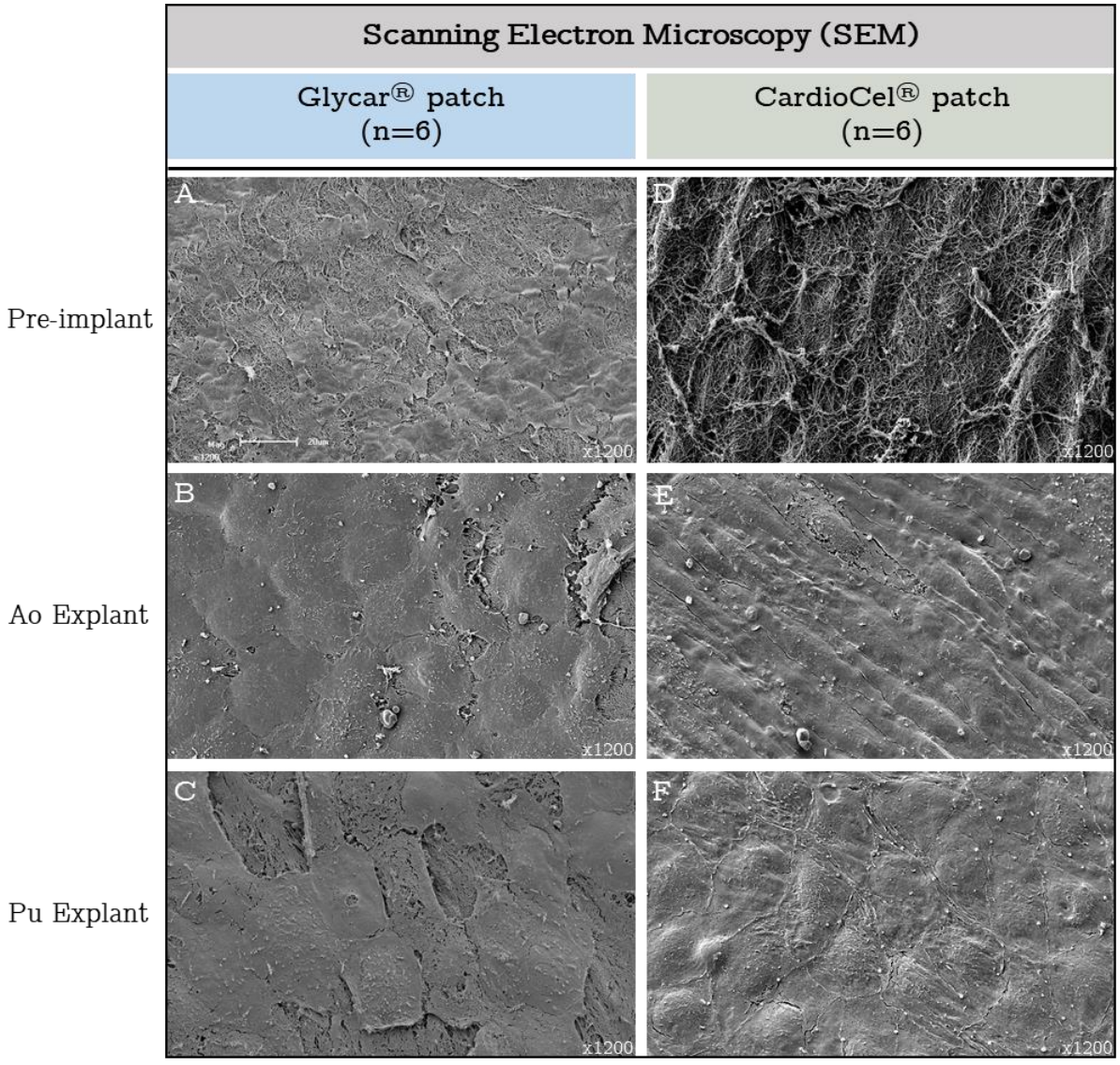

Figure 5.6 SEM of pre-implant and explanted aorta and pulmonary pericardium: Glycar® and CardioCel® patches. (A-F = 1200x magnification)

Transmission electron microscopy (TEM)

TEM demonstrated that both the pre-implanted Glycar® and CardioCel® patches had well-defined collagen fibers with transverse (a) and longitudinal (b) cut fibrils (Figure 5.7B, H). Elastin (black arrow) was visible on the pre-implant (A, G) and explanted patches (E, K) of both groups. A limited number of fibroblast-like cells (d) were seen on the explants (E, J, K) of both groups. However, the cells in the Glycar® patches were devitalized with loss of membrane integrity (C) and edema (F). In contrast the fibroblasts-like cells in the CardioCel® aorta explants demonstrated secretory vacuoles (arrow heads) in which procollagen is packaged from the Golgi complex (I, J).

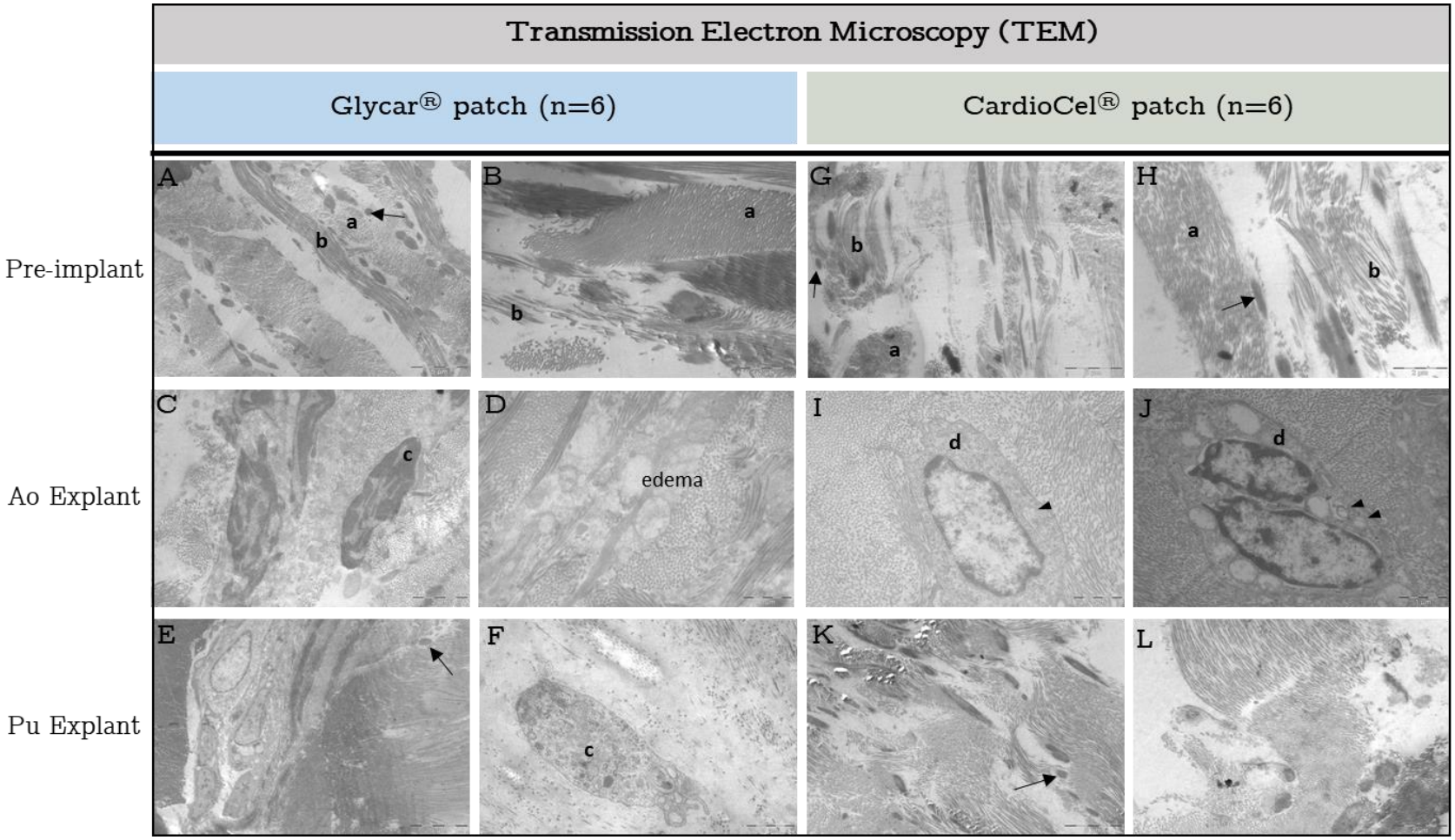

Figure 5.7 TEM of pre-implanted and explanted aorta and pulmonary pericardium: Glycar® patches and CardioCel® patches. (a) transverse cut fibrils, (b) longitudinal cut fibrils (c) devitalized fibroblast-like cells with loss of membrane integrity (d) cells displaying fibroblast-like properties, (↑) elastin fiber and (▲) secretory vacuoles (A, E, G, K = 3400x; B, C, I, H, L = 7900x; D, F, J =13500x magnification)

5.4.5 Pericardial thickness

The Glycar® and CardioCel® patch explants were significantly thicker at explantation compared to their pre-implantation counterparts (Figure 5.9). This could be attributed to the fibrous encapsulation that developed while implanted. However, if only the pericardial patch was measured, and the fibrous encapsulation ignored, both the Glycar® and CardioCel® patches did not substantially thicken over time.

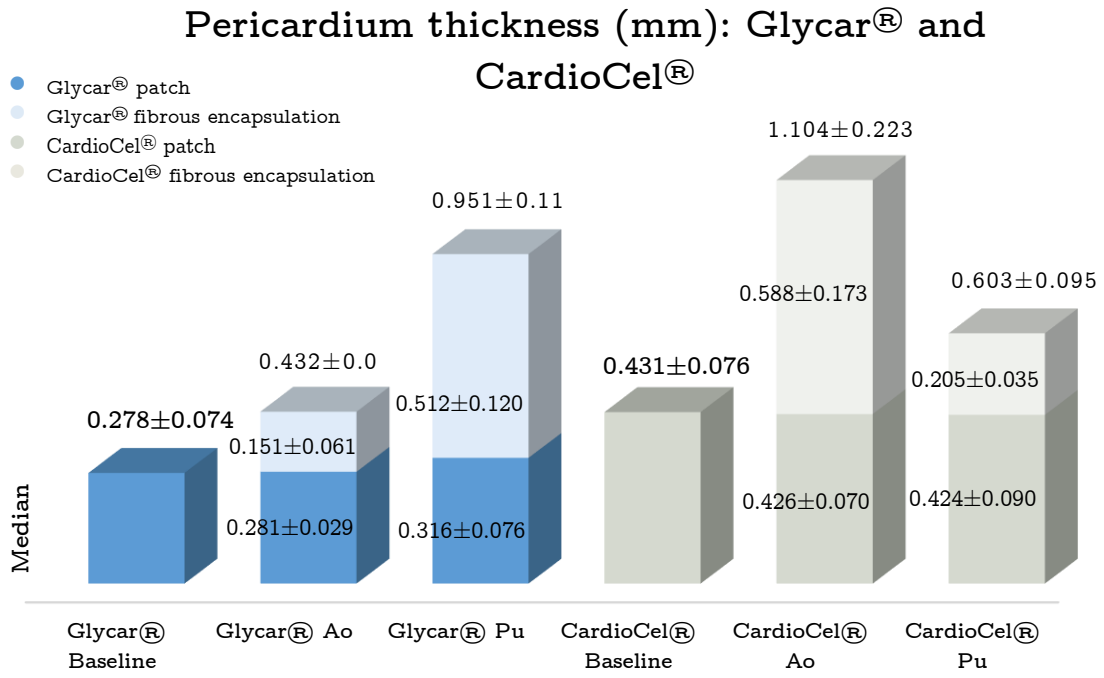

Figure 5.8 Pericardial thickness: Glycar® and CardioCel® patches

5.5 Discussion

Although GA remains the gold standard for crosslinking pericardium several processes have been developed to improve the functioning of long-term implants to prevent tissue degeneration and calcification. Detoxification processes addressing GA cytotoxicity employed by Glycar® has been successful in the past, but adding a

decellularization process to the development of a new generation of pericardial patch might have added benefits (Brizard et al., 2014; Remi et al., 2011). Theoretically it may provide a patch that is not only resistant to calcification but provide a lessor or no immunological target that may offer tissue ingrowth with remodeling potential.

Two (2) commercially available products were evaluated and compared; GA-crosslinked and detoxified Glycar® patches using EnCap technology and a decellularized and crosslinked CardioCel® bovine pericardial patch, using ADAPT TEP anticalcification technology. Both patches maintained adequate tissue strength and no evidence of calcification could be demonstrated during the implantation period. However, both groups developed a foreign body reaction with the development of a fibrous encapsulation. The CardioCel® patches were also not significantly more pliable than the Glycar® patches upon explantation whilst retaining similar strength. Importantly however, the CardioCel® patches demonstrated some recellularization with fibroblast-like cells. These cells demonstrated secretory activity and can potentially contribute to remodeling.

The TS of the pre-implanted pulmonary Glycar® patches (23.0 ± 4.72 Mpa) were higher compared to the CardioCel® patches (16.8 ± 2.58 Mpa) but at explantation no significant difference in strength were noted (p=0.4432). The increased TS values of the pre-implanted Glycar® patches could be attributed to the increased percentage of GA (0.625%) used in comparison to the 0.05% of CardioCel®. The amount of incorporated GA determines the degree of crosslinking, pliability and extent of calcification. The explanted TS of both the Glycar® and CardioCel® patches were still well above the minimum strength of the native human ascending aorta (1.8 ± 0.24 Mpa) (Sommer et al., 2008). Both tissues were more pliable at explantation compared to their per-implantation counterparts. It seems that the increased TS values of the Glycar® pericardium came at the expense of pliability

upon implantation. Neethling et al. (2018) demonstrated comparable pliability with non-crosslinked pericardial products. This is important as graft failure may result if processing protocols have a negative effect on tissue pliability by compromising compliance, hemodynamic performance and even the binding of host cells to the bio-patch when implanted (Kaiser and Coulombe, 2015; Neethling et al., 2018).

Prior to implantation the DAPI histological stain confirmed acellularity of the CardioCel® patches. All animals survived to term and no echocardiographic abnormalities were recorded prior to explantation. Macroscopically, at explantation the Glycar® and CardioCel® patches were in pristine condition with no signs of aneurysm formation, degeneration or calcific deposits. Calcification is commonly seen in GA-crosslinked pericardium (Saporito et al., 2011; Pires et al., 1999) but both Glycar® and CardioCel® employ anti-calcification strategies to minimize the possibility of calcification. The VK stain confirmed the absence of calcification in both the aorta and pulmonary explants of both groups. Similar results were reported by Neethling et al. (2018) and Brizard et al. (2014) for CardioCel® and van den Heever et al. (2013) and Crawford et al. (1986) for Glycar®. In contrast, Salameh et al. (2018) reported calcification of the CardioCel® patches when implanted in the aortic and pulmonary positions of minipigs after only 1 year but this did not occur in our study in an ovine model and might be attributed to interspecies differences of the models used.

The collagen bundles of the pulmonary and aortic CardioCel® patches were less compacted/dense and demonstrated a more separated and wavier appearance when compared to the Glycar® collagen bundles. The Glycar® collagen bundles were densely compacted/collapsed with no separation in between. The compactness of the collagen reduced the pore size which might influence recellularization negatively.

The SEM of the pre-implanted CardioCel® patches demonstrated that all patches were stripped of endothelial coverage after decellularization leaving only an ECM. At explantation an endothelial layer was present on the luminal side of both groups.

No host cell infiltration was seen in the Glycar® patches and an insignificant number of pyknotic fibroblast-like cells were visible at explantation. Although limited the CardioCel® aorta and pulmonary explant did demonstrate host cell infiltration. GA-fixation is known for its cytotoxic effects that prevents host cell infiltration (Umashankar et al., 2012; Neethling et al., 2010). Higher GA concentrations were used to crosslink the Glycar® patches compared to the CardioCel® patches. The higher concentration of GA could also be the reason for limited cell ingrowth into the Glycar® patch because the dense/compact collagen structure did not provide adequate pore size (Murphy & O'Brien, 2010) to promote cellular infiltration.

Both patches developed a fibrous encapsulation on both the inferior and posterior pericardial surface in which fibroblast-like cells were present in abundance. As previously described a typical foreign body reaction can be initiated due to surgical implants where a chronic inflammatory reaction is initiated which result in the dense accumulation of mononuclear cells mostly macrophages (Delgado et al., 2015; Ketchedjian et al., 2005). This reaction was not seen in this study or at least not at explantation. Nezhad et al. (2019) reported an inflammatory response after 1-month implantation of the Glycar® patch in a pig model and by 3-months a fibrous encapsulation developed that did not reduce after 1-year of implantation. The patch also showed degradation after 6-months but again this was not seen in this study. Neethling et al. (2018) also reported a typical immunological response towards the foreign CardioCel® material.

The presence of cellular remnants and GA cytotoxicity in the Glycar® patches may have contributed to this foreign body response and poor host cell infiltration (Poornejad et al., 2016; Stella et al., 2010). However, Neethling et al. (2018) reported remodeling of the CardioCel® patch 12-weeks after subcutaneous implants in a rat model. Although host cell infiltration was limited in the CardioCel® group transmission electron microscopy did show evidence of fibroblast-like cells containing numerous secretory vacuoles within the cytoplasm. These vacuoles play an important role in the secretion of procollagen from the cell (Canty & Kadler, 2005). If the explantation time of 180-days were extended host-cell infiltration might have been more significant in the CardioCel® patches. Brizard et al. (2014) reported the formation of new collagen once implanted in a juvenile ovine model but only after 7-months. The Glycar® patches demonstrated only devitalized fibroblast-like cells with loss of membrane integrity, edema and remains essentially acellular in this study.

The fibrous encapsulation contributed to an increase in the pericardial thickness from implantation to explantation in both groups. At implantation our thickness measurements of both the Glycar® and CardioCel® patches were within the prescribed manufacturers standards (Glycar® = 0.2-0.4 mm and CardioCel® <0.5 mm). The aortic patches had a median thickening of 55% in the Glycar® group and 135% in the CardioCel® group. The pulmonary patches had a median thickening of 197% in the Glycar® group and 46% in the CardioCel® group. Brizard et al. (2014) supported our findings and reported a 37% increase in CardioCel® thickness when used to replace the posterior leaflet of the pulmonary valve in a juvenile sheep model.

5.6 Conclusion

Clinically, the handling quality of both patches were satisfactory and demonstrated excellent clinical results with no signs of degradation, calcification or aneurysm formation. The structural integrity of the Glycar® and CardioCel® patches were

similar at pre-implantation and explantation with no difference in strength or pliability. No calcification occurred in any of the groups. Both pericardial patch groups developed a fibrous encapsulation. However, the collagen of the CardioCel® patches appeared healthier with a more wave-like, well-separated appearance which might contribute to host cell infiltration.

The important difference between the Glycar® and CardioCel® patch is the limited amount of recellularization. Although sparsely populated by fibroblast-like cells, the CardioCel® patches did show viability and secretory activity. Brizard et al. (2014) reported that longer term implants showed better host cell infiltration potential. This remains to be seen and could be a major advantage as initial structural integrity of CardioCel® seems to be equal to Glycar® in this study.

The development of a fibrous encapsulation in both groups remains a concern and seems to be immunologically linked as described by Neethling et al. (2018). The thickening caused by the fibrous encapsulation remains a challenge and further investigations is needed to minimize thickening especially when used for valvular leaflets. It is important to know whether the thickening is linked to the use of GA, and if not, what is the cause, and should alternative detoxification techniques be explored?

Limitations and Recommendation

Data provided by the juvenile sheep model cannot be unconditionally applied to human patients. Measuring pericardial thickness prior to processing was not available for Glycar® nor CardioCel® patches. Due to technical limitations, tissue implanted in the descending aorta did not allow a large enough tissue sample upon explantation for TS/YM determination.

For future studies we recommend that immunohistochemistry be added to the list of analyses to describe cell types and immunological processes involved.

References

Bell, D., Prabhu, S., Betts, K., Justo, R., Venugopal, P., Karl, T.R. & Alphonso, N. 2019. Durability of tissue-engineered bovine pericardium (CardioCel®) for a minimum of 24 months when used for the repair of congenital heart defects. *Interactive Cardiovascular and Thoracic Surgery*, 28(2): 284–290.

Brizard, C.P., Brink, J., Horton, S.B., Edwards, G.A., Galati, J.C. & Neethling, W.M.L. 2014. New engineering treatment of bovine pericardium confers outstanding resistance to calcification in mitral and pulmonary implantations in a juvenile sheep model. *Journal of Thoracic and Cardiovascular Surgery*, 148(6): 3194–3201.

Canty, E.G. & Kadler, K.E. 2005. Procollagen trafficking, processing and fibrillogenesis. *Journal of Cell Science*, 118(pt 7):1341-1353.

Cohen, S., Magal, S., Yakov, I., Sirabella, E., Bitman, A., Groisman, G. & Lotan, C. 2018. Tissue processing techniques for fabrication of covered stents for small-diameter vascular intervention. *Acta Biomaterialia*, 65: 248–258.

Collatusso, C., Roderjan, J.G., Vieira, E.D., Myague, N.I., Noronha, L. de & Costa, F.D.A. da. 2011. Decellularization as an anticalcification method in stentless bovine pericardium valve prosthesis: a study in sheep. Brazilian Journal of Cardiovascular Surgery, 26(3): 419–426.

Crawford, F.A., Sade, R.M. & Spinale F. 1986. Bovine pericardium for correction of congenital heart defects. *Annuals of Thoracic Surgery*, 41:602-605.

Delgado, L.M., Bayon, Y., Pandit, A. & Zeugolis, D.I. 2015. To cross-link or not to cross-link? Cross-linking associated foreign body response of collagen-based devices. *Tissue Engineering - Part B: Reviews*, 21(3): 298–313.

Kaiser, N.J. & Coulombe K.L.K. 2015. Physiologically inspired cardiac patchs for

tailored in vivo function and heart regeneration. BioMedical Materials, 10(3): 034003.

Ketchedjian, A., Jones, A.L., Krueger, P., Robinson, E., Crouch, K., Wolfinbarger, L. & Hopkins, R. 2005. Recellularization of decellularized allograft patchs in ovine great vessel reconstructions. *Annals of Thoracic Surgery*, 79(3): 888–896.

Lee, C., Kim, S.H., Choi, S.H. & Kim, Y.J. 2011. High-concentration glutaraldehyde fixation of bovine pericardium in organic solvent and post-fixation glycine treatment: In vitro material assessment and in vivo anticalcification effect. *European Journal of Cardiothoracic Surgery*, 39(3): 381–387.

Ma, B., Wang, X., Wu, C. & Chang, J. 2014. Crosslinking strategies for preparation of extracellular matrix-derived cardiovascular patchs. *Regenerative Biomaterials*, 1(1): 81–89.

Mallis, P., Michalopoulos, E., Dimitriou, C., Kostomitsopoulos, N. & Stavropoulos-Giokas, C. 2017. Histological and biomechanical characterization of decellularized porcine pericardium as a potential patch for tissue engineering applications. *Bio-Medical Materials and Engineering*, 28(5): 477–488.

Murphy, C.M. & O'Brien, F.J. 2010. Understanding the effect of mean pore size on cell activity in collagen-glycosaminoglycan patchs. *Cell Adhesion and Migration*, 4(3): 377–381.

Neethling, W.M.L., Glancy, R. & Hodge, A.J. 2010. Mitigation of calcification and cytotoxicity of a glutaraldehyde-preserved bovine pericardial matrix: improved biocompatibility after extended implantation in the subcutaneous rat model. *The Journal of Heart Valve Disease*, 19(6): 778–785.

Neethling, W.M.L., Puls, K. & Rea, A. 2018. Comparison of physical and biological properties of CardioCel® with commonly used biopatchs. *Interactive Cardiovascular and Thoracic Surgery*, 26(6): 985–992.

Neethling, W.M.L., Strange, G., Firth, L. & Smit, F.E. 2013. Evaluation of a tissue-engineered bovine pericardial patch in paediatric patients with congenital cardiac

anomalies: Initial experience with the ADAPT-treated CardioCel® patch. *Interactive Cardiovascular and Thoracic Surgery*, 17(4): 698–702.

Nezhad, M.Z., Poncelet, A., Fervaille, C. & Gianello, P. 2019. Comparing the host reaction to CorMatrix and different cardiac patch materials implanted subcutaneously in growing pigs. *Thoracic and Cardiovascular Surgeon*, 67(1): 44–49.

Pires, A.C., Saporito, W.F., Cardoso, S.H. & Ramaciotti, O. 1999. Bovine pericardium used as a cardiovascular patch. *The Heart Surgery Forum*, 2(1): 60–69.

Poornejad, N., Schaumann, L.B., Buckmiller, E.M., Momtahan, N., Gassman, J.R., Ma, H.H., Roeder, B.L., Reynolds, P.R., Cook, A.D. 2016. The impact of decellularization agents on renal tissue extracellular matrix. *Journal of Biomaterials Applications*, 31(4): 521–33.

Prabhu, A.S., Armes, J.E., Bell, D., Justo, R., Karl, T., Alphonso, N., Frcs, P.V., Fracs, T.K. & Fracs, N.A. 2017. Histological evaluation of explanted tissue engineered bovine pericardium (CardioCel). Seminars in Thoracic and Cardiovascular Surgery, 29(3): 356-363.

Remi, E., Khelil, N., Di, I., Roques, C., Ba, M., Medjahed-Hamidi, F., Chaubet, F., Letourneur, D., Lansac, E. & Meddahi-Pelle, A. 2011. Pericardial Processing: Challenges, Outcomes and Future Prospects. *Biomaterials Science and Engineering*. Retrieved from: http://www.intechopen.com/books/biomaterials-science-and-engineering/pericardial-processing-challenges-outcomes-and-future-prospects. [accessed 20 November 2018].

Salameh, A., Greimann, W., Vondrys, D. & Kostelka, M. 2018. Calcification or not. This is the question. A 1-year study of bovine pericardial vascular patches (CardioCel) in minipigs. *Seminars in Thoracic and Cardiovascular Surgery*, 30(1): 54–59.

Saporito, W.F., Pires, A.C., Cardoso, S.H., Correa, J.A., Carlos De Abreu, L., Valenti, V.E., Miller, L.M.R. & Colombari, E. 2011. Bovine pericardium retail preserved

in glutaraldehyde and used as a vascular patch. *BMC Surgery*, 11(37): 1-8.

Sommer, G., Gasser, T.C., Regitnig, P., Auer, M. & Holzapfel, G.A. 2008. Dissection properties of the human aortic media: An experimental study. *Journal of Biomechanical Engineering*, 130(2): 1-12.

Stella, J.A., D'Amore, A., Wagner, W.R., Sacks, M.S. 2010. On the biomechanical function of patchs for engineering load bearing soft tissue. *Acta Biomaterialia*, 6(7): 2365–2381.

Tran, H.L.B., Dinh, T.T.H., Nguyen, M.T.N., To, Q.M. & Pham, A.T.T. 2016. Preparation and characterization of acellular porcinepericardium for cardiovascular surgery. *Turkish Journal of Biology*, 40: 1243–1250.

Umashankar, P.R., Mohanan, P. V & Kumari, T. V. 2012. Glutaraldehyde treatment elicits toxic response compared to decellularization in bovine pericardium. *Toxicology International*, 19(1): 51–58.

Van Den Heever, J.J., Neethling, W.M., Smit, F.E., Litthauer, D. & Joubert, G. 2013. The effect of different treatment modalities on the calcification potential and cross-linking stability of bovine pericardium. *Cell Tissue Bank*, 14(1): 53-63.

Chapter 6 - Article 3

The impact of pericardial patch processing techniques after 180-days implantation in an ovine model: Glycar® versus a tissue engineered decellularized, glutaraldehyde-fixed and detoxified bovine pericardium

Botes L[1], Laker L[2], Dohmen PM[2&3], van den Heever JJ[2], Jordaan CJ[2], Goedhals J[4], Smit FE[2]

[1]*Department of Health Sciences, Central University of Technology, Free State, Bloemfontein, South Africa*

[2]*Department of Cardiothoracic Surgery, University of the Free State, Bloemfontein, South Africa*

[3]*Department of Cardiac Surgery, Heart Centre Rostock, University of Rostock, Germany*

[4]*Department of Anatomical Pathology, University of the Free State, Bloemfontein, South Africa*

Abstract

Introduction: Decellularization reduce scaffold stability and strength but might promote recellularization. Collagenous tissue can be strengthened by glutaraldehyde (GA)-crosslinking prior to implantation through the reaction of aldehyde groups of GA with the e-amine groups of lysine or hydroxylysine residues. Therefore, a decellularized patch that is GA-fixed might demonstrate adequate strength and recellularization potential when implanted. The study aimed to prove that a novel decellularized patch which is GA-fixed and detoxified (D-GAD) using the same detoxification process as Glycar®, was not structurally or morphologically inferior to the commercialized Glycar® patch and might have remodeling advantages when implanted in an ovine model. Methods: The impact of the processing methods on tissue strength and morphology was assessed prior to implantation. Bovine Glycar® pericardial patches (Group 1) were implanted in the descending aorta and main pulmonary artery of six (6) sheep and bovine decellularized, GA-fixed and detoxified (D-GAD) pericardial patches (Group 2) were implanted in six (6) sheep at the same anatomical locations. The clinical, mechanical and morphological integrity of the explants were evaluated and compared after 180-days of implantation. Results: The pre-implanted Group 2 patches were significantly weaker [tensile strength (TS), $p = 0.0001$)] but more pliable (Youngs modulus (YM), $p = 0.0150$) compared to the Group 1 patches. Group 1 demonstrated devitalized cells after processing and acellularity was confirmed in Group 2. The collagen in Group 1 was densely compacted while Group 2 demonstrated wavier more separated collagen bundles. The clinical performance of both groups was excellent, and echocardiography confirmed the absence of aneurysm formation, calcification or disintegration. The explanted pulmonary TS and YM was comparable between groups (TS, $p = 0.2567$; YM, $p = 0.1442$). Both groups initiated a foreign-body response and all implants developed a fibrous encapsulation. Calcification was absent in both groups. At explantation, Group 2 demonstrated better preservation of collagen and better fibroblast-like cellular infiltration compared to Group 1. Secretory vacuoles visible within the fibroblast-like cells can promote procollagen secretion. Patch thickness increased in Group 1 but remained similar in Group 2 when comparing implantation to explantation thickness. Conclusion: The decellularized, fixed and capped pericardial scaffolds were not structurally or morphologically inferior to the commercially available Glycar® patches. The recellularization potential demonstrated by the decellularized, fixed and capped scaffolds make this scaffold an attractive substitute to GA-fixed patches especially in younger patients.

Keywords: Pericardium, Glutaraldehyde, Decellularization, Strength, Calcification, Recellularization

6.1 Introduction

Today, bovine pericardium (BP) derived biomaterials are widely used and has established itself in cardiac and vascular reconstruction and closure surgery (Yoo et al., 2011). BP has superiority over autologous and porcine pericardium because it has a higher collagen content compared to porcine pericardium (Remi et al., 2011) and autologous pericardium tends to retract, thicken, become aneurysmal and develop fibrosis (Neethling et al., 2014).

Glutaraldehyde (GA)-fixated bovine pericardium improves handling, provides greater mechanical stability, and reduces the risk of aneurysmal dilation, especially for patches in the systemic circulation (Sinha et al., 2012). However, GA-fixation can also be costly with numerous reports of degradation, thickening, inflammation, calcification and the lack of in vivo tissue remodeling (Sinha et al., 2012; Saporito et al., 2011; Neethling et al., 2010). Therefore, it is important to overcome the aggressive recipient-graft-specific rejection response to allow utilization in clinical practice (Liu et al., 2016). Several approaches have been explored to reduce or overcome the antigenicity of GA-fixed BP for example, decellularization [e.g., sodium dodecyl sulphate (SDS), Triton X-100 (TX), trypsin], enzymatic removal of α-Gal (i.e. α-galactosidase), and solubilization-based antigen removal (Remi et al., 2011). Tissue engineered (TE) scaffolds which add decellularization to the process limits antigenicity because it removes cellular antigens and procalcifying remnants while preserving the ECM (Mendoza-Novelo & Valerio, 2011).

The decellularized BP three (3)-dimensional ECM is largely comprised of collagen fibers that lends elastic properties to allow conformity to complex anatomy (Bielli et al., 2018; Lam & Wu, 2012). The acellular ECM contains a mixture of structural and functional proteins, glycoproteins and

glycosaminoglycans arranged in a three (3)-dimensional architecture (Costa et al., 2017; Mendoza-Novelo et al., 2013).

Therefore, the ECM acts as a regenerative framework that supports new collagen deposition and remodeling (Keane et al., 2015). The ideal scaffold will gradually fully integrate into the host tissue, thus promoting cellular and vascular regeneration and de novo formation of tissue that mimics native tissue.

Exploring the development of more effective decellularization protocols for bovine pericardium to offer better ECM preservation and good biocompatibility is currently of major interest. Different decellularization methods have been developed over the years most of them based on TX, sodium deoxycholate (SDC) and SDS (Aguiari et al., 2017). Each of the agents used during the decellularization process affects the composition, strength and ultrastructure of the ECM and accordingly, affects the host tissue response to the ECM scaffold following implantation (Gilbert et al., 2006). In order to address these deteriorating characteristics brought upon by decellularization additional treatment options can be performed (Remi et al., 2011). Crosslinking the polypeptide chains of the ECM with GA reduce immunogenicity of the pericardium and its biodegradability by increasing its resistance to enzymatic degradation (Parenteau-Bareil et al., 2010). However, crosslinking with GA accelerate calcification and render poor regeneration ability in vivo and the cytotoxic effects can limit host cell attachment, migration and proliferation (Remi et al., 2011). Coating of pericardium with biopolymeric films (either chitosan or silk fibroin) after decellularization should improve graft integration at the site of implantation and decrease pericardial degradation. However, coating limits reendothelialization and increases calcification in vivo (Remi et al., 2011; Nogueira et al., 2010).

A tissue engineered BP patch incorporating our proprietary decellularization protocol was developed by the Frater Cardiovascular Research Centre. This process included GA-crosslinking followed by the removal of residual aldehyde toxicity by the Aldecap process. The aldehyde tanned tissue is treated with propylene glycol (2%) which cap any residual unlinked aldehyde groups and is referred to as the EnCap™ AC Technology used by Glycar®. The EnCap™ AC Technology was added to the decellularization process to provide additional strength to withstand the high-pressure environment of the systemic circulation. The aim of this study was firstly to evaluate if the tissue engineered decellularized GA detoxified bovine pericardial patch (D-GAD) demonstrated comparable mechanical and morphological integrity when compared to a commercial bovine GA and detoxified BP patch (Glycar®) using similar GA fixation, detoxification and storage technology after implantation in a juvenile ovine model. Secondly, to evaluate the remodeling potential of the D-GAD patch.

6.2 Materials and Methods

The study was performed at the RWM Frater Cardiovascular Research Centre, Department of Cardiothoracic Surgery, University of the Free State (UFS), South Africa. Ethical clearance was obtained from the Animal Ethics Committee of UFS (ETOVS Number: UFS-AED2015/0081, Appendix A1).

Glycar® bovine pericardial patch

For the detailed processing method of the Glycar® pericardial patch refer to section 4.2, Materials and methods, Article 1, Chapter 4.

Decellularized, GA-fixated and detoxified (D-GAD) bovine pericardial patch

The decellularization process was repeated in the exact manner as mentioned in section 4.2, Materials and methods, Article 1, Chapter 4. After the decellularization

step the pericardial patches were fixated with GA (0,625%) to limit immunogenicity followed by the removal of the residual aldehyde toxicity by treating the tissue with 75% propylene glycol which bind any residual unlinked aldehyde groups. This fixation and detoxification process are similar to the EnCap™ AC Technology used by Glycar®. The patches were stored in sterile water containing 2% propylene oxide.

6.2.1 Study design and layout

A prospective analytical cohort study design was followed. The clinical and mechanical integrity [tensile strength (TS) and Young's Modulus (YM)] tissue morphology [hematoxylin and eosin (H&E), modified Verhoeff's von Gieson (EvG), Von Kossa (VK) histological stains, scanning electron microscopy (SEM) and transmission electron microscopy (TEM)] and thickness were evaluated in both groups prior to implantation and after explantation. (Figure 6.1).

Glycar® and D-GAD patches were implanted into twelve (12) juvenile Dorper Wether sheep. After removal from the storage container the patches did not require any additional preparation. Six (6) sheep received two (2) Glycar® pericardial patches (control group, Group 1), the first implanted in the descending aortic arch and the second in the main pulmonary artery. In Group 2, six (6) sheep received two tissue engineered D-GAD BP patches implanted in the same surgical locations. Samples of each pericardial patch were taken prior to surgical implantation to evaluate processing impact and to establish pre-implantation values. This process was repeated when the patches were explanted after 180-days. Intraoperatively the functionality of the patches was evaluated using echocardiography.

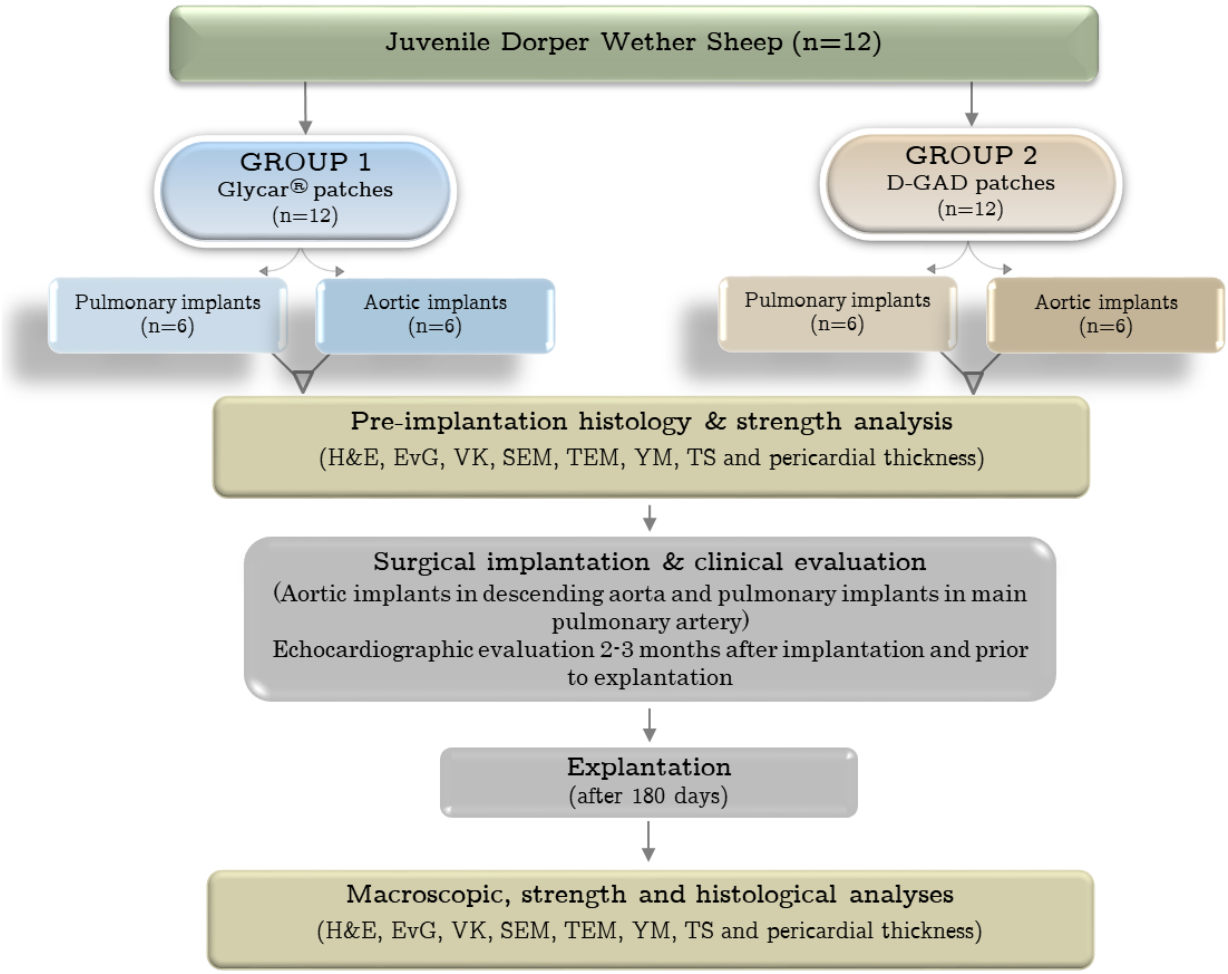

Figure 6.1 Study layout: Glycar® and decellularized GA-fixed and detoxified (D-GAD) patches. (Pu = pulmonary; Ao = Aorta; H&E = hematoxylin and eosin; EVG = modified Verhoeff's von Gieson; VK = Von Kossa; YM = Young's Modulus; TS = tensile strength; SEM = scanning electron microscopy; TEM = transmission electron microscopy]

6.2.2 Surgical protocol

A mini thoracotomy was performed on twelve (12) recipient sheep (aged 6-12 months; mean weight 30.41±5.53kg). Refer to section 4.2.2, Surgical protocol, Article 1, Chapter 4 for a detailed description of the surgical protocol.

6.2.3 Laboratory analysis

Prior to implantation and after explantation samples were taken from both the aorta and pulmonary Glycar® and D-GAD pericardial patches and evaluated for tissue strength and morphology. However, strength analysis (YM and TS) was only performed on the pulmonary explants in both groups due to limited tissue available.

6.2.3.1 Clinical evaluation

Echocardiographic examinations were performed 2-3 months after implantation and just before explantation to evaluate the patches for calcification, infective endocarditis and aneurysm formation.

6.2.3.2 Validation of acellularity

4', 6-Diamidino-2-Phenylindole (DAPI) staining

The Cardiovascular Research Unit of the University of Cape Town performed the DAPI stains to confirm acellularity after the decellularization step. Refer to section 4.2.3.2, Validation of accellularity, Article 1, Chapter 4 for a detailed description of the DAPI method.

6.2.3.3 Strength evaluation

Tensile strength (TS) and Young's Modulus (YM)

Refer to section 4.2.3.3, Strength evaluation, Article 1, Chapter 4 for a detailed description of the TS and YM methods.

6.2.3.4 Structural evaluation

Light Microscopy and electron microscopy

Refer to section 4.2.3.4, Structural evaluation, Article 1, Chapter 4 for detailed light and electron microscopy (SEM and TEM) methods.

6.2.4.5 Pericardial thickness and sizing

The measurement of pericardial thickness is described in section 4.2.3.5, Pericardial thickness, Article 1, Chapter 4.

6.3 Statistical analysis

Refer to section 4.3, Statistical analysis, Article 1, Chapter 4 for statistical methods used.

6.4 Results

6.4.1 Clinical evaluation

The handling quality of both patches were satisfactory. All twelve (12) sheep survived till they were euthanized after a minimum of 180-days. The echocardiographic and macroscopic (after explantation) evaluations of the Glycar® and D-GAD groups demonstrated no evidence of aneurysm formation, infective endocarditis or calcification.

6.4.2 Validation of acellularity: 4', 6-Diamidino-2-Phenylindole (DAPI) staining

The pre-implantation Glycar® and D-GAD patches demonstrated no evidence of intact cells. The DAPI stain (Figure 6.2) confirmed successful removal of cells after the decellularization step prior to implantation.

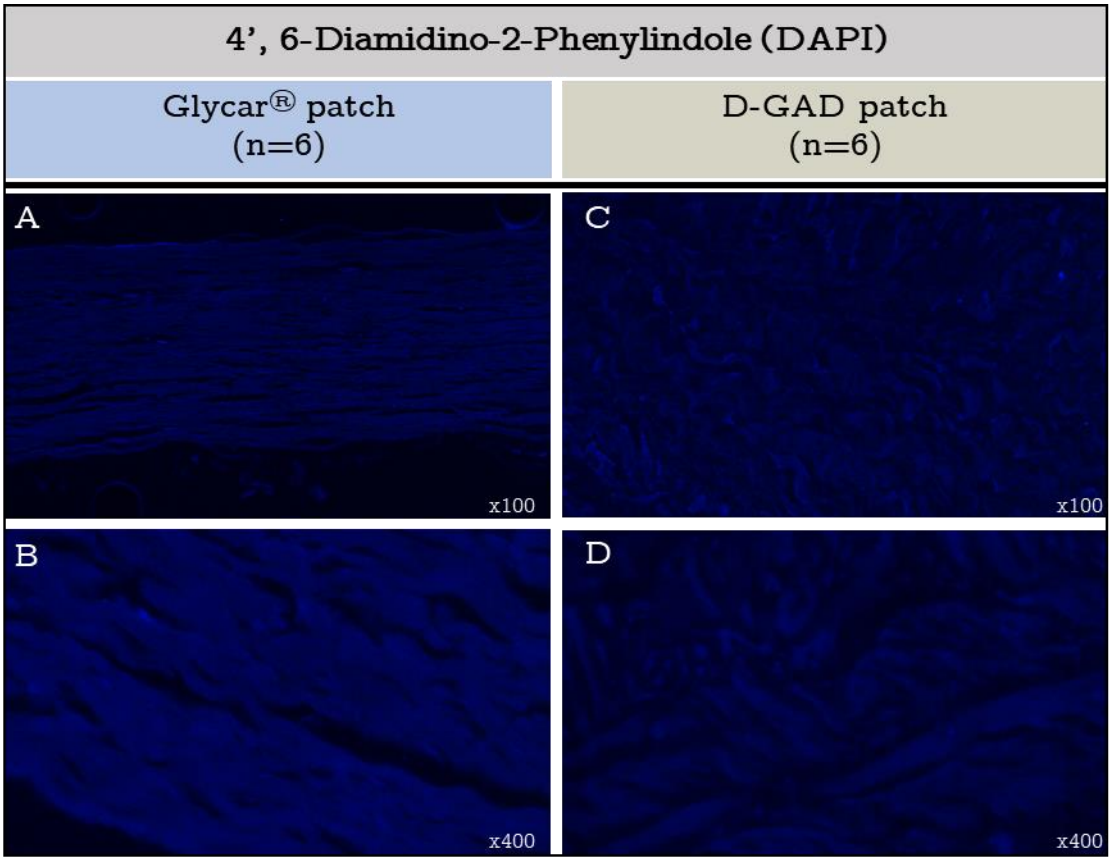

Figure 6.2 DAPI pre-implantation histological stain: Glycar® (A, B) and D-GAD patches (C, D). (A, C = 100x; B, D = 400x magnification)

6.4.3 Strength evaluation

The YM (p = 0.0027) and TS (p = 0.0004) significantly decreased from pre-implantation to explantation in the Glycar® patches. However, the decrease in TS from pre-implantation to explantation was not statistically significant (p=0.1051) in the D-GAD patches. The YM also decreased significantly from pre-implantation to explantation (p=0.0121) indicating that the explanted D-GAD tissue was more elastic and pliable compared to their pre-implanted counterparts (Table 6.1).

The pre-implanted Glycar® patches were significantly stronger (TS, p=0.0001) and significantly less pliable (YM, p=0.0150) compared to the pre-implanted D-GAD

patches. However, at explantation both the TS (p=0.2567) and YM (p=0.1442) did not statistically differ between the two (2) groups (Table 6.1).

Table 6.1 Strength analysis of pre-implanted and explanted pericardium: Glycar® and D-GAD patches

Variable	Glycar® patches (n=6) (Median ± SD)			D-GAD patches (n=6) (Median ± SD)		
	Pre-implantation patch	Explant (Pu)	Pre-implant vs. Explant	Pre-implantation scaffold	Explant (Pu)	Pre-implant vs. Explant
YM (MPa)	114.50±40.41	19.58±17.18	p=0.0027*	39.88±28.46	10.01±11.41	p=0.0121*
Glycar® vs D-GAD				p=0.0150*	0.1442	
TS (MPa)	23.02±4.72	6.02±0.96	p=0.0004*	9.91±2.53	5.30±1.40	p=0.1051
Glycar® vs D-GAD				p=0.0001*	p=0.2567	

*- Significant difference (p<0.05)(SD = Standard Deviation; Pu = Pulmonary; YM = Youngs modulus; TS = tensile strength; MPa=megapascals)

6.4.4 Structural evaluation

6.4.4.1 Light and electron microscopy

Hematoxylin and eosin (H&E)

The H&E stain demonstrated pyknotic cells (↑) in the pre-implanted Glycar® patches (Figure 6.3 B) but were absent in the D-GAD patches (J).

A fibrous encapsulation (↕) developed during implantation on the interior and posterior side of both the Glycar® (C, E) and D-GAD patches (H, I). Most cells were visible in the fibrous encapsulation of the explanted Glycar® patches with only limited pyknotic cells visible within the patch itself (C, D & E, F). However, most fibroblast-like cells were similarly also situated in the fibrotic encapsulation of the D-GAD patches (I, J & K, L) but cells were also visible within the patch itself (more in the pulmonary patch).

The collagen structure of the pre-implanted and explanted aortic and pulmonary Glycar® patches displayed densely compacted/collapsed interwoven collagen bundles (B, D, F). However, in comparison the D-GAD patches demonstrated collagen bundles that were wavier and more separated.

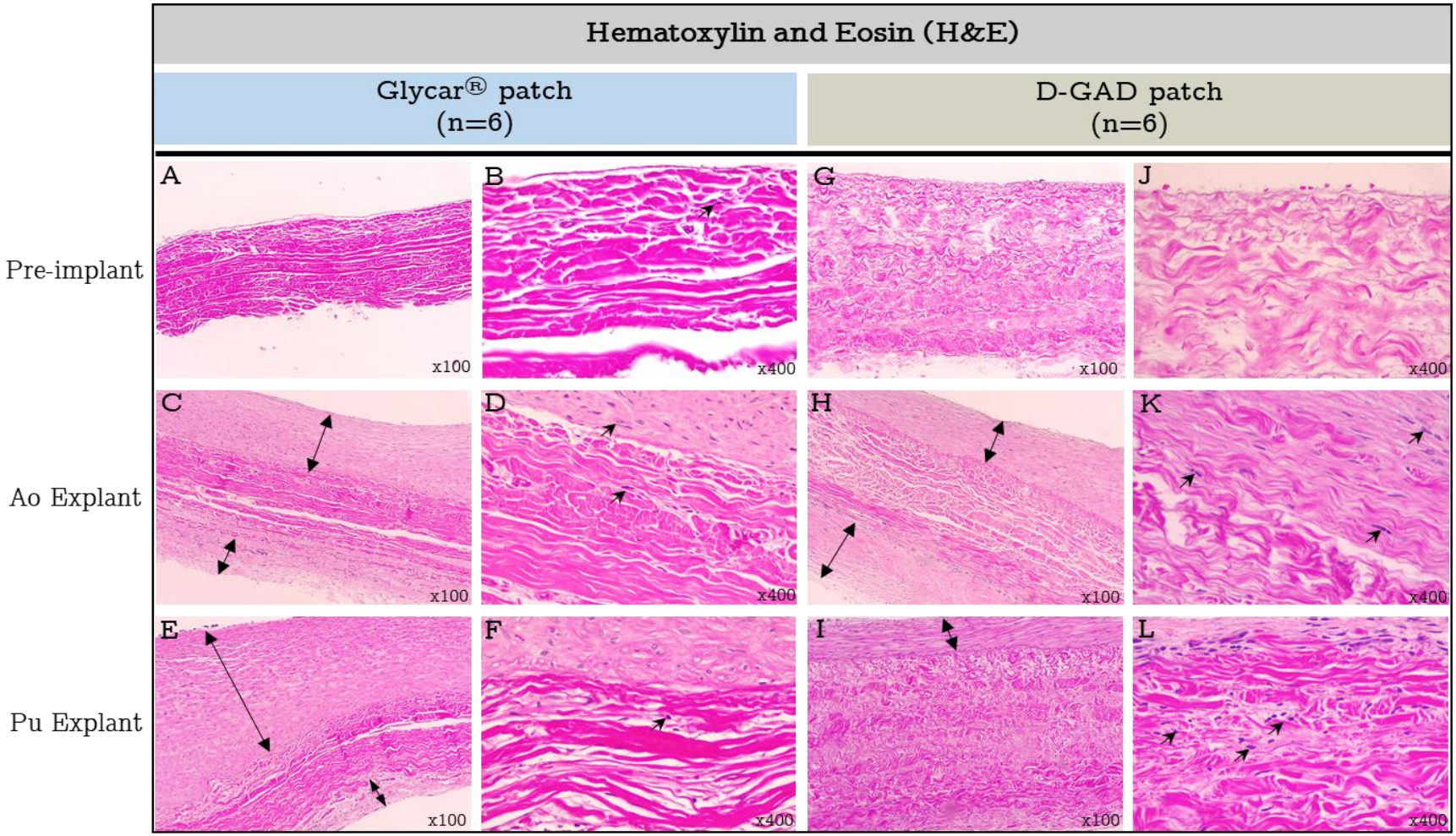

Figure 6.3 H&E of pre-implanted and explanted aortic and pulmonary pericardium: Glycar® and D-GAD patches. (↑) fibroblast-like cells; (↕) fibrous encapsulation. (A, C, E, G, H, I = 100x magnification and B, D, F, J, K, L = 400x magnification)

Modified Verhoeff von Gieson (EvG)

The Glycar® patches retained elastin (black fiber strains) from pre-implantation (Figure 6.4A) to explantation (B, C). Elastin was visible in the pre-implanted D-GAD patches (D) but decreased in the explanted aorta (E) and pulmonary patches (F). Most of the elastin present in both the explanted Glycar® and D-GAD patches were visible within the fibrous encapsulation.

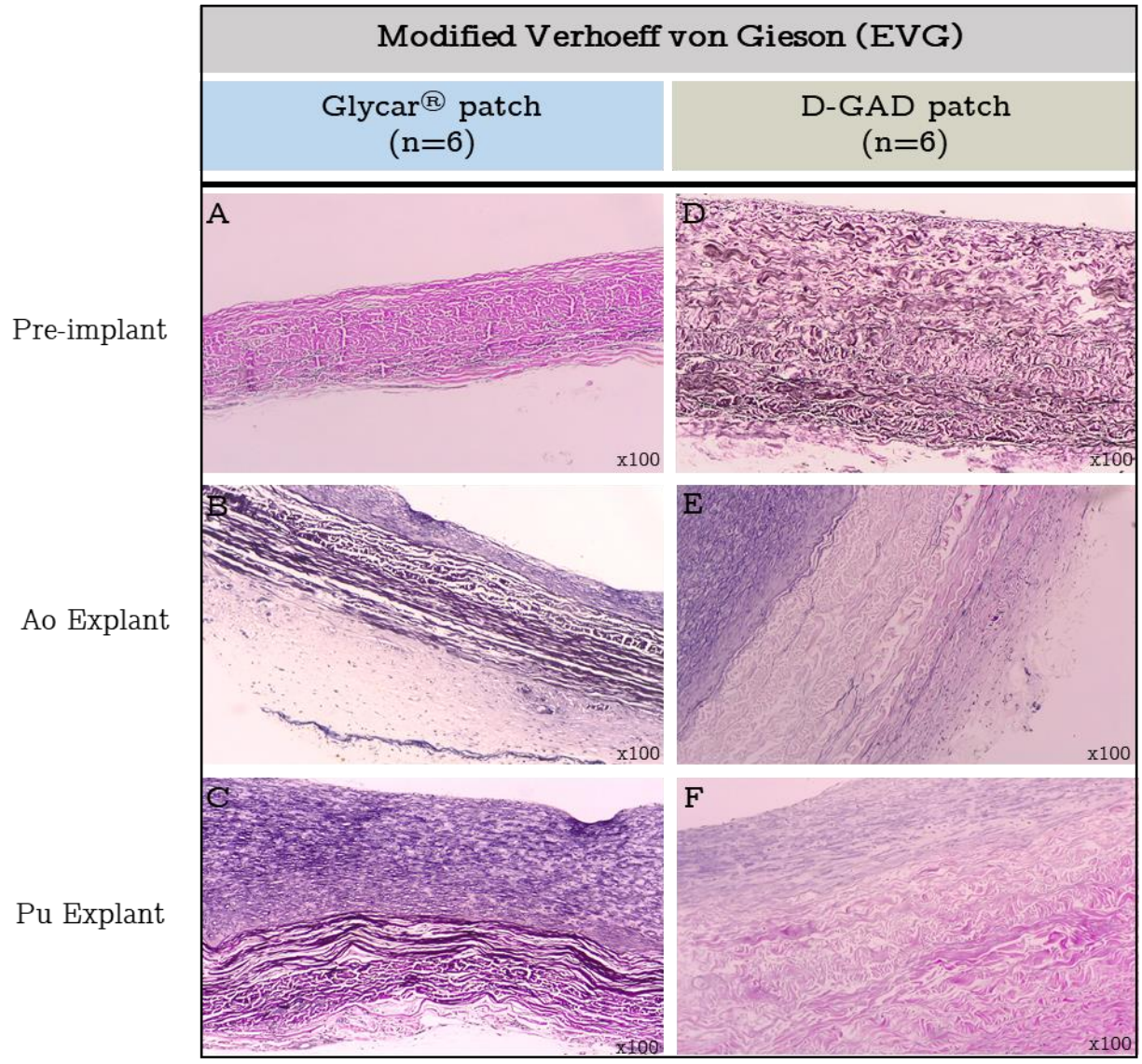

Figure 6.4 EVG histological stain of pre-implanted and explanted aortic and pulmonary pericardium: Glycar® and D-GAD patches. (A-F = 100x magnification)

Von Kossa (VK)

The VK stain confirmed the absence of calcific deposits (black) in the pre-implantation (A, D) and explanted samples of both the Glycar® (B, C) and D-GAD patches (E, F)(Figure 6.5).

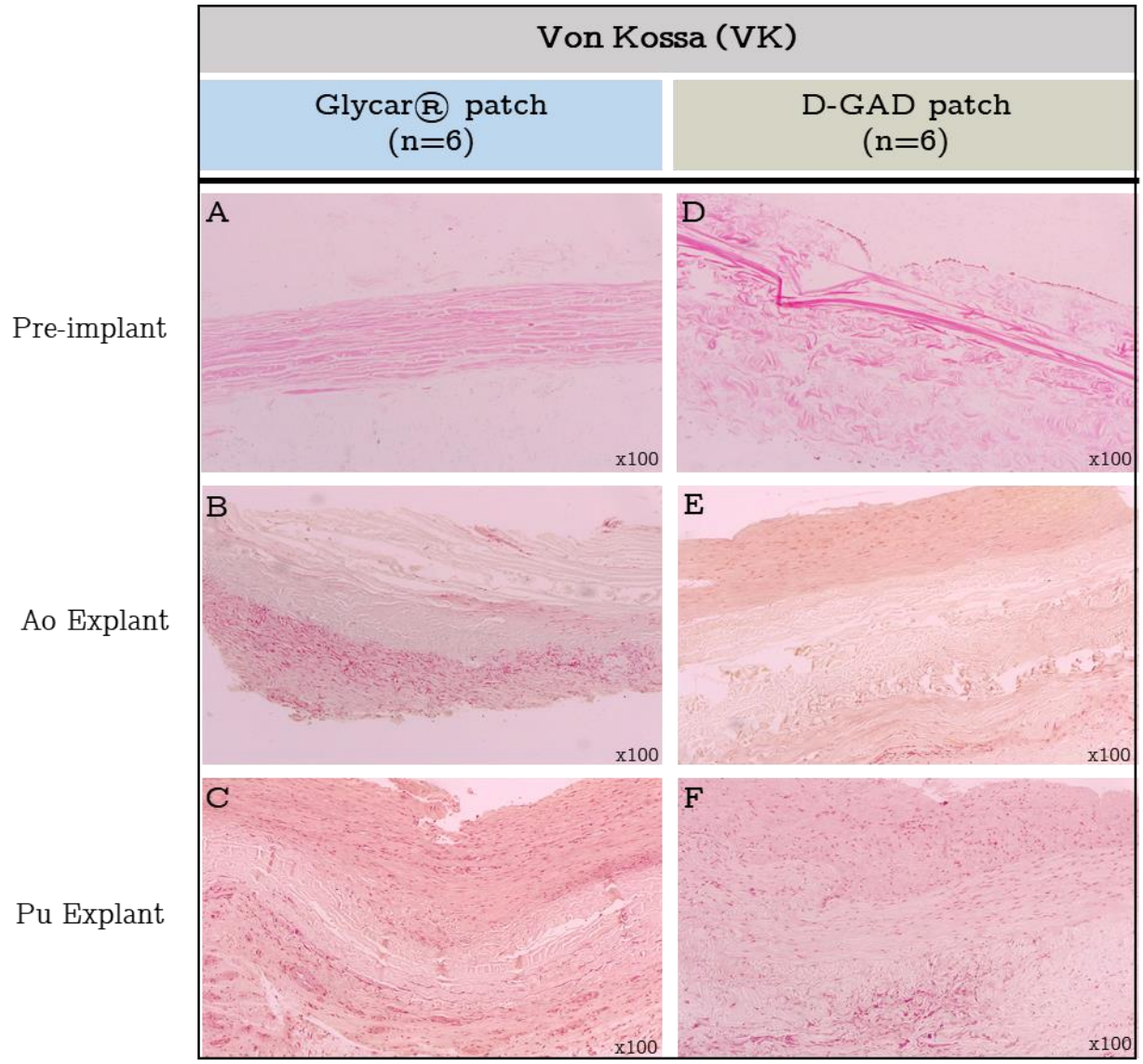

Figure 6.5 VK histological stain (VK) of pre-implanted and explanted aortic and pulmonary pericardium: Glycar® and D-GAD patches. (A-F = 100x magnification)

Scanning electron microscopy (SEM)

Scattered endothelial cells with collapsed extranuclear areas and areas of dehiscence from the basal membrane was seen on the pre-implanted Glycar® micrographs (Figure 6.6A). The decellularization step stripped the pre-implanted D-GAD patches of all endothelial cells leaving only the collagen scaffold (D) too remain.

At explantation the Glycar® (B, C) and D-GAD patches (E, F) demonstrated endothelial coverage which appeared in a confluent monolayer.

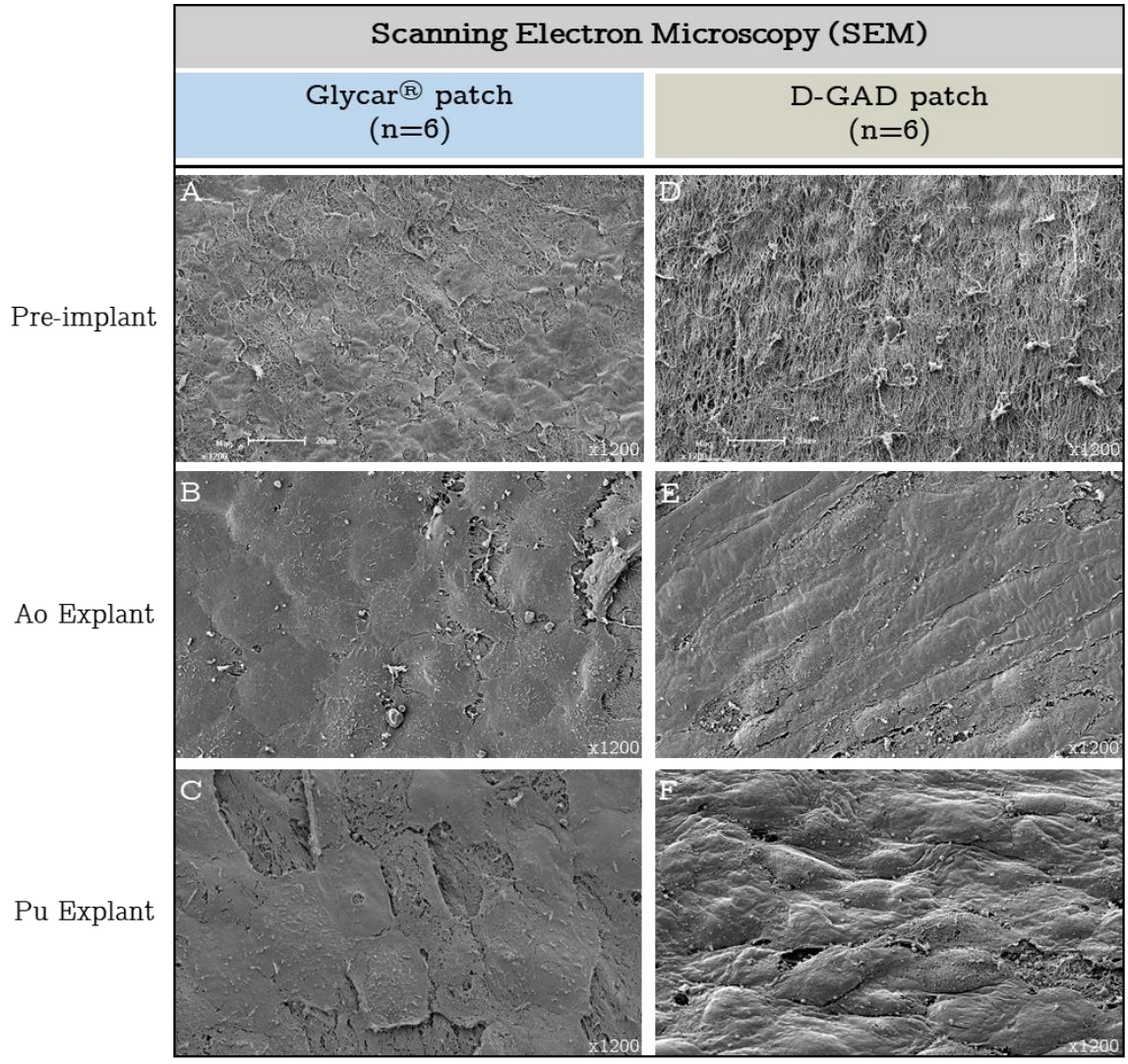

Figure 6.6 SEM of pre-implanted and explanted aorta and pulmonary pericardium: Glycar® and D-GAD patches. (A-F = 1200x magnification)

Transmission electron microscopy (TEM)

TEM demonstrated well-defined collagen fibers (black arrow) that included (a) transverse cut fibrils and (b) longitudinal cut fibrils on the pre-implanted and explanted Glycar® (Figure 6.7A-F) and D-GAD patches (G-L). The collagen of the Glycar® patches were densely compacted/collapsed (C, E) compared to the D-GAD patches (I, K). The absence of cells in micrograph G and H demonstrated acellularity of the implanted D-GAD patches. Devitalized fibroblast-like cells (e) were seen in the explanted Glycar® patches (C, F). However, fibroblast-like cells (d) with defined cellular structures, membranes and secretory vacuoles (arrow heads) were visible on the explanted aorta and pulmonary D-GAD patches (J, L). The secretory vacuoles have the potential to produce new collagen.

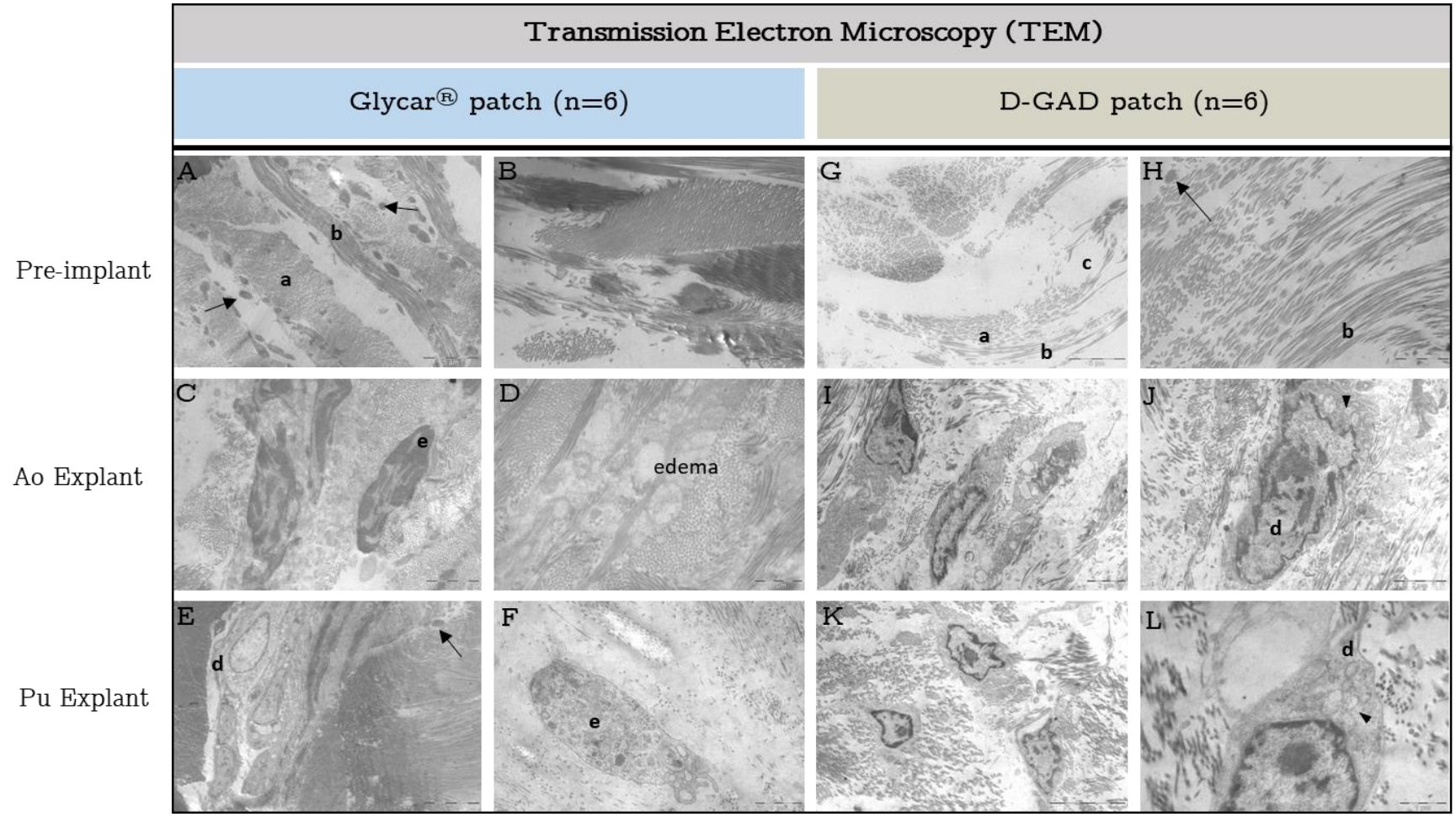

Figure 6.7 TEM of pre-implanted and explanted aorta and pulmonary pericardium: Glycar® and D-GAD patches. (a) transverse cut fibrils, (b) longitudinal cut fibrils (c) devitalized fibroblast-like cells with loss of membrane integrity (d) cells displaying fibroblast-like properties, (↑) elastin fiber and (▲) secretory vacuoles (A, E, G, K = 3400x; B, C, H, I, J = 7900x; D, F, L =13500x magnification)

6.4.5 Pericardial thickness

Prior to processing, Glycar® patches are standardized and selected based on pericardial thickness however, this was not done for the D-GAD patches and only a homogenous part of the pericardium was selected. Therefore, each group served as its own control and the groups were not compared.

The explanted Glycar® aortic (median 0.403 ± 0.085) and pulmonary patches (median 0. 951 ± 0.116) were significantly thicker compared to the pre-implantation values (0.278 ± 0.074) due to the developed fibrous encapsulation (Figure 6.8). When only comparing the patch thickness, the thickness of the Glycar® patch did not remarkably increased from pre-implantation to explantation in both the aorta (0.281 ± 0.029) and pulmonary patch (0.316 ± 0.076).

At explantation the thickness of the D-GAD pulmonary patch (median 1.053 ± 0.386) did not differ much from the initial pre-implanted patch (median 0.808 ± 0.326). The D-GAD aortic patch decreased in thickness from pre-implantation (median 0.808±0.326) to explantation (median 0.734 ± 0.383) whilst retaining comparable strength to the Glycar® patches.

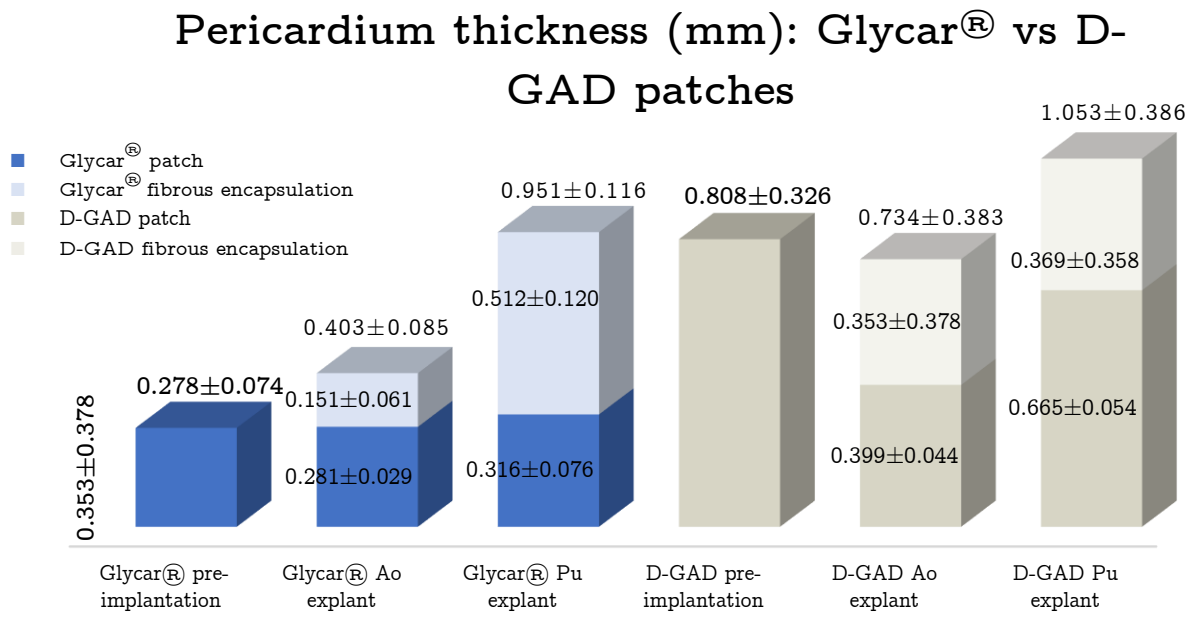

Figure 6.8 Pericardial thickness: Glycar® and D-GAD patches

6.5 Discussion

Clinically, both patches did not develop any signs of calcification, infective endocarditis or aneurysms. The structure and morphological characteristics of the D-GAD patch was not inferior to the commercialized Glycar® patch after being implanted in the aortic and pulmonary circulation of a juvenile ovine model for 180-days. In both the Glycar® and D-GAD groups the tissue integrity and structure were well preserved. Importantly, the D-GAD patches demonstrated recipient cell infiltration and complete reendothelialization.

Synergy between the decellularized detergents used in our decellularization /sterilization process was confirmed by Dr L Laker, PhD, 2019 and Bester et al., 2017). However, after the decellularization process the tissue was fixed with GA (0.625%) to increase scaffold stability and strength followed by the removal of residual aldehyde toxicity with 75% propylene glycol.

As expected, the pre-implanted Glycar® pulmonary pericardial patches were significantly stronger (TS, p=0.0001) and less pliable (YM, p=0.0150) than the pre-implanted pulmonary D-GAD patches. However, at explantation both the TS and YM was comparable between the two (2) groups with no statistical differences. The TS of both groups exceeded the strength of the native human ascending aorta (1.8 ± 0.24 MPa) as published by Sommer et al. (2008).

The D-GAD patches were successfully decellularized as no nuclear remnants could be detected by routine H&E or DAPI staining prior to implantation. Dr L Laker, PhD (2019) confirmed the absence of DNA with a quantitative DNA analysis.

Echocardiographic and macroscopic evaluations demonstrated no signs of calcification, infective endocarditis or aneurysm formation at explantation. Thus, both groups demonstrated resistance to calcification in an aggressive juvenile ovine model for the study period. In GA-fixated BP the mechanism of calcification has been attributed to both chronic immune responses (Kim et al., 2015; Manji et al., 2006 Human & Zilla, 2001) and fixation processes (Golomb et al., 1987; Levy et at., 1986). Specifically, damaged collagen may become a nucleus for calcium deposition in implanted xenografts (Wong et al., 2016). Sinha et al., (2012) reported the presence of calcification when the GA-concentration exceeded 0.625%. The GA exposure time to fixation were also similar between groups.

The elastin of the aorta and pulmonary Glycar® patches were better preserved from implantation to explantation compared to the aorta and pulmonary patches of the D-GAD group.

The collagen of the Glycar® patches were densely compacted/collapsed while the collagen of the D-GAD patches had a more separated and wavier appearance. The

D-GAD patches demonstrated host cell infiltration of fibroblast-like cells in both the explanted aorta and pulmonary patches. The Glycar® patches demonstrated no host cell infiltration into the patch itself but fibroblast-like cells were seen in the fibrous encapsulation. GA-fixed bovine pericardium is known to show early deterioration with limited remodeling, regeneration, and growth potential (Wong et al., 2016; Dohmen et al., 2014; Valente et al., 1992; Kirklin et al., 1989; Fiddler et al., 1983). Liao et al. (2008) reported that decellularization protocols based on SDS, Trypsin and TX resulted in a disrupted collagen network and the ECM pore size varied as a function of the protocol used. According to Murphy & O'Brien, (2010) the mean pore size between collagen promotes host cell infiltration. The collagen of the explanted D-GAD patches was well-separated providing a more suitable mean pore size for cellular infiltration. This explains why more fibroblast-like cells were seen in the explanted D-GAD patches compared to the Glycar® patches.

The fibroblast-like cells seen in the explanted D-GAD patches demonstrated large nuclei, cytoplasm and clear cellular borders. The cells contained numerous secretory vacuoles which can promote the formation of new collagen fibrils and bundles by playing an integral role in the secretion of procollagen (Canty & Kadler, 2005; Cross & Mercer, 1993). In contrast, the limited number of cells seen in the explanted Glycar® patches were pyknotic, fibroblast-like cells displaying loss of membrane integrity.

SEM demonstrated that the decellularization step removed all endothelial cells from the D-GAD patches prior to implantation and the endothelial cells of the Glycar® patch were severely dehydrated with collapsed extra nuclear areas and areas of dehiscence from the basal membrane but with minimal loss of fiber architecture. However, at explantation the surface area of the aorta and pulmonary patches of both groups displayed endothelial coverage.

The aortic and pulmonary patches of both groups developed a fibrous encapsulation on the interior and posterior side of the surgical implants. Numerous fibroblast-like cells were visible within these encapsulations. Chemical fixation with GA alters the ultrastructure, composition, and surface topology of tissues promoting a foreign-body response mediated by the formation of a fibrous encapsulation because the innate cells is unbale to recognize the implant as self (Badylak, 2014). However, no mononuclear cells were visible within the fibrous encapsulation of both groups. McPherson et al. (1986) examined the influence of GA-treatment concentrations (ranging from 0.01 to 1.0%) on the biological responses of collagen implants. An inflammatory response was initiated against the implants in all these concentrations with the most severe response documented with implants crosslinked with 1% GA (Badylak, 2007).

In the Glycar® patches, the fibrous encapsulation contributed to an increase in patch thickness from implantation (0.278 ± 0.074) to explantation (Ao, 0.403 ± 0.085; Pu, 0.951 ± 0.116). However, if only patch thickness was compared, the thickness of the explanted patches (Ao, 0.281 ± 0.029; Pu, 0.316 ± 0.076) compared well with the thickness of the pre-implanted patches and did not remarkably thicken over time. However, the pre-implanted D-GAD patches were significantly thicker compared to the Glycar® patches because the D-GAD patches were not selected based on patch thickness but the Glycar® patches were. SDS used in the decellularization process can cause an increase in scaffold thickness because it is an ionic detergent capable of promoting swelling in tissue (Li et al., 2018; Mallis et al., 2017). If the thickness of the fibrous encapsulation was not taken into consideration the thickness of the D-GAD patches declined from implantation (0.808 ± 0.326) to explantation in both the aortic (0.399 ± 0.044) and pulmonary (0.665 ± 0.054) patches. However, at explantation both groups demonstrated similar strength despite the difference in patch thickness.

6.6 Conclusion

The tissue strength and pliability of both groups were comparable and demonstrated adequate strength to withstand implantation in the aortic and pulmonary circulation for 180-days. Both the Glycar® and D-GAD patches developed a fibrous encapsulation on the interior and posterior side of the patch as a result of a foreign body response. However, no mononuclear cells were visible within this fibrous encapsulation in both groups. None of the aortic or pulmonary implants demonstrated evidence of calcification, infective endocarditis, aneurysm formation or degeneration.

The major difference between the Glycar® and D-GAD patches were the amount of recellularization demonstrated. The D-GAD patches demonstrated much better cellular infiltration compared to the Glycar® patches. This could be attributed to (i) the better preservation of the collagen matrix and (ii) adequate pore size to promote cellular infiltration.

The D-GAD patches were not structurally or morphologically inferior to the commercially available Glycar® patches. In addition, the recellularization/remodeling potential demonstrated by the D-GAD patches makes this patch a very attractive option especially in younger patients.

Limitations and recommendations

Data provided by the juvenile sheep model cannot be unconditionally applied to human patients. Measuring pericardial thickness prior to processing was not available for Glycar® nor D-GAD patches. Due to technical limitations, tissue implanted in the descending aorta did not allow a large enough tissue sample upon explantation for TS/YM determination.

For future studies we recommend that immunohistochemistry be added to the list of analyses to describe cell types and immunological processes involved. Extending the implantation time might render better host-cell infiltration in the D-GAD patch.

References

Aguiari, P., Iop, L., Favaretto, F., Fidalgo, C.M.L., Naso, F., Milan, G., Vindigni, V., Spina, M., Bassetto, F., Bagno, A., Vettor, R. & Gerosa, G. 2017. In vitro comparative assessment of decellularized bovine pericardial patches and commercial bioprosthetic heart valves. *Biomedical Materials*, 12(1): 1-12.

Badylak, S.F. 2014. Decellularized allogeneic and xenogeneic tissue as a bioscaffold for regenerative medicine: factors that influence the host response. *Annuals of Biomedical Engineering*, 42: 1517–1527.

Badylak, S.F. 2007. The extracellular matrix as a biologic scaffold material. *Biomaterials*, 28(25): 3587–3593.

Bester, D., Smit, F.E., van den Heever, J.J., Botes, L., Dohmen P. M. C. E. Detoxification and stabilization of implantable or transplantable biological material. Patent 16702008.0-1455, EU, 2017.

Bielli, A., Bernardini, R., Varvaras, D., Rossi, P., Di Blasi, G., Petrella, G., Buonomo, O.C., Mattei, M. & Orlandi, A. 2018. Characterization of a new decellularized bovine pericardial biological mesh: Structural and mechanical properties. *Journal of the Mechanical Behavior of Biomedical Materials*, 78(2018): 420–426.

Canty, E.G. & Kadler, K.E. 2005. Procollagen trafficking, processing and fibrillogenesis. *Journal of Cell Science*, 1:118(Pt 7): 1341-1353.

Costa, A., Naranjo, J.D., Londono, R. & Badylak, S.F. 2017. Biologic scaffolds. *Cold Spring Harbor Perspectives in Medicine*, 7(9): 1–24.

Cross, P.C, Mercer, K.L. 1993. Cell and Ultrastructure. WH Freeman publishers, 2nd edition. pages 70-75.

Dohmen, P.M., da Costa, F., Lopes, S.V., Vilani, R., Bloch, O. & Konertz, W. 2014. Successful implantation of a decellularized equine pericardial patch into the systemic circulation. *Medical Science Monitor Basic Research*, 20: 1–8.

Fiddler, G.I., Gerlis, L.M., Walker, D.R., Scott, O. & Williams, G.J. 1983. Calcification of glutaraldehyde-pre- served porcine and bovine xenograft valves in young children. *Annuals of Thoracic Surgery*, 35(3): 257–261.

Gilbert, T.W., Sellaro, T.L. & Badylak, S.F. 2006. Decellularization of tissues and organs. *Biomaterials*, 27(19): 3675–3683.

Human, P. & Zilla, P. 2001. Characterization of the immune response to valve bioprostheses and its role in primary tissue failure. *Annuals of Thoracic Surgery*, 71: S385–S388.

Keane, T.J., Swinehart, I.T. & Badylak, S.F. 2015. Methods of tissue decellularization used for preparation of biologic scaffolds and in vivo relevance. *Methods*, 84: 25–34.

Kim, M.S., Jeong, S., Lim, H.G. & Kim, Y.J. 2015. Differences in xenoreactive immune response and patterns of calcification of porcine and bovine tissues in α-Gal knock-out and wild-type mouse implantation models. *European Journal of Cardiothoracic Surgery*, 48(3): 392–399.

Kirklin, J.K., Kirklin, J.W., Blackstone, E.H., Milano, A. & Pacifico, A.D. 1989. Effect of transannular patching on outcome after repair of tetralogy of Fallot. *Annuals of Thoracic Surgery*, 48(6): 783–791.

Laker L. The evaluation of a novel decellularization and sterilization process on bovine pericardial tissue. PhD Thesis, University of the Free State, South Africa, 2019.

Lam, M.T. & Wu, J.C. 2012. Biomaterial applications in cardiovascular tissue repair and regeneration. *Expert Review of Cardiovascular Therapy*, 10(8): 1039–1049.

Levy, R.J., Schoen, F.J., Sherman, F.S., Nichols, J., Hawley, M.A. & Lund, S.A. 1986.

Calcification of subcutaneously implanted type I collagen sponges. Effects of formaldehyde and glutaraldehyde pretreatments. *American Journal of Pathology,* 122(1): 71–82.

Liao, J., Joyce, E.M. & Sacks, M.S. 2008. Effects of decellularization on the mechanical and structural properties of the porcine aortic valve leaflet. *Biomaterials*, 29(8): 1065–1074.

Li, N., Li, Y., Gong, D., Xia, C., Liu, X. & Xu, Z. 2018. Efficient decellularization for bovine pericardium with extracellular matrix preservation and good biocompatibility. *Interactive CardioVascular and Thoracic Surgery*, 26(5): 768–776.

Liu, Z.Z., Wong, M.L. & Griffiths, L.G. 2016. Effect of bovine pericardial extracellular matrix scaffold niche on seeded human mesenchymal stem cell function. *Scientific Reports*, 6: 1–12.

Mallis, P., Michalopoulos, E., Dimitriou, C., Kostomitsopoulos, N. & Stavropoulos-Giokas, C. 2017. Histological and biomechanical characterization of decellularized porcine pericardium as a potential scaffold for tissue engineering applications. *Bio-Medical Materials and Engineering*, 28(5): 477–488.

Manji, R.A., Zhu, L.F., Nijjar, N.K., Rayner, D.C., Korbutt, G.S., Churchill, T.A., Rajotte, R.V., Koshal, A. & Ross, D.B. 2006. Glutaraldehyde-fixed bioprosthetic heart valve conduits calcify and fail from xenograft rejection. *Circulation*, 114: 318–327.

McPherson, J.M., Sawamura, S. & Armstrong, R. 1986. An examination of the biologic response to injectable, glutaraldehyde crosslinked collagen implants. *Journal of Biomedical Materials Research*, 20: 93-107.

Mendoza-Novelo, B., Alvarado-Castro, D.I., Mata-Mata, J.L., Cauich-Rodríguez, J. V., Vega-González, A., Jorge-Herrero, E., Rojo, F.J. & Guinea, G. V. 2013. Stability and mechanical evaluation of bovine pericardium cross-linked with polyurethane prepolymer in aqueous medium. *Materials Science and*

Engineering C, 33(4): 2392–2398.

Mendoza-Novelo, B. & Valerio, J. 2011. Decellularization, stabilization and functionalization of collagenous tissues used as cardiovascular biomaterials. *Biomaterials - Physics and Chemistry* - New Edition. Retrieved from: https://www.intechopen.com/books/biomaterials-physics-and-chemistry/decellularization-stabilization-and-functionalization-of-collagenous-tissues-used-as-cardiovascular- [accessed 20 August 2019].

Murphy, C.M. & O'Brien, F.J. 2010. Understanding the effect of mean pore size on cell activity in collagen-glycosaminoglycan scaffolds. *Cell Adhesion and Migration*, 4(3): 377–381.

Neethling, W., Brizard, C., Firth, L. & Glancy, R. 2014. Biostability, durability and calcification of cryopreserved human pericardium after rapid glutaraldehyde-stabilization versus multistep ADAPT® treatment in a subcutaneous rat model. *European Journal of Cardiothoracic Surgery*, 45(4): 110–117.

Neethling, W.M.L., Glancy, R. & Hodge, A.J. 2010. Mitigation of calcification and cytotoxicity of a glutaraldehyde-preserved bovine pericardial matrix: improved biocompatibility after extended implantation in the subcutaneous rat model. *The Journal of Heart Valve Disease*, 19(6): 778–785.

Nogueira, G.M., Rodas, A.C.D., Weska, R.F., Aimoli, C.G., Higa, O.Z., Maizato, M., Leiner, A.A., Pitombo, R.N.M., Polakiewicz, B. & Beppu, M.M. 2010. Bovine pericardium coated with biopolymeric films as an alternative to prevent calcification: In vitro calcification and cytotoxicity results. *Materials Science and Engineering C*, 30(4): 575–582.

Parenteau-Bareil, R., Gauvin, R. & Berthod, F. 2010. Collagen-based biomaterials for tissue engineering applications. *Materials*, 3(3): 1863–1887.

Remi, E., Khelil, N., Di, I., Roques, C., Ba, M., Medjahed-Hamidi, F., Chaubet, F., Letourneur, D., Lansac, E. & Meddahi-Pelle, A. 2011. Pericardial Processing: Challenges, Outcomes and Future Prospects. *Biomaterials Science and*

Engineering. Retrieved from: http://www.intechopen.com/books/biomaterials-science-and-engineering/pericardial-processing-challenges-outcomes-and-future-prospects. [accessed 20 October 2019].

Saporito, W.F., Pires, A.C., Cardoso, S.H., Correa, J.A., Carlos De Abreu, L., Valenti, V.E., Miller, L.M.R. & Colombari, E. 2011. Bovine pericardium retail preserved in glutaraldehyde and used as a vascular patch. *BioMed Central Surgery*, 11:37-44.

Sinha, P., Zurakowski, D., Susheel Kumar, T.K., He, D., Rossi, C. & Jonas, R.A. 2012. Effects of glutaraldehyde concentration, pretreatment time, and type of tissue (porcine versus bovine) on postimplantation calcification. *Journal of Thoracic and Cardiovascular Surgery*, 143(1): 224–227.

Sommer, G., Gasser, T.C., Regitnig, P., Auer, M. & Holzapfel, G.A. 2008. Dissection properties of the human aortic media: An experimental study. *Journal of Biomechanical Engineering*, 130(2): 1-12.

Valente, M., Laborde, F., Thiene, G., Milano, A., Talenti, E. & Gallix P. 1992. Glutaraldehyde-fixed bovine iliac veins used as bioprosthetic conduits: an experimental animal study. *Journal of Cardiac Surgery*, 7(2): 156–162.

Wong, M.L., Wong, J.L., Vapniarsky, N., Griffiths, L. G. 2016. In vivo xenogeneic scaffold fate is determined by residual antigenicity and extracellular matrix preservation. *Biomaterials*, 92: 1-12.

Yoo, J.S., Kim, Y.J., Kim, S.H. & Choi, S.H. 2011. Study on genipin: A new alternative natural crosslinking agent for fixing heterograft tissue. *Korean Journal of Thoracic and Cardiovascular Surgery*, 44(3): 197–207.

Chapter 7 - Article 4

Comparison of the tissue integrity and morphology between decellularized bovine pericardial scaffolds with and without glutaraldehyde fixation in a 180-day implant study in the juvenile ovine model

Botes L[1], Laker L[2], Dohmen PM[2&3], van den Heever JJ[2], Jordaan CJ[2], Goedhals J[4], Smit FE[2]

[1]*Department of Health Sciences, Central University of Technology, Free State, Bloemfontein, South Africa*

[2]*Department of Cardiothoracic Surgery, University of the Free State, Bloemfontein, South Africa*

[3]*Department of Cardiac Surgery, Heart Centre Rostock, University of Rostock, Germany*

[4]*Department of Anatomical Pathology, University of the Free State, Bloemfontein, South Africa*

Abstract

Introduction:
The potential to use a decellularized pericardial scaffold assumes that the major cellular immunogenic components have been removed, and that the remaining extracellular matrix (ECM) should retain its mechanical properties and functional design. Decellularization agents are known to reduce mechanical strength of pericardial scaffolds. Glutaraldehyde (GA)-fixation is known to improve scaffold strength. This study compared the impact of a novel decellularization method with and without GA-fixation on the tissue integrity and morphology of bovine pericardial scaffolds in an ovine model. Methods: The impact of the processing methods on tissue strength and morphology was assessed prior to implantation. Bovine decellularized pericardial scaffolds (BPS, Group 1) were implanted in the descending aorta and main pulmonary artery of six (6) sheep and bovine decellularized, GA-fixed and detoxified (D-GAD patches, Group 2) were implanted in six (6) sheep at the same anatomical locations. The clinical, mechanical and morphological integrity of the explanted scaffolds were evaluated and compared after 180-days of implantation. Results: The tensile strength (TS, $p = 0.0514$) and the Youngs Modulus (YM, $p = 0.0605$) of the pre-implanted BGS and D-GAD groups were comparable. Acellularity was confirmed in both Group 1 and 2 after processing. The collagen bundles in both groups were well preserved prior to implantation but the collagen in Group 1 was a bit wavier and more separated compared to Group 2. The clinical performance of both groups was excellent, and echocardiography confirmed the absence of aneurysm formation, calcification or disintegration. The explanted pulmonary TS and elastic modulus was comparable between groups (TS, $p = 0.0628$; YM, $p = 0.3121$) and above the minimum native human ascending aorta strength (1.8 ± 0.24 MPa). Calcification was absent in the explanted aorta and pulmonary scaffolds/patches of both groups. Compared to Group 2, the explanted collagen of Group 1 had a wavier appearance and were less dense that promoted more fibroblast-like cellular infiltration. Secretory vacuoles visible within the fibroblast-like cells can promote procollagen secretion. Group 2 developed a fibrous encapsulation as a result of a foreign body response. The BPS did not thicken over time. Conclusion: Decellularization in combination with GA-fixation did not add any benefits to the structural and morphological integrity of the decellularized pericardial scaffold after 180-days. Extending the explantation time might provide a clearer indication if GA-fixation with decellularization do provide additional benefits compared to decellularization alone.

Keywords: Bovine, pericardium, glutaraldehyde, fixation, decellularization, strength, morphology, calcification

7.1 Introduction

Decellularization of biological materials were introduced to minimize the host-tissue response, as xenogeneic cellular antigens induce an immune response contributing to chronic tissue rejection (Gates et al., 2017).

Different combinations and concentrations of decellularization agents/detergents have different effects on the structural and mechanical properties of the scaffolds ECM (Bielli et al., 2018; Gilpin & Yang, 2017). Numerous decellularization protocols have been introduced and are adapted to provide the best decellularization efficiency for a specific target tissue and implantation site. Remi et al. (2011) and Gilpin & Yang, 2017 provides excellent summaries of the different decellularization methods developed and their effects on tissue integrity and morphology. The majority of these decellularization methods used Triton X-100 (TX), sodium deoxycholate (SDC) and sodium dodecyl sulfate (SDS) (Aguiari et al., 2017) as detergents.

Standard decellularization protocols includes several steps starting with lysis of the cell membrane, enzymatic treatments to separate cellular components from the ECM, and solubilization of nuclear and cytoplasmic cellular components followed by extensive washing to remove residual chemicals (Gilbert, 2006).

Each of the agents used during the process affects the composition and ultrastructure of the ECM and accordingly, affects the host tissue response to the ECM scaffold following implantation (Gilbert et al., 2006). SDS (ionic detergent) solubilizes both cytoplasmic and nuclear cellular membranes but is cytotoxic which requires extensive washing and alters pericardial microstructure (collagen fibers and structural and signaling proteins) (Li et al., 2018; Gilpin & Yang, 2017; Tran et al., 2016). Furthermore, SDS can also promote tissue swelling (Mallis et al., 2017) and

Mendoza-Novelo and Cauich-Rodríguez, 2009 reported that irreversible swelling in decellularized bovine pericardium was associated with a 50% reduction in tissue strength when compared to native tissue and tissue treated with TX. TX (nonionic detergent) disrupts lipid-lipid and lipid-protein interactions and is often used to remove remnants of SDS and is less harsh on the tissue's structural integrity compared to SDS (Li et al., 2018; Gilpin & Yang, 2017). SDC (ionic detergent) seldomly used alone is effective to remove cellular remnants, solubilize cell membranes and can cause agglutination of DNA on the tissue's surface (Gilpin & Yang, 2017; Cissell et al., 2014).

Additional treatment options after decellularization may improve the mechanical and biological features of a scaffold (Remi et al., 2011). These treatments include crosslinking (i.e., GA, genipin, epoxy compounds, carbodiimides, dye-mediated photo-oxidation processes etc.)(Yoo et al., 2011; Remi et al., 2011) coating with biopolymeric films (i.e., chitosan, silk fibroin etc.)(Nogueira et al., 2010) and anti-calcification treatments (i.e., GA, L-glutamic acid, L-arginine etc.)(Remi et al., 2011; Grabenwoger et al., 1992). GA-fixation was added to our decellularization protocol to evaluate its impact on tissue strength and recellularization potential.

A decellularization protocol was developed by the Frater Cardiovascular Center in which synergy was demonstrated between the combination of detergents, washing and fixation techniques used. This resulted in excellent retention of scaffold strength equaling that of untreated native bovine pericardium (Dr L Laker, PhD, 2019). Two (2) decellularized bovine pericardial (BP) products were developed; one without GA crosslinking resulting in a bovine pericardial scaffold (BPS) and one that includes GA crosslinking and detoxification (D–GAD). The aim of this study was to compare the tissue integrity and morphology between the BPS and the D-GAD patch in a juvenile ovine model.

7.2 Materials and Methods

The study was initiated and performed by the RWM Frater Cardiovascular Research Centre, Department of Cardiothoracic Surgery, University of the Free State (UFS), South Africa. Ethical approval was obtained from the Animal Ethics Committee of the UFS prior to commencement (ETOVS Number: UFS-AED2015/0081, Appendix A1).

Bovine pericardial scaffolds (BPS) and decellularized GA-fixed and detoxified (D-GAD) patches

Refer to section 4.2, Materials and methods, Article 1, Chapter 4 for a detailed description of the decellularized method.

Refer to section 6.2, Materials and methods, Article 3, Chapter 6 for a detailed description of the D-GAD method.

7.2.1 Study design and layout

The study design was a prospective analytical cohort. The clinical and mechanical integrity [tensile strength (TS) and Young's Modulus (YM)] tissue morphology [hematoxylin and eosin (H&E), modified Verhoeff's von Gieson (EvG), Von Kossa (VK) histological stains, scanning electron microscopy (SEM) and transmission electron microscopy (TEM)] and thickness were evaluated in both groups prior to implantation and after explantation (Figure 7.1).

The BPS and D-GAD patches were implanted into twelve (12) juvenile Dorper Wether sheep. Six (6) sheep received two (2) BPS (Group 1), implanted in the descending aortic arch and the main pulmonary artery and six (6) sheep received two (2) D-GAD patches (Group 2) in the same anatomical locations as Group 1 (Figure 7.1).

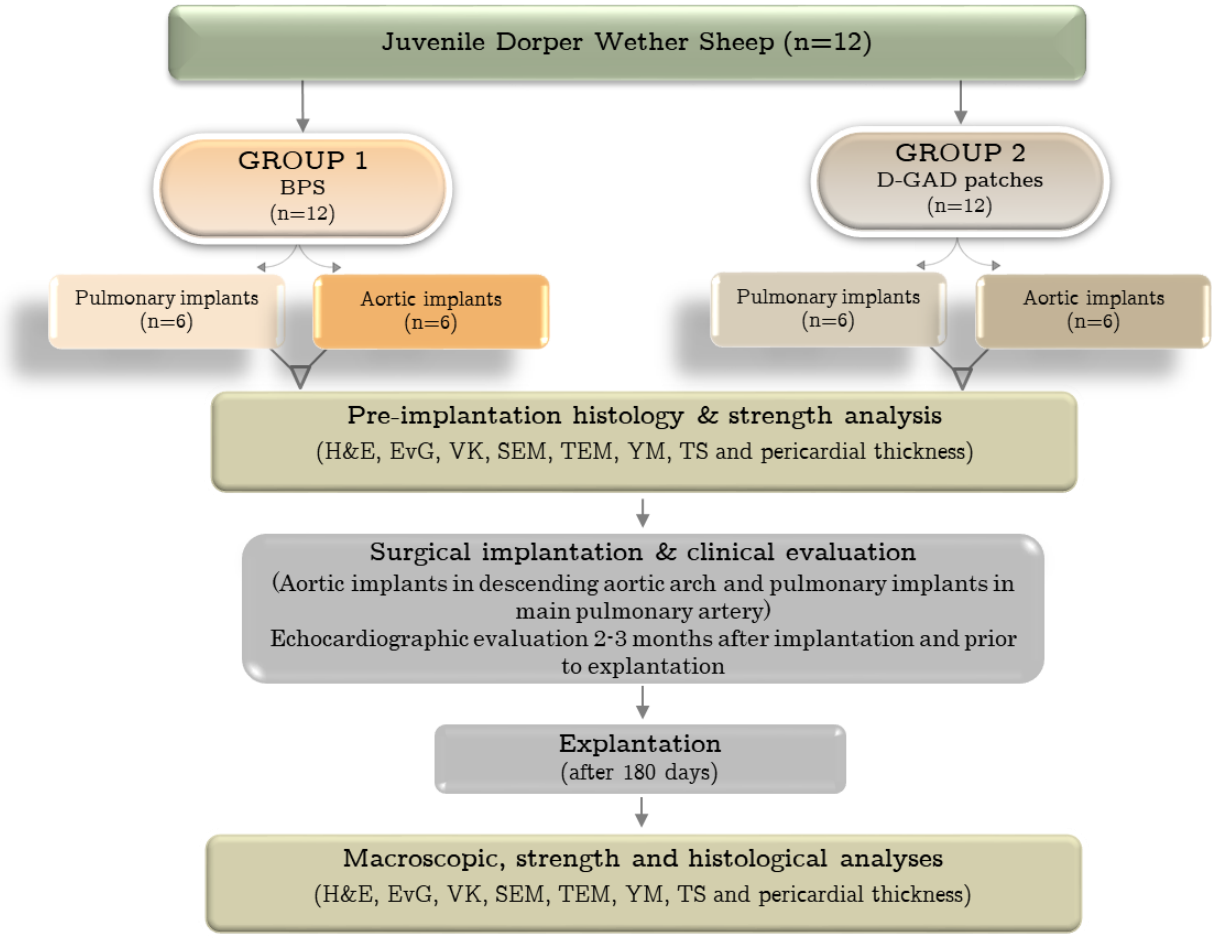

Figure 7.1 Study layout: Decellularized bovine pericardial scaffold (BPS) and decellularized GA-fixed and detoxified (D-GAD) patch (Pu = pulmonary; Ao = Aorta; H&E = hematoxylin and eosin; EvG = modified Verhoeff's von Gieson; VK = Von Kossa; YM = Young's modulus; TM = transmission electron microscopy; SEM = scanning electron microscopy; TEM = transmission electron microscopy)

7.2.2 Surgical protocol

A mini thoracotomy was performed on twelve (12) recipient sheep (aged 6-12 months; mean weight 25.75 ±2.13kg). Refer to section 4.2.2, Surgical protocol, Article 1, Chapter 4 for a detailed description of the surgical protocol.

7.2.3 Laboratory analysis

Samples of the twelve (12) BPS and D-GAD patches were taken from both the aorta and pulmonary BPS and D-GAD patches prior to implantation and at explantation after a minimum implantation period of 180-days. TS and YM analysis was only performed on the pulmonary patch because the implanted aortic BPS and D-GAD patches did not provide adequate tissue size to perform analysis.

7.2.3.1 Clinical evaluation

Echocardiographic examinations were performed 2-3 months after implantation and just before explantation to evaluate the patches for calcification, infective endocarditis and aneurysm formation.

7.2.3.2 Validation of acellularity

4', 6-Diamidino-2-Phenylindole (DAPI) staining

Refer to section 4.2.3.2, Validation of accellularity, Article 1, Chapter 4 for a detailed description of the DAPI method. The DAPI stains were performed by the Cardiovascular Research Unit of the University of Cape Town according to their standard operating procedure.

7.2.3.3 Strength evaluation

Tensile strength (TS) and Young's Modulus (YM)

Refer to section 4.2.3.3, Strength evaluation, Article 1, Chapter 4 for a detailed description of the TS and YM methods.

7.2.3.4 Structural Evaluation

Light Microscopy and electron microscopy

Refer to section 4.2.3.4, Structural evaluation, Article 1, Chapter 4 for detailed light and electron microscopy (SEM and TEM) methods.

7.2.3.5 Pericardial thickness

The measurement of pericardial thickness is described in section 4.2.3.5, Pericardial thickness, Article 1, Chapter 4.

7.3 Statistical analysis

Refer to section 4.3, Statistical analysis, Article 1, Chapter 4 for statistical methods used.

7.4 Results

7.4.1 Clinical evaluation

The handling quality of both patches were satisfactory, but the BPS were more slippery compared to the D-GAD patch. All twelve (12) sheep survived till they were euthanized after a minimum of 180-days. The echocardiographic and macroscopic (after explantation) evaluations of the BPS and D-GAD groups demonstrated no evidence of aneurysm formation, infective endocarditis or calcification. One (1) sheep developed a false aneurysm (3 x 4 mm) on the suture line of the explanted aortic BPS.

7.4.2 Validation of acellularity

The DAPI (4', 6-Diamidino-2-Phenylindole) stain revealed no evidence of intact cell nuclei in both the BGS and the D-GAD pericardial scaffolds (Figure 7.2). The DAPI stain confirmed that acellularity was achieved in both groups after the decellularization process.

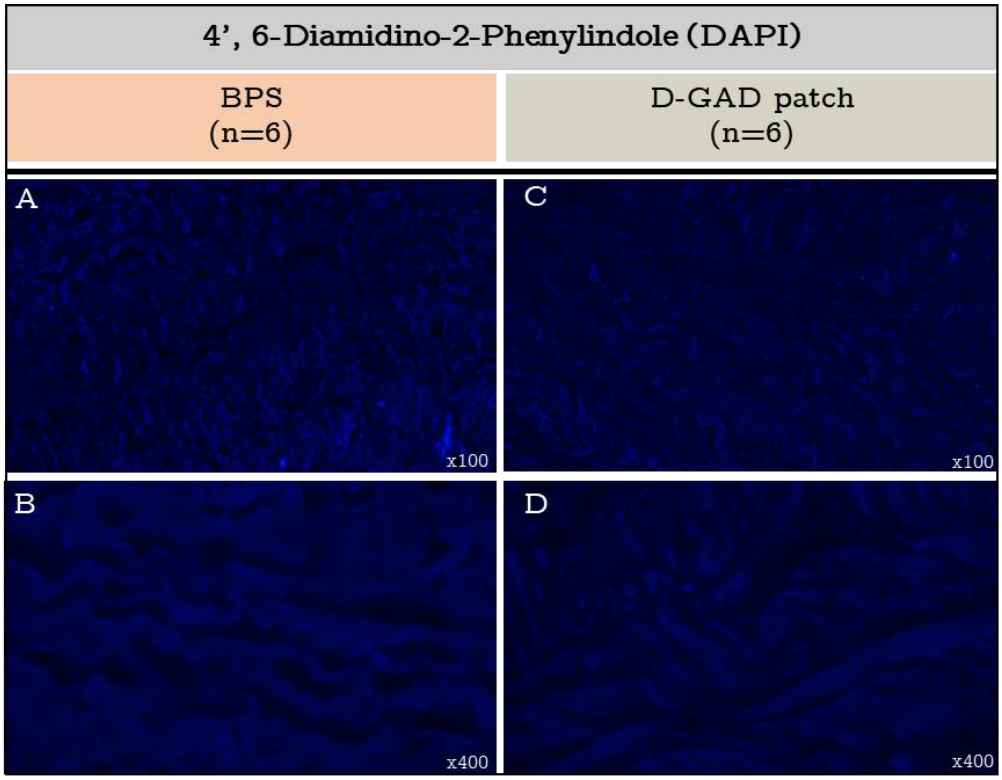

Figure 7.2 DAPI pre-implantation histological stain: BPS (A, B) and D-GAD patches (C, D). (A, C = 100x magnification and B, D = 400x magnification)

7.4.3 Strength evaluation

The two (2) groups demonstrated comparable strength and pliability prior to implantation (TS, p=0.0514; YM, 0.0605) and after explantation (TS, p = 0.0628; YM,p = 0.3121)(Table 7.1).

In both groups the TS decreased from implantation to explantation but only the BPS showed a statistically significant difference (p = 0.0004). The YM decreased from pre-implantation to explantation in both groups, but a significant difference was only observed in the D-GAD patches (p = 0.0121). The decrease in YM indicates an increase in elasticity/pliability of the explanted pericardial scaffolds/patches.

Table 7.1 Strength analysis of pre-implanted and explanted pericardium: BPS and D-GAD patches

Variable	BPS (n=6) (Median ± SD)			D-GAD (n=6) (Median ± SD)		
	Pre-implantation scaffold	Explant (Pu)	Pre-implant vs. Explant	Pre-implantation scaffold	Explant (Pu)	Pre-implant vs. Explant
YM (MPa)	16.69±9.87	9.81±3.55	p=0.2228	39.88±28.46	10.01±11.41	p=0.0121*
BPS vs D-GAD				p=0.0605	p=0.3121	
TS (MPa)	15.02±3.25	3.60±1.28	p=0.0004*	9.91±2.53	5.30±1.40	p=0.1051
BPS vs D-GAD				p=0.0514	p=0.0628	

*- Significant difference ($p<0.05$)(SD = Standard Deviation; Pu = Pulmonary; YM = Youngs modulus; TS = tensile strength; MPa=megapascals)

7.4.4 Structural evaluation

7.4.4.1 Light and electron microscopy

Hematoxylin and eosin (H&E)

The pericardial tissue structure was evaluated by light (H&E, EVG, VK)(Figure 7.3-7.4) and electron microscopy (SEM and TEM)(Figure 7.5-7.6). The H&E stain confirmed the absence of cells in both groups after the decellularization step prior to implantation (Figure 7.3A, B, G & J). The aorta (C, D & H, K) and pulmonary explants (E, F & I, J) in both groups demonstrated cellular ingrowth (↑) into the scaffolds/patches however, it was significantly more in the BPS explanted aorta (C, D) and pulmonary scaffolds (E, F). Furthermore, only the D-GAD patches developed a fibrous encapsulation (↕) on the interior and posterior side of the patch (I, K).

The collagen of both groups was well preserved, but the collagen bundles of the BPS had a wavier and well-separated appearance (B, D, F) compared to the collagen of the D-GAD patches (H, J, L).

Importantly, the aortic (D) and pulmonary (F) BPS was completely remodeled after the implantation time of 180-days. Both groups demonstrated endothelium on the pericardial surface area.

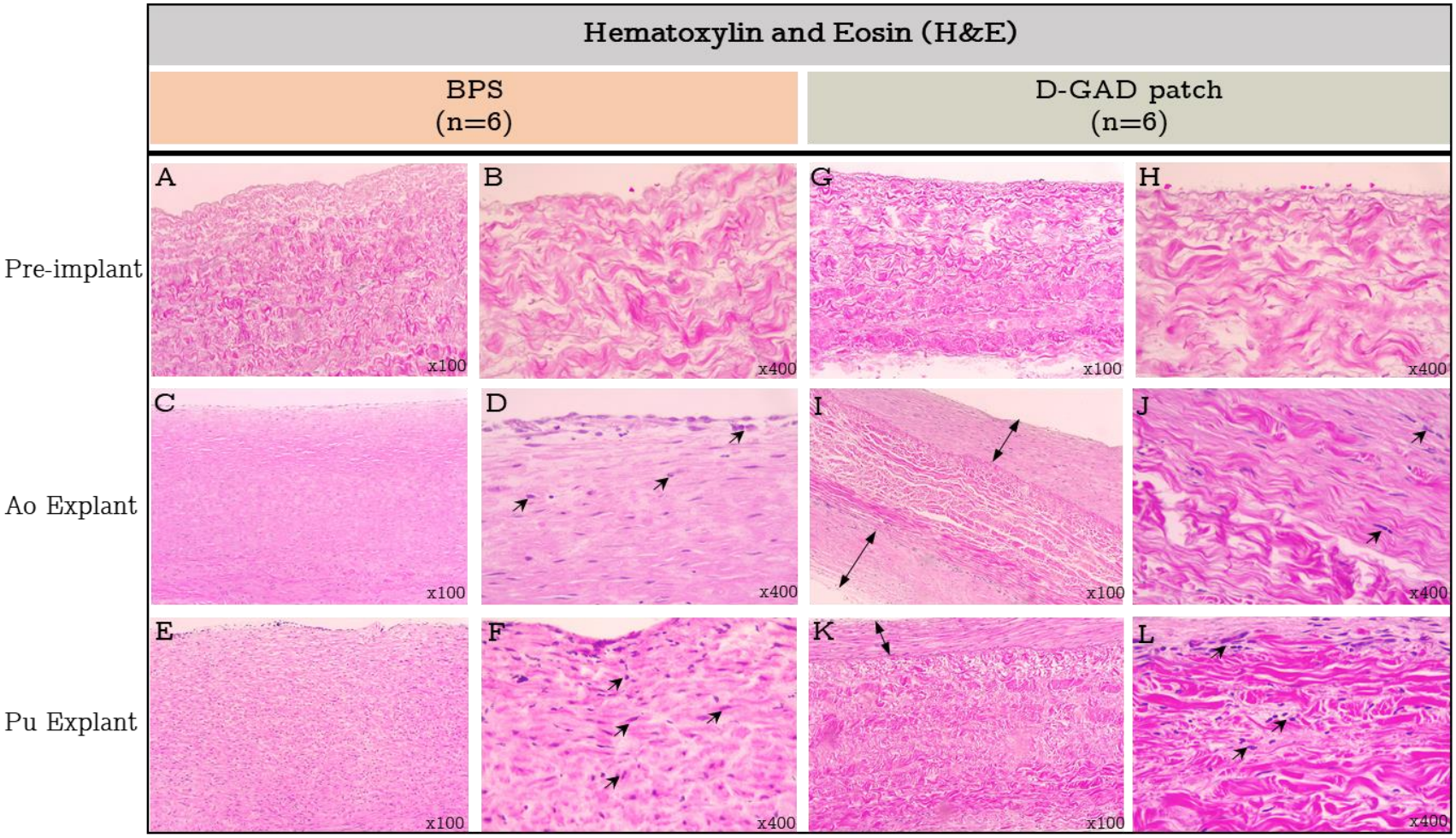

Figure 7.3 H&E of pre-implanted and explanted aortic and pulmonary pericardium: BPS and D-GAD patches. (↑) fibroblast-like cells; (↕) fibrous encapsulation. (A, C, E, G, H, I = 100x magnification and B, D, F, J, K, L = 400x magnification)

Modified Verhoeff von Gieson (EvG)

The pre-implantation EVG stains demonstrated elastin (black fiber strains) in both groups (Figure 7.4A & D) but were significantly less at explantation in the aortic (B & E) and pulmonary scaffolds (C & F) of both groups. However, most of the elastin present in the explanted D-GAD patches were seen in the fibrous encapsulation (E, F)(Figure 7.4).

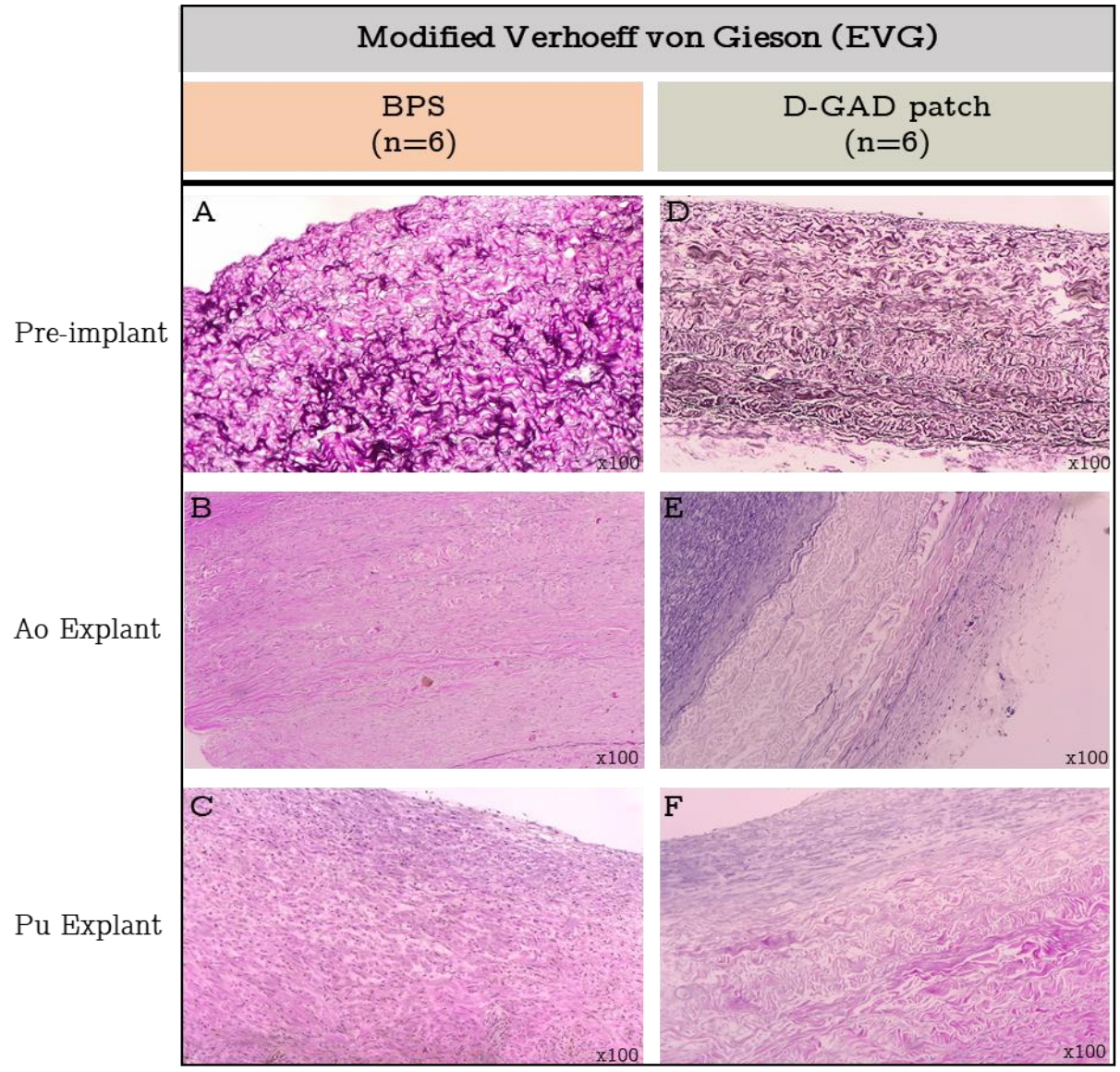

Figure 7.4 EVG histological stain of pre-implanted and explanted aortic and pulmonary pericardium: BPS and D-GAD patches. (A-F = 100x magnification)

Von Kossa (VK)

The VK stain confirmed that no calcification deposits (black) were visible in any of the pre-implanted or explanted aortic or pulmonary BPS or D-GAD groups (Figure 7.5).

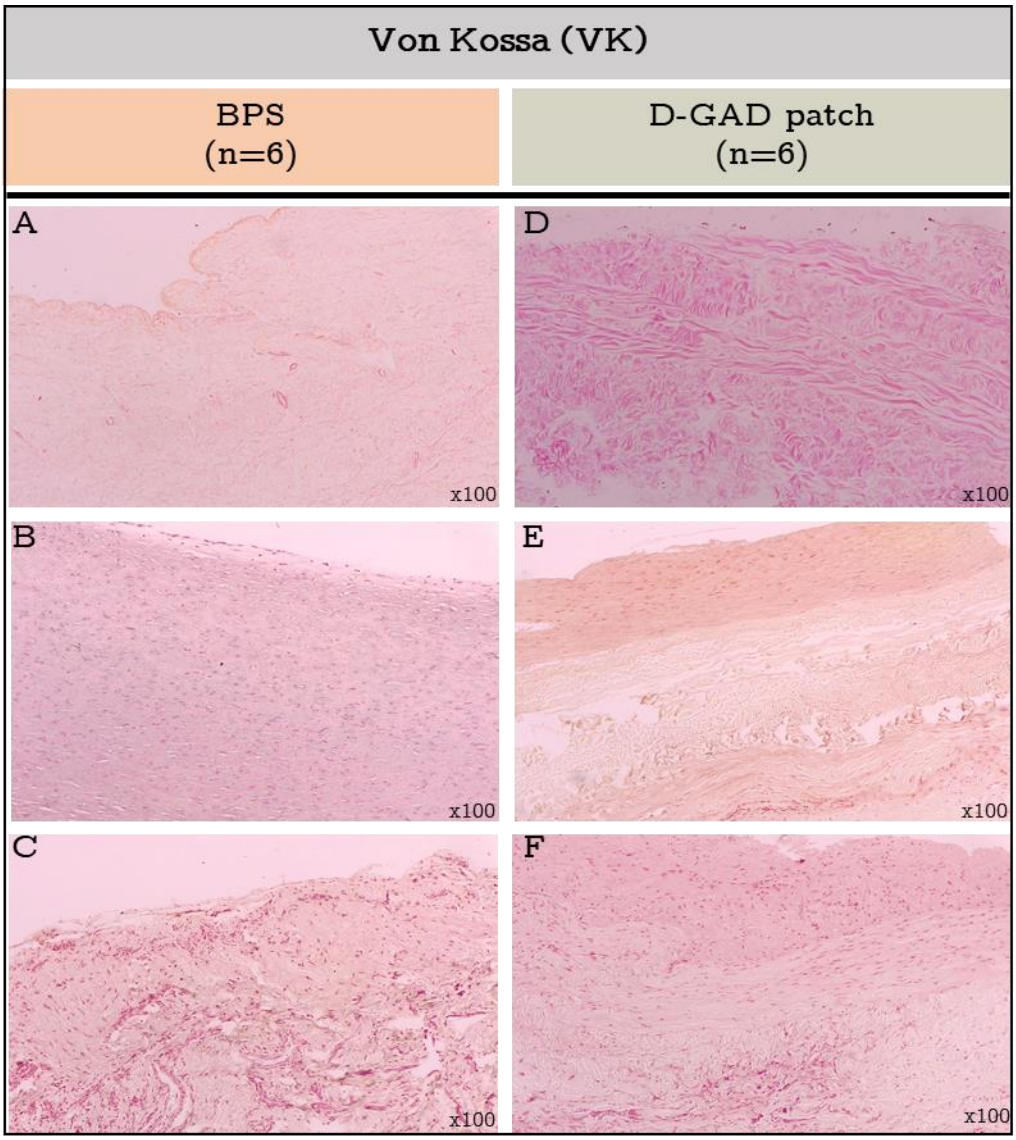

Figure 7.5 VK histological stain of pre-implanted and explanted aortic and pulmonary pericardium: BPS and D-GAD patches. (A-F = 100x magnification)

Scanning electron microscopy (SEM)

SEM demonstrated similar surface morphology between the two (2) groups. The pre-implantation micrographs of both groups (Figure 7.6A & D) demonstrated no endothelial cells or basal membrane with only a collagen scaffold that remained after the decellularization process. However, the serosa of both the aorta (B & E) and pulmonary explants (C & F) of both groups showed cobblestone-like endothelial cells in various amounts forming a confluent monolayer of cells.

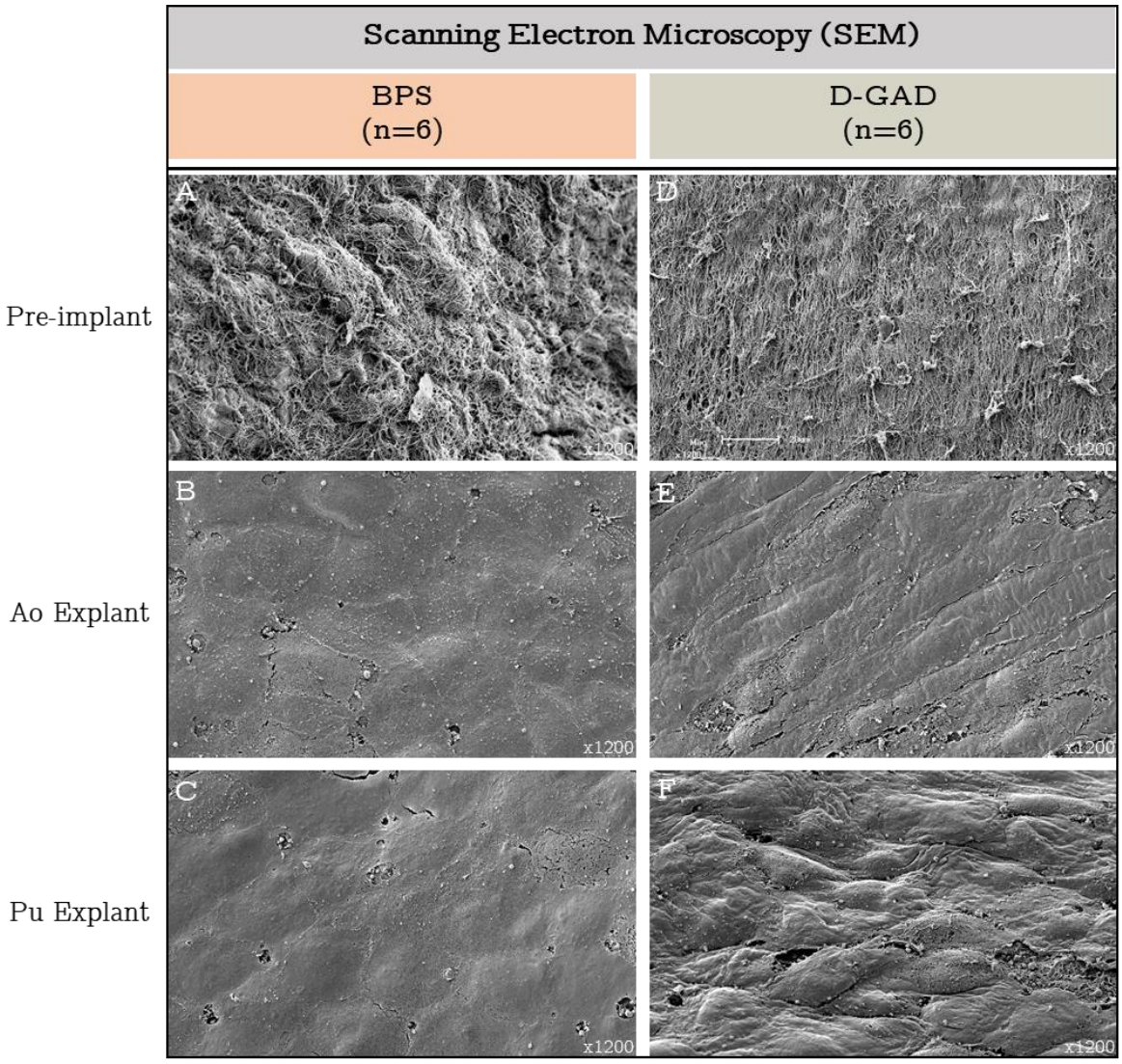

Figure 7.6 SEM of pre-implanted and explanted aorta and pulmonary pericardium: BPS and D-GAD patches. (A-F = 1200x magnification)

Transmission electron microscopy (TEM)

The ultrastructure of both the BPS and D-GAD demonstrated well-defined collagen fibers (Figure 7.7). Micrographs A & G indicated collagen fibers present as (a) transverse cut fibrils and (b) longitudinal cut fibrils. The pre-implanted BGS and D-GAD patches demonstrated no cells (A, B, & G, H). Cells displaying fibroblast-like properties (d) with well-defined cellular structures and membranes can be seen on the explanted aorta and pulmonary scaffolds (D, F & J, L) of both groups. The arrow heads (D, E, F & J, L) indicates secretory vacuoles in which procollagen is packaged from the Golgi complex. The collagen was more abundant in the BPS compared to D-GAD patches.

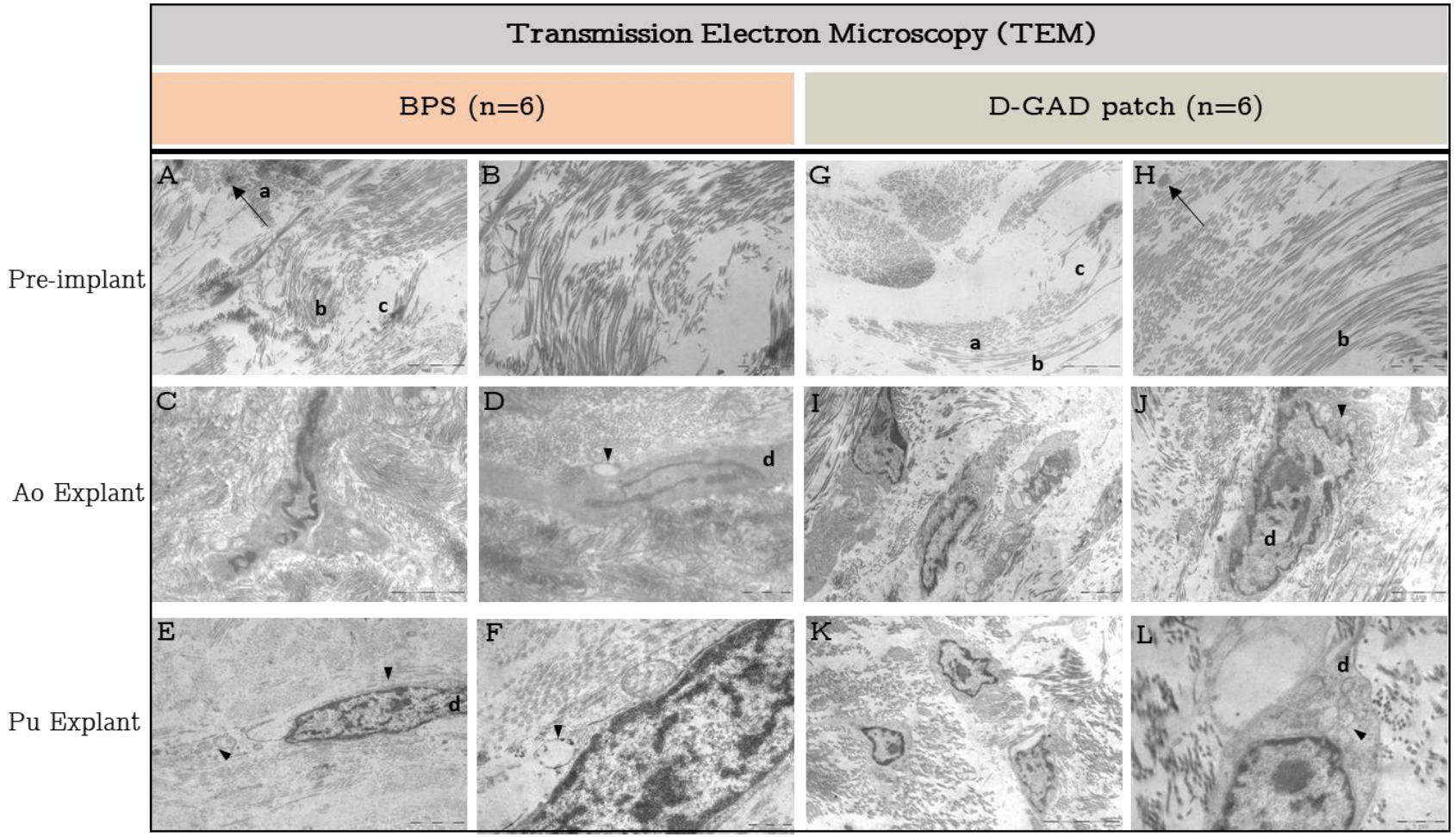

Figure 7.7 TEM of pre-implanted and explanted aorta and pulmonary pericardium: BPS and D-GAD patches. (a) transverse cut fibrils, (b) longitudinal cut fibrils (c) devitalized fibroblast-like cells with loss of membrane integrity (d) cells displaying fibroblast-like properties, (↑) elastin fiber and (▲) secretory vacuoles. (A, G, K = 3400x; B, C, E, H, J, I, = 7900x; L, D = 13500x ; F= 25000x magnification)

7.4.5 Pericardial thickness

Both the BPS and D-GAD patches were not selected based on pericardial thickness. Scaffolds/patches were cut from a homogenous part of the pericardium without taking thickness into consideration. Therefore, each group served as its own control and the groups were not compared.

The BPS did not develop a fibrous encapsulation and both the explanted aorta (median 1.416 ± 0.456) and explanted pulmonary scaffolds (median 1.054 ± 0.533) did not thicken over time when compared to the pre-implantation thickness (1.452 ± 0.129).

If only considering patch thickness, the D-GAD patches decreased in thickness from pre-implantation (median 0.808 ± 0.326) to explantation in both the aorta (median 0.399 ± 0.044) and pulmonary patches (median 0.665 ± 0.054). However, if the patch and fibrous encapsulation thickness was combined the aorta patch (median 0.734 ± 0.383) still did not exceed the pre-implantation thickness but the pulmonary explant did (median 1,053 ± 0.386).

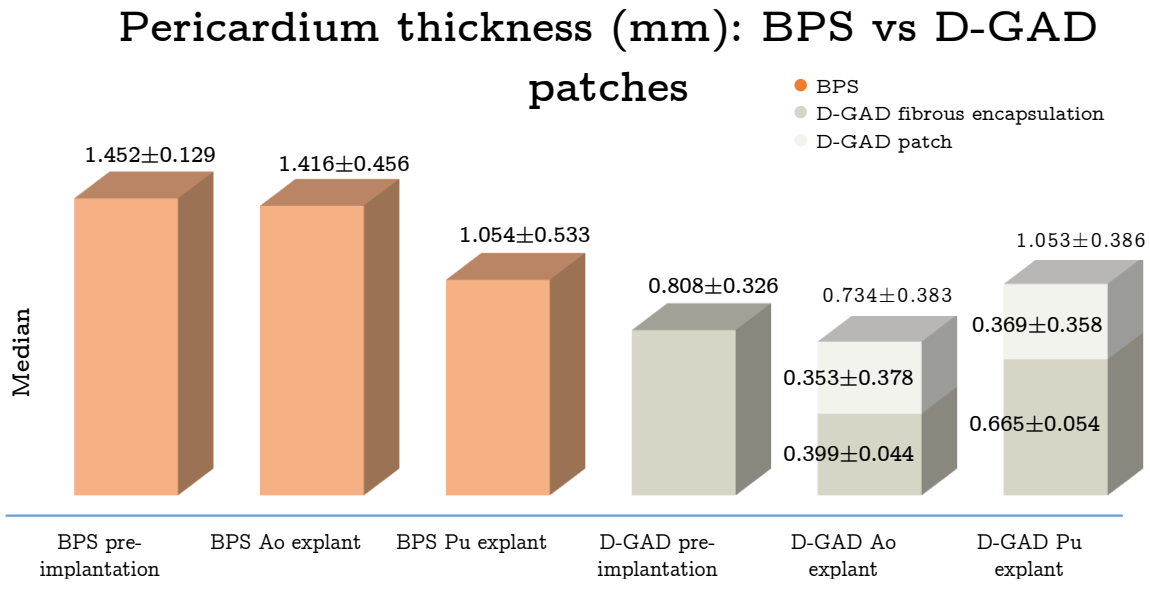

Figure 7.8 Pericardial thickness: BPS and D-GAD patches

7.5 Discussion

The potential to use a decellularized pericardial scaffold is based on the assumption that the major cellular immunogenic components have been removed, and that the remaining extracellular matrix (ECM) retains its mechanical properties and functional design (Li et al., 2018). Essentially it needs to be implanted in a high-pressure environment without disintegrating or becoming aneurysmal. Decellularization agents, especially SDS is known to reduce the mechanical strength of pericardial scaffolds (Li et al., 2018; Gilpin & Yang, 2017). As the outcome of the BPS implantations were unknown, a control group of D-GAD patches were prepared. Therefore, to conceptually avoid initial mechanical failure of the BPS we added GA-fixation and detoxification (Encap™ AC Technology used by Glycar®) to our proprietary decellularization protocol. Therefore, this study evaluated and compared the impact of our decellularization method with and without GA-fixation on the tissue integrity and morphology of bovine pericardial scaffolds/patches implanted in an ovine model after 180-days.

No clinical failures, or evidence of aneurysm formation, infective endocarditis or calcification were observed in any of the BPS or G-GAD patches. However, one (1) sheep developed a false aneurysm on the suture line of an aortic BPS.

This study demonstrated that the structure and tissue integrity of the BPS and D-GAD patches were both well preserved. This was demonstrated in the aortic and pulmonary scaffolds explanted after 180-days in a juvenile ovine model. Both the BPS and D-GAD patches demonstrated recipient cell infiltration and reendothelialization. However, although some recipient cell infiltration could be demonstrated in the D-GAD group, the BPS group showed extensive recellularization and remodeling, especially in the pulmonary explants. No residual BPS could be identified in the aorta or pulmonary explants and we conclude that the tissue was thus completely remodeled. Badylak & Gilbert, (2009) reported

that 60% of the mass of the ECM is degraded and resorbed between one (1) and three (3)-months after in vivo grafting.

Decellularization agents/detergents have different effects on the ECM of a biological scaffolds (Bielli et al., 2018; Gilpin & Yang, 2017). Our decellularization protocol used a combination of 0.5% SDS, 1% SDC and 1% TX. Synergy was demonstrated for the decellularization/sterilization process developed at our institution with well retained pericardial strength and structure (Dr L Laker, PhD, 2019; Patent No./ 16702008.0 – 1455).

The TS ($p = 0.0628$) of the pulmonary BPS and D-GAD patches decreased from implantation to explantation but did not demonstrate a significant difference ($p=0.0628$). However, the TS of both groups were still well above the minimum strength of the native human ascending aorta (1.8 ± 0.24MPa)(Sommer et al., 2008). As previously describe GA-fixation provides greater mechanical stability to the tissue (Sinha et al., 2012) because GA crosslinking involves a heterogenous crosslinking distribution occurring only on the surface of fibrils and fibers, leading to predominant intermolecular crosslinks that connects collagen molecules (Delgado et al., 2015). However, although the pre-implanted BPS were stronger than the D-GAD patches it was still not statistically significant ($p=0.0514$). The strength of the pulmonary BPS explants might relate to tissue remodeling, ECM regeneration and even the influx of glycosaminoglycans (GAGs) and needs further investigation.

Both the BPS and D-GAD patches were more elastic/pliable than their pre-implantation counterparts with the D-GAD patches demonstrating a statistically significant difference ($p=0.0121$). However, between groups the explanted YM were similar. Hulsmann et al. (2012) reported that decellularization has allowed for decreases in the elastic modulus relative to GA treatment in bovine

pericardium. Pliability is an important characteristic of scaffold performance in vivo and the lack thereof may negatively influence compliance and hemodynamic performance. The lack therefore can contribute to graft failure (Neethling et al., 2018) especially when used to manufacture biological valves.

The DAPI and H&E stain confirmed effective decellularization by detecting no traces of cells or cellular remnants in the pre-implanted aortic and pulmonary patches and scaffolds of both groups using our decellularization process. Dr L Laker, PhD (2019) confirmed the absence of DNA with a quantitative DNA analysis. In most commercially available biological scaffolds residual DNA fragments still remains after decellularization with minimal impact on their clinical efficacy (Bielli et al., 2018) but might contribute to calcification and tissue rejection (Mallis et al., 2017).

The collagen-elastin matrix was well preserved in both groups with no signs of calcific deposits. The collagen of both groups' mimics that of fresh pericardial tissue but the collagen of the BPS was a bit wavier and less dense than the collagen of the D-GAD patches. Elastin was preserved in both decellularized groups but decreased from implantation to explantation.

The BPS and D-GAD groups demonstrated recellularization with fibroblast-like cells. However, recellularization was more abundant in the pulmonary BPS compared to the pulmonary D-GAD patches. The low pressure within the pulmonary artery could promote recellularization compared to the high pressure environment of the aorta. Dohmen et al. (2014) reported the presence of fibroblast-like and myofibroblast-like cells displaying partially large nuclei, characteristic of young fibroblasts on decellularized equine pericardium implanted in the systemic circulation. The decreased number of fibroblast-like cells in the D-GAD patches could be attributed to the (i) GA cytotoxicity and (ii) reduced mean pore sizes

within the collagen. GA-fixation reduces bacterial contamination but prevents host cell infiltration, migration and proliferation (Remi et al., 2011; Jayakrishnan & Jameela, 1996). However, it is still important to ensure sterility of the BPS prior to implantation.

The D-GAD patches developed a fibrous encapsulation during implantation. Most fibroblast-like cells were present within this fibrous encapsulation that developed on the interior and posterior side of the implanted patch. The encapsulation could result from a proinflammatory response initiated by macrophage activation, predominant M1 macrophage population and increased proinflammatory cytokine release which typically represents a foreign body response seen in surgical implants of many types (Ketchedjian et al., 2005; Delgado et al., 2015). This fibrous encapsulation might also act as a precursor for future calcification. However, no mononuclear cells were visible within these encapsulations. More importantly the fibrous encapsulation contributed to an increase in patch thickness which could influence pliability.

The fibroblast-like cells seen in both groups demonstrated numerous secretory vacuoles within the cytoplasm, which are normally associated with the transport of protein complexes synthesized within the rough endoplasmic reticulum, to the Golgi apparatus (Hodgson et al., 1990). Moreover, many of these vacuoles play an integral role in the secretion of procollagen from the cell (Canty & Kadler, 2005). These collagen-containing vacuoles might be an important indicator of young fibroblast-like cells actively involved in the production of new collagen fibrils and bundles.

SEM of both decellularized groups demonstrated a well-preserved collagen fiber network prior to implantation and at explantation a confluent monolayer of endothelial cells were visible.

From implantation (0.808 ± 0.326) to explantation the development of the fibrous encapsulation caused the pulmonary D-GAD patches to thicken (1.053 ± 0.386) but the aorta patches did not (0.734 ± 0.383). The aorta D-GAD patches and BPS did not thicken from implantation to explantation The use of SDS as decellularization detergent can promote swelling of the tissue (Mallis et al., 2017; Remi et al., 2011; Courtman et al., 1994).

7.6 Conclusion

The BPS and D-GAD patches demonstrated sufficient strength by exceeding the TS of the native human ascending aorta. Between groups, the explanted pulmonary D-GAD patches were not significantly stronger or less pliable than the explanted BPS. The surface of both scaffolds was reendothelialized at explantation and the explants did not show any evidence of calcification. However, the D-GAD patches did initiate a foreign body response with the development of a fibrous encapsulation. No mononuclear cells were seen within this encapsulation. The BPS demonstrated excellent recellularization potential and were completely remodeled. Despite the marked lesser recellularization in the D-GAD patches, the fibroblast-like cells in both groups contained secretory vacuoles in which procollagen can be packaged from the Golgi complex. The BPS did not thicken over time due to the lack of the development of a fibrous encapsulation.

Compared to the BPS, it seems that GA-fixation surprisingly did not add any benefits to the structural and morphological integrity of the pericardial patch at 180-day explantation. Moreover, the fixation came at a cost with the development of a fibrous encapsulation, potential thickening and reduced cellular infiltrates that could potentially contribute to fibrosis, calcification and possible long-term failure. The GA-fixation did not provide additional strength to the BPS and both the implanted pulmonary and aortic scaffolds were strong enough to withstand the 180-day implantation time (exceeding the 1.8 ± 0.24 MPa strength

of the native human aorta). However, GA might be important to ensure sterility and to mask epitopes when implanted in a primate model. Recellularization of the D-GAD patch has been claimed by Brizard et al. (2014) if implantation times were extended.

The BPS showed great potential after evaluating its structural and morphological characteristics in an ovine model. These scaffolds might be an attractive option especially in younger patients and warrant further investigation.

Limitations and recommendations

Data provided by the juvenile sheep model cannot be unconditionally applied to human patients. Measuring pericardial thickness prior to processing was not done for the BPS nor the D-GAD patches. Due to technical limitations, tissue implanted in the descending aorta did not allow a large enough tissue sample upon explantation for TS/YM determination.

For future studies we recommend that immunohistochemistry be added to the list of analyses to describe cell types and immunological processes involved. Extending the explantation time might provide a clearer indication if GA-fixation with decellularization do provide additional benefits compared to decellularization alone.

References

Aguiari, P., Iop, L., Favaretto, F., Fidalgo, C.M.L., Naso, F., Milan, G., Vindigni, V., Spina, M., Bassetto, F., Bagno, A., Vettor, R. & Gerosa, G. 2017. In vitro comparative assessment of decellularized bovine pericardial patches and commercial bioprosthetic heart valves. *Biomedical Materials*, 12(1): 1-12.

Badylak, S.F., & Gilbert, T.W. 2009. Immune response to biologic scaffold materials. Seminars of Immunology. *Seminars in Immunology*, 20(2): 109–

116.

Bielli, A., Bernardini, R., Varvaras, D., Rossi, P., Di Blasi, G., Petrella, G., Buonomo, O.C., Mattei, M. & Orlandi, A. 2018. Characterization of a new decellularized bovine pericardial biological mesh: Structural and mechanical properties. *Journal of the Mechanical Behavior of Biomedical Materials*, 78(2018): 420–426.

Canty, E.G. & Kadler, K.E. 2005. Procollagen trafficking, processing and fibrillogenesis. *Journal of Cell Science*, 1:118(Pt 7): 1341-1353.

Cissell, D.D., Hu, J.C., Griffiths, L.G. & Athanasiou, K.A. 2014. Antigen removal for the production of biomechanically functional, xenogeneic tissue grafts. *Journal of Biomechanics*, 47(9): 1987–1996.

Courtman, D.W., Pereira, C.A., Kashef, V., McComb, D., Lee, J.M. & Wilson, G.J. 1994. Development of a pericardial acellular matrix biomaterial: Biochemical and mechanical effects of cell extraction. *Journal of Biomedical Materials Research*, 28(6): 655–666.

Delgado, L.M., Bayon, Y., Pandit, A. & Zeugolis, D.I. 2015. To cross-link or not to cross-link? Cross-linking associated foreign body response of collagen-based devices. *Tissue Engineering - Part B: Reviews*, 21(3): 298–313.

Dohmen, P.M., da Costa, F., Lopes, S.V., Vilani, R., Bloch, O. & Konertz, W. 2014. Successful implantation of a decellularized equine pericardial patch into the systemic circulation. *Medical Science Monitor Basic Research*, 20: 1–8.

Gates, K. V., Dalgliesh, A.J. & Griffiths, L.G. 2017. Antigenicity of bovine pericardium determined by a novel immunoproteomic approach. *Scientific Reports*, 7(1): 1–10.

Gilbert, T.W., Sellaro, T.L. & Badylak, S.F. 2006. Decellularization of tissues and organs. *Biomaterials*, 27(19): 3675–3683.

Gilpin, A. & Yang, Y. 2017. Decellularization strategies for regenerative medicine: From processing techniques to applications. *BioMed Research*

International, 2017:1-13.

Grabenwoger, M., Grimm, M., Eybl, E., Leukauf, C., Muller, M.M., Plenck, H.J. & Bock, P. 1992. Decreased tissue reaction to bioprosthetic heart valve material after L-glutamic acid treatment. A morphological study. *Journal of Biomedical Materials Research*, 26(9): 1231–1240.

Jayakrishnan, A. & Jameela, S.R. 1996. Glutaraldehyde as a fixative in bioprostheses and drug delivery matrices. *Biomaterials*, 17(5): 471–484.

Ketchedjian, A., Jones, A.L., Krueger, P., Robinson, E., Crouch, K., Wolfinbarger, L. & Hopkins, R. 2005. Recellularization of decellularized allograft scaffolds in ovine great vessel reconstructions. *Annals of Thoracic Surgery*, 79(3): 888–896.

Li, N., Li, Y., Gong, D., Xia, C., Liu, X. & Xu, Z. 2018. Efficient decellularization for bovine pericardium with extracellular matrix preservation and good biocompatibility. *Interactive Cardiovascular and Thoracic Surgery*, 26(5): 768–776.

Mallis, P., Michalopoulos, E., Dimitriou, C., Kostomitsopoulos, N. & Stavropoulos-Giokas, C. 2017. Histological and biomechanical characterization of decellularized porcine pericardium as a potential scaffold for tissue engineering applications. *Bio-Medical Materials and Engineering*, 28(5): 477–488.

Mendoza-Novelo, B. & Cauich-Rodríguez, J. V. 2009. The effect of surfactants, crosslinking agents and L-cysteine on the stabilization and mechanical properties of bovine pericardium. *Journal of Applied Biomaterials and Biomechanics*, 7(2): 123–131.

Neethling, W.M.L., Puls, K. & Rea, A. 2018. Comparison of physical and biological properties of CardioCel® with commonly used bioscaffolds. *Interactive Cardiovascular and Thoracic Surgery*, 26(6): 985–992.

Nogueira, G.M., Rodas, A.C.D., Weska, R.F., Aimoli, C.G., Higa, O.Z., Maizato, M., Leiner, A.A., Pitombo, R.N.M., Polakiewicz, B. & Beppu, M.M. 2010. Bovine pericardium coated with biopolymeric films as an alternative to prevent

calcification: In vitro calcification and cytotoxicity results. *Materials Science*

Remi, E., Khelil, N., Di, I., Roques, C., Ba, M., Medjahed-Hamidi, F., Chaubet, F., Letourneur, D., Lansac, E. & Meddahi-Pelle, A. 2011. Pericardial Processing: Challenges, Outcomes and Future Prospects. *Biomaterials Science and Engineering*. Retrieved from: http://www.intechopen.com/books/biomaterials-science-and-engineering/pericardial-processing-challenges-outcomes-and-future-prospects. [accessed 20 November 2018].

Sinha, P., Zurakowski, D., Susheel Kumar, T.K., He, D., Rossi, C. & Jonas, R.A. 2012. Effects of glutaraldehyde concentration, pretreatment time, and type of tissue (porcine versus bovine) on postimplantation calcification. *Journal of Thoracic and Cardiovascular Surgery*, 143(1): 224–227.

Sommer, G., Gasser, T.C., Regitnig, P., Auer, M. & Holzapfel, G.A. 2008. Dissection properties of the human aortic media: An experimental study. *Journal of Biomechanical Engineering*, 130(2): 1-12.

Tran, H.L.B., Dinh, T.T.H., Nguyen, M.T.N., To, Q.M. & Pham, A.T.T. 2016. Preparation and characterization of acellular porcine pericardium for cardiovascular surgery. *Turkish Journal of Biology*, 40: 1243–1250.

Yoo, J.S., Kim, Y.J., Kim, S.H. & Choi, S.H. 2011. Study on genipin: A new alternative natural crosslinking agent for fixing heterograft tissue. *Korean Journal of Thoracic and Cardiovascular Surgery*, 44(3): 197–207.

Chapter 8 - General Conclusion

The use of cardiac patches remains one of the main therapeutic solutions for surgical treatment. They are mostly used for the reconstruction of the aorta and pulmonary vessels, closure of interatrial and interventricular defects, and reconstruction of atrioventricular valves. Cardiovascular patches are either synthetic or biological. Synthetic materials like GORE-TEX® and Dacron® polyutetrafluoroethylene (PTFE) have become less popular over the years because they are rigid with poor flexibility, are difficult to handle surgically and biocompatibility remains a challenge. Synthetic materials are also prone to endocarditis and local inflammatory reactions that contributes to fibrotic processes and calcification. Furthermore, these synthetic materials also have no regeneration potential. Autologous pericardium tends to retract, thicken, become aneurysmal and develop fibrosis once implanted. As a result, the use of xenogeneic transplanted tissue dominated by bovine pericardium has become an attractive alternative. The ideal biological patch should include the following characteristics; (i) acceptable surgical handling, (ii) anti-thrombogenicity, (iii) non-calcification, (iv) hemostasis, (v) non-immunogenicity (vi) reendothelialization capability and (vii) acceptable off the shelve storage.

To overcome the aggressive recipient graft-specific rejection responses, ensure sterility and to increase durability and mechanical stability, GA-fixation of bovine xenograft pericardium was introduced in 1971 by Ionescu but not without consequences. The residual GA toxicity and host immune responses seen in GA-preserved bovine pericardium causes degenerative processes that involves structural changes causing rigidity, shrinkage, calcium deposition and subsequent failure of the pericardial patch. Furthermore, GA also limits host cell infiltration, remodeling and fails to remove or mask all animal specific antigens such as

Galalpha1,3-Galbeta1-4GlcNAc-R (α-gal) and N-glycolylneuraminic acid (Neu5Gc) epitopes that contributes to chronic rejection.

This resulted in several strategies to reduce the side-effects of GA-fixation like lyophilization, heparin or sulphonated poly (ethylene oxide) treatments and modified adipic dihydrazide hyaluronic acid treatments. Alternatives to GA as a crosslinking agent like genipin, epoxy compound, carbodiimides, glycerol or dye-mediated photo-oxidation to name but a few has also been investigated but with mixed results.

To address the concerns of the initiated immune response caused by GA-fixation [(i) lack of host cell infiltration and (ii) masking/removal of epitopes] basic research is focused to produce a scaffold with reduced antigenicity while maintaining structural integrity and create recellularization potential. Attempts to reduce antigenicity included decellularization (e.g., SDS, TX, trypsin), enzymatic or gene knockout removal of epitopes, and solubilization-based antigen removal. Various decellularization methods have been developed through the years but the perfect one still eludes us.

The Frater Cardiovascular Research Centre developed a proprietary decellularization protocol. Dr L Laker completed her PhD thesis titled "*The evaluation of a novel decellularization and sterilization process on bovine pericardial tissue*" in 2019 and demonstrated synergy between the decellularization detergents used in vitro. Importantly, she also demonstrated the retention of strength and structure of the bovine pericardial scaffold after using our proprietary decellularization method. In order to evaluate the potential application of this technology a study was designed to compare the structural and morphological performance of decellularized tissue in several settings after being implanted in a juvenile ovine model for 180-days;

(i) decellularized bovine pericardial scaffold was compared to a commercially available GA-fixated and detoxified patch (Glycar®),

(ii) the newer generation CardioCel® patch, that has been decellularized and fixated using a low concentration of monomeric GA was compared with the established Glycar® GA-fixated and detoxified patch,

(iii) decellularized GA-fixated and detoxified (D-GAD) patch was compared to the Glycar® patch and

(iv) the decellularized bovine pericardial scaffold (BPS) was compared to the D-GAD patch to assess the impact of GA-fixation and detoxification.

Therefore, the aim of this study was to develop a BPS that maintains tissue integrity, restrict calcification and provide recellularization potential in vivo. Furthermore, to demonstrate mechanical and morphological non-inferiority when compared to two (2) commercially available pericardial patches (Glycar® and CardioCel®). The results of each setting (i-iv) is summarized below:

Article 1

Advantages of decellularized bovine pericardial scaffolds compared to glutaraldehyde fixed bovine pericardial patches demonstrated in a 180-day implant ovine study

GA-fixed bovine pericardial patches remain the industry standard in cardiovascular surgery despite numerous reports of degradation, thickening, inflammation, calcification and the lack of in vivo tissue remodeling. Decellularization provides us the opportunity to attenuate some of these immune mediated processes. As decellularization methods might weaken tissue it is important to demonstrate structural integrity of decellularized scaffolds in large animal models before human implants is undertaken. In this study the impact of our decellularization process was evaluated and compared to the Glycar® patch in a juvenile ovine model, expecting in vivo recellularization and tissue remodeling.

The BPS demonstrated adequate strength prior to implantation. Clinically, all scaffolds performed well with no evidence of aneurysm formation, calcification or disintegration at 180-days. The explanted aortic and pulmonary scaffolds demonstrated recellularization, tissue remodeling, resistance to calcification, reendothelialization and strength in excess of the native human aorta of 1.8 ± 0.24 MPa (Sommer et al., 2008). Histology demonstrated a wave-like appearance of well-separated collagen fibers that provided pore sizes adequate to promote fibroblast infiltration with new collagen formation after an implantation time of 180-days.

Therefore, BPS should be considered as an alternative to GA-fixed pericardial patches for it demonstrated excellent remodeling and growth potential. This could be an ideal scaffold for younger patients.

Article 2

Comparing the impact of processing techniques between Glycar® and CardioCel® bovine pericardial patches after 180-days implantation in a juvenile ovine model

Clinically, the handling quality of both patches were satisfactory and demonstrated excellent clinical results with no signs of degradation, calcification or aneurysm formation. The structural integrity of the Glycar® and CardioCel® patches were similar at pre-implantation and explantation with no difference in strength or pliability. No calcification occurred in any of the groups. Both pericardial patch groups developed a fibrous encapsulation. However, the collagen of the CardioCel® patches appeared healthier with a more wave-like, well-separated appearance which might contribute to host cell infiltration.

An important difference between Glycar® and CardioCel® is the amount of recellularization. Glycar® showed limited recellularization. CardioCel®, although

sparsely populate, showed fibroblast-like cells with secretory activity. Brizard et al. (2014) reported that longer term implants showed better host cell infiltration potential. This remains to be seen and could be a major advantage as initial structural integrity of CardioCel® seems to be equal to Glycar® in this study.

The development of a fibrous encapsulation in both groups remains a concern and seems to be immunologically linked as described by Neethling et al. (2018). The thickening caused by the fibrous encapsulation remains a challenge and further investigations is needed to minimize thickening especially when used for valvular leaflets.

Article 3

The impact of pericardial patch processing techniques after 180-days implantation in an ovine model: Glycar® versus a tissue engineered decellularized, glutaraldehyde-fixed and detoxified bovine pericardium

The tissue strength and pliability of both groups were comparable and demonstrated adequate strength to withstand implantation in the aortic and pulmonary circulation for 180-days. Both the Glycar® and D-GAD patches developed a fibrous encapsulation on the interior and posterior side of the patch as a result of a foreign body response. However, no mononuclear cells were visible within this fibrous encapsulation in both groups. None of the aortic or pulmonary implants demonstrated evidence of calcification, infective endocarditis, aneurysm formation or degeneration.

The major difference between the Glycar® and D-GAD patches were the amount of recellularization demonstrated. The D-GAD patches demonstrated much better cellular infiltration compared to the Glycar® patches. This could be attributed to (i) the better preservation of the collagen matrix and (ii) adequate pore size to promote cellular infiltration.

The D-GAD patches were not structurally or morphologically inferior to the commercially available Glycar® patches. In addition, the recellularization/remodeling potential demonstrated by the D-GAD patches makes this patch a very attractive option especially in younger patients.

Article 4

Comparison of the tissue integrity and morphology between decellularized bovine pericardial scaffolds with and without glutaraldehyde fixation in a 180-day implant study in the juvenile ovine model

The PBS and D-GAD patches demonstrated sufficient strength by exceeding the TS of the native human ascending aorta. Between groups, the explanted pulmonary D-GAD patches were not significantly stronger or less pliable than the explanted PBS. The surface of both scaffolds was reendothelialized at explantation and the explants did not show any evidence of calcification. However, the D-GAD patches did initiate a foreign body response with the development of a fibrous encapsulation. No mononuclear cells were seen within this encapsulation. The PBS demonstrated excellent recellularization potential and the decellularized PBS patches were completely remodeled. Despite the marked lesser recellularization in the D-GAD patches, the fibroblast-like cells in both groups contained secretory vacuoles in which procollagen can be packaged from the Golgi complex. The PBS did not thicken over time due to the lack of the development of a fibrous encapsulation.

Compared to the BPS, it seems that GA-fixation surprisingly did not add any benefits to the structural and morphological integrity of the pericardial patch at 180-day explantation. Moreover, the fixation came at a cost with the development of a fibrous encapsulation, potential thickening and reduced cellular infiltrates that could potentially contribute to fibrosis, calcification and possible long-term failure. The GA-fixation did not provide additional strength to the BPS

and both the implanted pulmonary and aortic scaffolds were strong enough to withstand the 180-day implantation time (exceeding the 1.8 ± 0.24 MPa strength of the native human aorta. However, GA might be important to ensure sterility and to mask epitopes when implanted in a primate model. Recellularization of the D-GAD patch has been claimed by Brizard et al. (2014) if implantation times were extended.

The PBS showed great potential after evaluating its structural and morphological characteristics in an ovine model. These scaffolds might be an attractive option especially in younger patients and warrant further investigation.

The key results of the study are summarized in Table 8.1.

It is important to note the following:

(i) *that the TS of each bovine pericardial patch and scaffold was considered adequate if the TS exceeded the minimum strength of the native human aorta (1.8 ± 0.24 MPa) as published by Sommer et al. (2008).*

(ii) *the Glycar® and CardioCel® bovine pericardial patches is selected based on adequate strength and thickness (according to manufacturer). However, the thickness of the decellularized BPS and D-GAD scaffolds were not taken into consideration when selected and only a homogenous part of the pericardium was chosen and processed.*

Table 8.1 Summary of study results

Variable	Glycar®		CardioCel®		D-GAD		BPS	
Pre-implantation								
Clinical								
Calcification	N		N		N		N	
Strength								
YM (MPa)	114.50±40.41		63.97±18.43		39.88±28.46		16.69±9.87	
TS (MPa)	23.02±4.72		16.81±2.58		9.91±2.53		15.02±3.25	
Morphology								
DAPI								
Cells	Acellular		Acellular		Acellular		Acellular	
H&E								
Collagen	Densely compacted/collapsed		Compacted		Compacted		Wavy, well-separated	
EVG								
Elastin	Y		Y		Y		Y	
VK								
Calcification	N		N		N		N	
SEM								
Endothelium	Y		N		N		N	
TEM								
Fibroblast-like cells	Pyknotic, extremely limited		N		N		N	
Implant Thickness								
Patch (mm)	0.278±0.074		0.431±0.076		0.808±0.326		1.452±0.129	
Explantation								
	Aorta	Pulmonary	Aorta	Pulmonary	Aorta	Pulmonary	Aorta	Pulmonary
Clinical								
Handling	Satisfactory	Satisfactory	Satisfactory	Satisfactory	Satisfactory	Satisfactory	Satisfactory but slippery	Satisfactory but slippery
Calcification	N	N	N	N	N	N	N	N
Aneurysm	N	N	N	N	N	N	1x False	N
Infective Endocarditis	N	N	N	N	N	N	N	N

Disintegration	N	N	N	N	N	N	N	N
Strength								
YM (MPa)	nd	19.58±17.18	nd	12.22±8.04	nd	10.01±11.41	nd	9.81±3.55
TS (MPa)	nd	6.02±0.96	nd	6.99±3.18	nd	5.30±1.40	nd	3.60±1.28
Morphology								
H&E								
Collagen	Densely compacted/collapsed	Densely compacted/collapsed	Compacted	Compacted	Compacted	Compacted	Wavy, well-separated	Wavy, well-separated
Fibrous encapsulation	Y	Y	Y	Y	Y	Y	N	N
Host cell infiltration	0/10	0/10	3/10	3/10	3/10	4/10	7/10	9/10
Remodeling	N	N	N	N	N	N	Y	Y
EVG								
Elastin	Y	Y	Y (<than pre-implant)	Y (<than pre-implant)	Y (<than pre-implant)	Y (<than pre-implant)	Y (<than pre-implant)	Y (<than pre-implant)
VK								
Calcification	N	N	N	N	N	N	N	N
SEM								
Reendothelialization	Y	Y	Y	Y	Y	Y	Y	Y
TEM								
Fibroblast-like cells	Devitalized	Devitalized	Y	Y	Y	Y	Y	Y
Thickness								
Patch (mm)	0.281±0.029	0.316±0.076	0.426±0.070	0.424±0.090	0.399±0.044	0.665±0.054	1.416±0.456	1.054±0.533
Fibrous encapsulation (mm)	0.151±0.061	0.512±0.120	0.588±0.173	0.205±0.035	0.353±0.378	0.369±0.358	-	-
Combined (mm)	0.403±0.085	0.951±0.116	1.104±0.223	0.603±0.095	0.734±0.383	1.053±0.386	-	-

[D-GAD = Decellularized GA-fixed and detoxified; BGS = Decellularized bovine pericardial scaffold; Y = Yes; N = No; nd = not done]

8.1 Summary of key results

8.1.1 Glycar® bovine pericardial patch

Pre-implantation: Adequate strength, less pliable, no calcification, fixated non-viable cells, densely compacted/collapsed collagen, elastin, severely dehydrated endothelial cells, thin

Ao-explant: No calcification, no aneurysm, no infective endocarditis, no disintegration, no host cell infiltration, densely compacted/collapsed collagen, elastin retained from pre-implantation, fibrous encapsulation, no remodelling, reendothelialized, thickened

Pu-explant: No calcification, no aneurysm, no infective endocarditis, no disintegration, adequate strength, more pliable, no host cell infiltration, densely compacted/collapsed collagen, elastin retained from pre-implantation, fibrous encapsulation, no remodelling, reendothelialized, thickened

8.1.2 CardioCel® bovine pericardial patch

Pre-implantation: Adequate strength, pliable, no calcification, acellular, compact collagen, elastin, no endothelial cells, thin

Ao-explant: No calcification, no aneurysm, no infective endocarditis, no disintegration, limited host cell infiltration, compacted collagen, elastin but less than pre-implant, fibrous encapsulation, no remodelling, reendothelialized, thickened

Pu-explant: No calcification, no aneurysm, no infective endocarditis, no disintegration, strength adequate, more pliable, limited host cell infiltration, compacted collagen, elastin but less than pre-implant, fibrous encapsulation, no remodelling, reendothelialized, thickened

8.1.3 Decellularized GA-fixed and detoxified (D-GAD) bovine pericardial patch

Pre-implantation: Adequate strength, pliable, no calcification, acellular, compact collagen, elastin, no endothelial cells, thick

Ao-explant: No calcification, no aneurysm, no infective endocarditis, no disintegration, limited host cell infiltration, compacted collagen, elastin but less than pre-implant, fibrous encapsulation, no remodelling, reendothelialized, thickened

Pu-explant: No calcification, no aneurysm, no infective endocarditis, no disintegration, adequate strength, more pliable, limited host cell infiltration, compacted collagen, elastin but less than pre-implant, fibrous encapsulation, no remodelling, reendothelialized, thickened

8.1.4 Decellularized bovine pericardial scaffold (BGS)

Pre-implantation: Adequate strength, pliable, no calcification, acellular, wavy well separated collagen, elastin but less than pre-implant, no endothelial cells, thick

Ao-explant: No calcification, one false aneurysm, no infective endocarditis, no disintegration, host cell infiltration, wavy well-separated collagen, elastin but less than pre-implant, no fibrous encapsulation, complete remodelling, reendothelialized, did not thickened

Pu-explant: No calcification, no aneurysm, no infective endocarditis, no disintegration, adequate strength, more pliable, host cell infiltration, wavy well-separated collagen, elastin but less than pre-implant, no fibrous encapsulation, complete remodelling, reendothelialized, did not thickened

8.2 Conclusions

Developing new bovine pericardial tissue for use as tissue substitutes in cardiovascular surgery remains a challenge. Glutaraldehyde-fixed and detoxified (GAD) and decellularized (D-GAD) solutions represent the state of the art in commercially available products. The impact of GAD technology on tissue seems to be constant, irrespective whether the tissue was decellularized or not. On the one hand, all the GAD tissues handled well, had excellent clinical outcomes and did not calcify. A fibrous encapsulation was present on all these explants in the

juvenile ovine model, explaining thickening of tissues as described by various researchers. Adding decellularization to the process benefits the collagen matrix, by making the collagen less dense/compact thus allowing for larger pore sizes. This may allow better recellularization, especially in the absence of cells or cellular debris, evoking an immunological reaction. The long-term benefit of the limited recellularization seen in both D-GAD products remains to be clearly demonstrated. The importance of remodelling may be beneficial to the long-term outcomes especially in the younger age group recipients.

On the other hand, decellularized BPS demonstrated acceptable pre-implant structural integrity and morphology. The TS of the pulmonary artery was deemed satisfactory because it exceeded the strength of the native human aorta. The collagen was well preserved in the decellularized BPS. Tissue handling was acceptable, though slippery compared to other patches.

Clinical outcomes demonstrated no disintegration, calcification or aneurysmal dilatation of the scaffold material. Tissue integrity and strength was also well retained upon explantation, and although weaker than fixed products it still exceeded the strength of the native human aorta (1.8 ± 0.24 MPa). Morphological assessment showed extensive recellularization and almost complete remodelling with no fibrous encapsulating and complete endothelialisation. The decellularized BPS retained its implantation thickness and did not thicken as a result of the formation of a fibrous encapsulation.

Although all the tissue products assessed provided excellent protection against calcification in the juvenile ovine model, the study supports the further assessment of decellularized BPS with in vivo recellularization as a viable alternative for cardiovascular tissue replacement applications. Furthermore, it also demonstrates the need for ongoing research in the development of alternative or

modified GA-fixation, sterilisation and storage technology that does not result in the formation of a fibrous encapsulation. The impact of limited recellularization in D-GAD products needs to be clarified in long-term studies to determine the exact impact on tissue maintenance, ECM structure and remodelling.

8.3 Limitations and Recommendations

The study was limited by:

(i) Data provided by the juvenile sheep model cannot be unconditionally applied to human patients.

(ii) Not selecting decellularized BPS and D-GAD patches according to thickness prior to processing made comparison to Glycar® and CardioCel® patches impossible. However, the measurement of pericardial thickness prior to processing was also not available for Glycar® nor CardioCel® patches.

(iii) Due to technical limitations, tissue implanted in the descending aorta did not allow a large enough tissue sample upon explantation for TS/YM determination.

(iv) The small sample sizes always make TS testing challenging

Future considerations:

(i) We recommend that immunohistochemistry be added to the list of analyses to confirm cell types and immunological processes involved.

(ii) Viability testing should be included.

(iii) Extending the explantation time might provide a clearer indication if GA-fixation with decellularization do provide additional benefits compared to decellularization alone.

(iv) Modifications to GA-fixation, sterilisation and storage technology that does not result in the formation of a fibrous encapsulation.

(v) The impact of limited recellularization in D-GAD products needs to be clarified in long-term studies to determine the exact impact on tissue maintenance, ECM structure and remodelling.

References

Aamodt, J.M. and Grainger, D.W. 2016. Extracellular matrix-based biomaterial scaffolds and the host response. *Biomaterials*, 86: 68-82.

Admedus Innovative Health Solutions. n.d. ADAPT® tissue engineering process. Retrieved from https://www.google.com/search?q=Admedus+processing+technology&rlz=1C1GCEU_enZA863ZA863&source=lnms&tbm=isch&sa=X&ved=2ahUKEwiLwa2I4aXnAhUTWsAKHYueCgoQ_AUoAnoECA0QBA&biw=1920&bih=937#imgrc=mpqpjsUOYYyWlM: [accessed 20 July 2019].

Aguiari, P., Iop, L., Favaretto, F., Fidalgo, C.M.L., Naso, F., Milan, G., Vindigni, V., Spina, M., Bassetto, F., Bagno, A., Vettor, R. & Gerosa, G. 2017. In vitro comparative assessment of decellularized bovine pericardial patches and commercial bioprosthetic heart valves. *Biomedical Materials*, 12(1): 1-12.

Al-bayati, A.H.F. & Hameed, F.M. 2018. Effect of acellular bovine pericardium and dermal matrixes on cutaneous wounds healing in male rabbits : Histopathological evaluation. *Journal of Entomology and Zoology Studies*, 6(2): 1976–1986.

Athar, Y., Lailatul, S., Zainuddin, A., Berahim, Z. & Hassan, A. 2014. Bovine Pericardium : A Highly Versatile Graft Material Bovine Pericardium : A Highly Versatile Graft Material. *International medical Journal*, 21(3): 321–324.

Badylak, S.F. 2007. The extracellular matrix as a biologic scaffold material. *Biomaterials*, 28(25): 3587–3593.

Badylak, S.F. 2002. The extracellular matrix as a scaffold for tissue reconstruction. *Seminars in cell & developmental biology*, 13(5): 377–383.

Badylak, S.F., Freytes, D.O. & Gilbert, T.W. 2015. Reprint of: Extracellular matrix as a biological scaffold material: Structure and function. *Acta Biomaterialia*, 23(S): S17–S26.

Badylak, S.F. & Gilbert, T.W. 2009. Immune response to biologic scaffold materials. Seminars of Immunology, 20(2): 109-116.

Bell, D., Prabhu, S., Betts, K., Justo, R., Venugopal, P., Karl, T.R. & Alphonso, N. 2019. Durability of tissue-engineered bovine pericardium (CardioCel®) for a minimum of 24 months when used for the repair of congenital heart defects. *Interactive Cardiovascular and Thoracic Surgery*, 28(2): 284-290.

Bielli, A., Bernardini, R., Varvaras, D., Rossi, P., Di Blasi, G., Petrella, G., Buonomo, O.C., Mattei, M. & Orlandi, A. 2018. Characterization of a new decellularized bovine pericardial biological mesh: Structural and mechanical properties. *Journal of the Mechanical Behavior of Biomedical Materials*, 78(2018): 420–426.

Carpentier, A. 1989. From valvular xenograft to valvular bioprosthesis: 1965-1970. *The Annals of Thoracic Surgery*, 48(Suppl 3): S73-74.

Carpentier, A., Lemaigre, G., Robert, L., Carpentier, S. & Dubost, C. 1969. Biological factors affecting long-term results of valvular heterografts. *The Journal of Thoracic and Cardiovascular Surgery*, 58(4): 467–483.

Chan, B.P. & Leong, K.W. 2008. Scaffolding in tissue engineering: General approaches and tissue-specific considerations. *European Spine Journal*, 17(Suppl 4): 467-479.

Cheung, D.T., Perelman, N. & Nimni, M.E. 1985. Mechanisms of crosslinking of proteins by glutaraldehyde III. Reaction with collagen in tissues. *Connective Tissue Research*, 1985, 13(2): 109-115.

Cigliano, A., Gandaglia, A., Lepedda, A.J., Zinellu, E., Naso, F., Gastaldello, A., Aguiari, P., De Muro, P., Gerosa, G., Spina, M. & Formato, M. 2012. Fine structure of glycosaminoglycans from fresh and decellularized porcine cardiac valves and pericardium. *Biochemistry Research International*, 2012: 1-10.

Ciubotaru, A., Cebotari, S., Tudorache, I., Beckmann, E., Hilfiker, A. & Haverich, A. 2013. Biological heart valves. *Biomedizinische Technik*, 58(5): 389–397.

Corda, S., Samuel, J. & Rappaport, L. 2000. Extracellular Matrix and Growth Factors During Heart Growth. *Heart Failure Reviews*, 5(2): 119-130.

Costa, A., Naranjo, J.D., Londono, R. & Badylak, S.F. 2017. Biologic scaffolds.

Cold Spring Harbor Perspectives in Medicine, 7(9): 1–24.

Costa, J.N.L., Pomerantzeff, P.M.A., Braile, D.M., Ramirez, V.A., Goissis, G. & Stolf, N.A.G. 2005. Comparison between the decellularized bovine pericardium and the conventional bovine pericardium used in the manufacture of cardiac bioprostheses. *Brazilian Journal of Cardiovascular Surgery*, 20(1): 14–22.

Courtman, D.W., Pereira, C.A., Kashef, V., McComb, D., Lee, J.M. & Wilson, G.J. 1994. Development of a pericardial acellular matrix biomaterial: Biochemical and mechanical effects of cell extraction. *Journal of Biomedical Materials Research*, 28(6): 655–666.

Crapo, P.M., Gilbert, T.W. & Badylak, D.V.M. 2011. An overview of tissue and whole organ decellularization processes. *Biomaterials*, 32(12): 3233–3243.

Czum, J.M., Silas, A.M. & Althoen, M.C. 2014. Evaluation of the Pericardium with CT and MR. *International Scholarly Research Notices Cardiology*, 2014: 1–11.

Di Franco, S., Amarelli, C., Montalto, A., Loforte, A. & Musumeci, F. 2018. Biomaterials and heart recovery: Cardiac repair, regeneration and healing in the MCS era: A state of the 'heart'. *Journal of Thoracic Disease*, 10(1): S2346–S2362.

Di Lullo, G.A., Sweeney, S.M., Korkk, J., Ala-Kokko, L. & San Antonio, J.D. 2002. Mapping the ligand-binding sites and disease-associated mutations on the most abundant protein in the human, type I collagen. *Journal of Biological Chemistry*, 277(6): 4223–4231.

Galla, S., Mathapati, S., Nayak, V.M., Cherian, K.M. & Guhathakurta, S. 2010. Analytical study to evaluate the extracellular matrix in processed acellular xenografts. *Indian Journal of Thoracic and Cardiovascular Surgery*, 26(2): 132–138.

García Páez, J.M., Herrero, E.J., San Martín, A.C., García Sestafe, J. V., Téllez, G., Millán, I., Salvador, J., Cordón, A. & Castillo-Olivares, J.L. 2000. The

influence of chemical treatment and suture on the elastic behavior of calf pericardium utilized in the construction of cardiac bioprostheses. *Journal of Materials Science: Materials in Medicine*, 11(5): 273–277.

Gates, K. V., Dalgliesh, A.J. & Griffiths, L.G. 2017. Antigenicity of bovine pericardium determined by a novel immunoproteomic approach. *Scientific Reports*, 7(1): 1–10.

Ghatak, S., Maytin, E. V., Mack, J.A., Hascall, V.C., Atanelishvili, I., Moreno Rodriguez, R., Markwald, R.R. & Misra, S. 2015. Roles of proteoglycans and glycosaminoglycans in wound healing and fibrosis. *International Journal of Cell Biology*, 2015: 1-20.

Gilbert, T.W., Sellaro, T.L. & Badylak, S.F. 2006. Decellularization of tissues and organs. *Biomaterials*, 27(19): 3675–3683.

Glycar South Africa. n.d. Glycar pericardial patch with Aldecap. Retreived from http://glycar.co.za/downloads/Glycar_Patch_Brochure.pdf [accessed 30 March 2019].

Goetz, W.A., Lim, H.S., Lansac, E., Weber, P.A. & Duran, C.M. 2002. A temporarily stented, autologous pericardial aortic valve prosthesis. *Journal of Heart Valve Disease*, 11(5): 696–702.

Gonçalves, A., Griffiths, L., Anthony, R. & Orton, C. 2005. Decellularization of bovine pericardium for tissue-engineering by targeted removal of xenoantigens. *Journal of Heart Valve Disease*, 14(2): 212-217.

Grande-Allen, K.J., Osman, N., Ballinger, M.L., Dadlani, H., Marasco, S. & Little, P.J. 2007. Glycosaminoglycan synthesis and structure as targets for the prevention of calcific aortic valve disease. *Cardiovascular Research*, 76(1): 19–28.

Gumbiner, B.M. 1996. Cell adhesion: The molecular basis of tissue architecture and morphogenesis. *Cell*, 84(3): 345–357.

Halees, Z. Al, Shahid, M. Al, Sanei, A. Al, Sallehuddin, A. & Duran, C. 2005. Up to 16 years follow-up of aortic valve reconstruction with pericardium: A

stentless readily available cheap valve? *European Journal of Cardio-thoracic Surgery*, 28(2): 200–205.

Huang-Lee, L.L., Cheung, D.T., Nimni, M.E. 1990. Biochemical changes and cytotoxicity associated with the degradation of polymeric glutaraldehyde derived crosslinks. *Journal of Biomaterials Research*, 24(9): 1185-1201.

Ionescu, M.I., Tandon, A.P., Mary, D.A. & Abid, A. 1977. Heart valve replacement with the Ionescu-Shiley pericardial xenograft. *The Journal of Thoracic and Cardiovascular Surgery*, 73(1): 31–42.

Iop, L., Palmosi, T., Sasso, E.D. & Gerosa, G. 2018. Bioengineered tissue solutions for repair, correction and reconstruction in cardiovascular surgery. *Journal of Thoracic Disease*, 10(Suppl 20): S2390–S2411.

Jaganathan, S.K., Supriyanto, E., Murugesan, S., Balaji, A. & Asokan, M.K. 2014. Biomaterials in cardiovascular research: Applications and clinical implications. *BioMed Research International*, 2014: 1-11.

Jana, S., Tefft, B.J., Spoon, D.B. & Simari, R.D. 2014. Scaffolds for tissue engineering of cardiac valves. *Acta Biomaterialia*, 10(7): 2877-2893.

Jang, W., Choi, S., Kim, S.H., Yoon, E., Lim, H.G. & Kim, Y.J. 2012. A comparative study on mechanical and biochemical properties of bovine pericardium after single or double crosslinking treatment. *Korean Circulation Journal*, 42(3): 154–163.

Jaworska-Wilczynska, M., Trzaskoma, P., Szczepankiewicz, A.A. & Hryniewiecki, T. 2016. Pericardium: Structure and function in health and disease. *Folia Histochemica et Cytobiologica*, 54(3): 121–125.

Jayakrishnan, A. & Jameela, S.R. 1996. Glutaraldehyde as a fixative in bioprostheses and drug delivery matrices. *Biomaterials*, 17(5): 471–484.

Jorge-Herrero, E., Fonseca, C., Barge, A.P., Turnay, J., Olmo, N., Fernández, P., Lizarbe, M.A. & Garcia Páez, J.m. 2010. Biocompatibility and calcification of bovine pericardium employed for the construction of cardiac bioprostheses

treated with different chemical crosslink methods. *Artificial Organs*, 34(5): E168-176.

Jorge-Herrero, E., Garcia Paez, J.M. & Del Castillo-Olivares Ramos, J.L. 2005. Tissue heart valve mineralization: Review of calcification mechanisms and strategies for prevention. *Journal of Applied Biomaterials & Biomechanics,* 3(2): 67–82.

Kanwar, Y.S., Carone, F.A., Kumar, A., Wada, J., Ota, K. & Wallner, E.I. 1997. Role of extracellular matrix, growth factors and proto-oncogenes in metanephric development. *Kidney International*, 52(3): 589–606.

Khandaker, M.H., Espinosa, R.E., Nishimura, R.A., Sinak, L.J., Hayes, S.N., Melduni, R.M. & Oh, J.K. 2010. Pericardial disease: Diagnosis and management. *Mayo Clinic Proceedings*, 85(6): 572–593.

Kiernan, J.A. 2000. Formaldehyde, formalin, paraformaldehyde and glutaraldehyde: What they are and what they do. *Microscopy Today*, 8(1): 8–13.

Kubota, H., Endo, H., Noma, M., Tsuchiya, H., Yoshimoto, A., Takahashi, Y., Inaba, Y., Matsukura, M. & Sudo, K. 2012. Equine pericardial roll graft replacement of infected pseudoaneurysm of the ascending aorta. *Journal of Cardiothoracic Surgery*, 7(1): 2–5.

Kular, J.K., Basu, S. & Sharma, R.I. 2014. The extracellular matrix: Structure, composition, age-related differences, tools for analysis and applications for tissue engineering. *Journal of Tissue Engineering*, 5: 1-17.

Lahir, Y.K. 2015. A dynamic component of tissues - exstracellular matrix: structural, functional and adaptive approach. *Biochemical and Cellular Archives*, 15(2): 331-347.

Lam, M.T. & Wu, J.C. 2012. Biomaterial applications in cardiovascular tissue repair and regeneration. *Expert Review of Cardiovascular Therapy*, 10(8): 1039–1049.

Lee, C., Kim, S.H., Choi, S.H. & Kim, Y.J. 2011. High-concentration

glutaraldehyde fixation of bovine pericardium in organic solvent and post-fixation glycine treatment: In vitro material assessment and in vivo anticalcification effect. *European Journal of Cardiothoracic Surgery*, 39(3): 381–387.

Lee, J.M. Rereira C.A. & Kan L.W.K. 1994. Effect of molecular structure of poly(glycidyl ether) reagents on crosslinking and mechanical properties of bovine pericardial xenograft materials. *Journal of Biomedical Materials Research*, 28(9): 981-992.

Levy, R.J., Schoen, F.J., Anderson, H.C., Harasaki, H., Koch, T.H., Brown, W., Lian, J.B., Cumming, R. & Gavin, J.B. 1991. Cardiovascular implant calcification: a survey and update. *Biomaterials*, 12(8): 707–714.

Li, X., Guo, Y., Ziegler, K., Model, L., Eghbalieh, S.D.D., Brenes, R., Kim, S., Shu, C. & Dardik, A. 2011. Current usage and future directions for the bovine pericardial patch. *Annals of Vascular Surgery*, 25(4): 561–568.

Li, N., Li, Y., Gong, D., Xia, C., Liu, X. & Xu, Z. 2018. Efficient decellularization for bovine pericardium with extracellular matrix preservation and good biocompatibility. *Interactive CardioVascular and Thoracic Surgery*, 26(5): 768–776.

Liao, J., Joyce, E.M. & Sacks, M.S. 2008. Effects of decellularization on the mechanical and structural properties of the porcine aortic valve leaflet. *Biomaterials*, 29(8): 1065–1074.

Lin, C.H., Yang, J.R., Chiang, N.J., Ma, H. & Tsay, R.Y. 2014. Evaluation of decellularized extracellular matrix of skeletal muscle for tissue engineering. *The International Journal of Artificial Organs*, 37(7): 546–555. extracellular-matrix-of-skeletal-muscle-for-tissue-engineering.

Lin, K., Zhang, D., Macedo, M.H., Cui, W., Sarmento, B., Shen, G. 2018. Advanced collagen-based biomaterials for regenerative biomedicine. *Advanced Functional Materials*, 29(3): 1-16.

Liu, Z.Z., Wong, M.L. & Griffiths, L.G. 2016. Effect of bovine pericardial

extracellular matrix scaffold niche on seeded human mesenchymal stem cell function. *Scientific Reports*, 6: 1–12.

Lu, P., Weaver, V.M. & Werb, Z. 2012. The extracellular matrix: A dynamic niche in cancer progression. *Journal of Cell Biology*, 196(4): 395–406.

Ma, B., Wang, X., Wu, C. & Chang, J. 2014. Crosslinking strategies for preparation of extracellular matrix-derived cardiovascular scaffolds. *Regenerative Biomaterials*, 1(1): 81–89.

Maestro, M.M., Turnay, J., Olmo, N., Fernández, P., Suárez, D., Páez, J.M.G., Urillo, S., Lizarbe, M.A. & Jorge-Herrero, E. 2006. Biochemical and mechanical behavior of ostrich pericardium as a new biomaterial. *Acta Biomaterialia*, 2(2): 213–219.

Mallis, P., Michalopoulos, E., Dimitriou, C., Kostomitsopoulos, N. & Stavropoulos-Giokas, C. 2017. Histological and biomechanical characterization of decellularized porcine pericardium as a potential scaffold for tissue engineering applications. *Bio-Medical Materials and Engineering*, 28(5): 477–488.

Manji, R.A., Menkis, A.H., Ekser, B. & Cooper, D.K.C. 2012. Porcine bioprosthetic heart valves: The next generation. *American Heart Journal*, 164(2): 177–185.

McGraw-Hill Education. n.d. The anatomy of pericardium. [Pinterest post]. Retrieved from: https://za.pinterest.com/pin/293789575686345506/ [accessed August 2018]

Med Info Education. n.d. Structure of proteoglycans. Retrieved from: http://medinfo.ufl.edu/pa/chuck/summer/handouts/images/gag.jpg [assessed October 2018].

Mendoza-Novelo, B., Avila, E.E., Cauich-Rodríguez, J. V., Jorge-Herrero, E., Rojo, F.J., Guinea, G. V. & Mata-Mata, J.L. 2011. Decellularization of pericardial tissue and its impact on tensile viscoelasticity and glycosaminoglycan content. *Acta Biomaterialia*, 7(3): 1241–1248.

Mendoza-Novelo, B. & Cauich-Rodríguez, J. V. 2009. The effect of surfactants,

crosslinking agents and L-cysteine on the stabilization and mechanical properties of bovine pericardium. *Journal of Applied Biomaterials and Biomechanics*, 7(2): 123–131.

Migneault, I., Dartiguenave, C., Bertrand, M.J. & Waldron, K.C. 2004. Glutaraldehyde: Behavior in aqueous solution, reaction with proteins, and application to enzyme crosslinking. *BioTechniques*, 37(5): 790–802.

Mirsadraee, S., Wilcox, H.E., Korossis, S.A., Kearney, J.N., Watterson, K.G., Fisher, J. & Ingham, E. 2006. Development and characterization of an acellular human pericardial matrix for tissue engineering. *Tissue engineering*, 12(4): 763–773.

Mirsadraee, S., Wilcox, H.E., Watterson, K.G., Kearney, J.N., Hunt, J., Fisher, J. & Ingham, E. 2007. Biocompatibility of acellular human pericardium. *Journal of Surgical Research*, 143(2): 407–414.

Miyamotto, M., Del Valle, C.E., Moreira, R.C.R. & Timi, J.R.R. 2009. Comparative analysis of rupture resistance between glutaraldehyde-treated bovine pericardium and great saphenous vein. *Jornal Vascular Brasileiro*, 8: 103–111.

Mosier, J., Nguyen, N., Parker, K. & Simpson, C.L. 2018. Calcification of biomaterials and diseased states. *Biomaterials - Physics and Chemistry - New Edition*. Retrieved from: http://www.intechopen.com/books/biomaterials-physics-and-chemistry-new-edition/calcification-of-biomaterials-and-diseased-states [accesed 12 March 2019].

Muto, A., Nishibe, T., Dardik, H. & Dardik, A. 2009. Patches for carotid artery endarterectomy: Current materials and prospects. *Journal of Vascular Surgery*, 50(1): 206–213.

Neethling, W., Brizard, C., Firth, L. & Glancy, R. 2014. Biostability, durability and calcification of cryopreserved human pericardium after rapid glutaraldehyde-stabilization versus multistep ADAPT® treatment in a

subcutaneous rat model. *European Journal of Cardiothoracic Surgery*, 45(4): 110–117.

Neethling, W.M.L., Cooper, S., Van Den Heever, J.J., Hough, J. & Hodge, A.J. 2002. Evaluation of kangaroo pericardium as an alternative substitute for reconstructive cardiac surgery. *The Journal of Cardiovascular Surgery*, 43(3): 301–306.

Neethling, W.M.L., Glancy, R. & Hodge, A.J. 2010. Mitigation of calcification and cytotoxicity of a glutaraldehyde-preserved bovine pericardial matrix: improved biocompatibility after extended implantation in the subcutaneous rat model. *The Journal of Heart Valve Disease*, 19(6):778-785.

Neethling, W.M.L., Strange, G., Firth, L. & Smit, F.E. 2013. Evaluation of a tissue-engineered bovine pericardial patch in paediatric patients with congenital cardiac anomalies: Initial experience with the ADAPT-treated CardioCel® patch. *Interactive Cardiovascular and Thoracic Surgery*, 17(4): 698–702.

O'Brien, F.J. 2011. Biomaterials & scaffolds for tissue engineering. *Materials Today*, 14(3): 88–95.

Olde Damink, L.H.H., Dijkstra, P.J., Van Luyn, M.J.A., Van Wachem, P.B., Nieuwenhuis, P. & Feijen, J. 1995. Glutaraldehyde as a crosslinking agent for collagen-based biomaterials. *Journal of Materials Science: Materials in Medicine*, 6(8): 460–472.

OpenLearn University. n.d. Sschematic diagram showing how the extracellular matrix is linked to some cells, via integrin molecules, which span the cell membrane. Outside the cell, integrin links via fibronectin to collagen. Inside the cell, another type of protein links integrin to actin filaments. retrieved from https://www.open.edu/openlearn/science-maths-technology/science/tour-the-cell/content-section-5.1 [accessed 20 October 2018].

Parenteau-Bareil, R., Gauvin, R. & Berthod, F. 2010. Collagen-based biomaterials

for tissue engineering applications. *Materials*, 3(3): 1863–1887.

Pibarot, P. & Dumesnil J.G. 2009. Prosthetic heart valves: selection of the optimal prosthesis and lon-term management. *Circulation*, 119(7): 1034-1048.

Ramasamy, V., Mayosi, B.M., Sturrock E.d. & Ntsekhe M. 2018. Established and novel pathophysiological mechanisms of pericardial injury and constrictive pericarditis. *World Journal of Cardiology*, 10(9):87-96.

Rana, D., Zreiqat, H., Benkirane-Jessel, N., Ramakrishna, S. & Ramalingam, M. 2017. Development of decellularized scaffolds for stem cell-driven tissue engineering. *Journal of Tissue Engineering and Regenerative Medicine*, 11(4): 942–965.

Remi, E., Khelil, N., Di, I., Roques, C., Ba, M., Medjahed-Hamidi, F., Chaubet, F., Letourneur, D., Lansac, E. & Meddahi-Pelle, A. 2011. Pericardial Processing: Challenges, Outcomes and Future Prospects. *Biomaterials Science and Engineering*. Available online: http://www.intechopen.com/books/biomaterials-science-and-engineering/pericardial-processing-challenges-outcomes-and-future-prospects. [accessed 20 November 2018].

Robinson, K.A., Li, J., Mathison, M., Redkar, A., Cui, J., Chronos, N.A.F., Matheny, R.G. & Badylak, S.F. 2005. Extracellular matrix scaffold for cardiac repair. *Circulation*, 112(Suppl 9): 135–143.

Rodriguez, E.R. & Tan, C.D. 2017. Structure and Anatomy of the Human Pericardium. *Progress in Cardiovascular Diseases*, 59(4): 327–340.

Sajith, S. 2017. Comparative study of two decellularization protocols on a biomaterial for tissue engineering. *Journal of Clinical & Experimental Cardiology*, 8(5): 3–6.

Schoen, F. & J. Levy, R. 1999. Tissue heart valves: Current challenges and future research perspectives. *Journal of Biomedical Materials Research*, 47(4): 439-465.

Schoen, F.J. & Levy, R.J. 2005. Calcification of tissue heart valve substitutes:

Progress toward understanding and prevention. *Annals of Thoracic Surgery*, 79(3): 1072–1080.

Schoen, F.J., Tsao, J.W. & Levy, R.J. 1986. Calcification of bovine pericardium used in cardiac valve bioprostheses. Implications for the mechanisms of bioprosthetic tissue mineralization. *The American Journal of Pathology*, 123(1): 134–45.

Schultz, G.S. & Wysocki, A. 2009. Interactions between extracellular matrix and growth factors in wound healing. *Wound Repair and Regeneration*, 17(2): 153–162.

Selçuk Kapisiz, N., Kapisiz, H.F., Doğan, O.V., Dolgun A. & Yücel E. 2008. Gluteraldehyde fixation of autologous pericardial patches. *Medical Journal of Trakya University*, 25(2): 124-129.

Simon, P., Kasimir, M.T., Rieder, E. & Weigel, G. 2006. Tissue engineering of heart valves - Immunologic and inflammatory challenges of the allograft scaffold. *Progress in Pediatric Cardiology*, 21(2): 161–165.

Singhal, P., Luk, A. & Butany, J. 2013. Bioprosthetic Heart Valves: Impact of implantation on biomaterials. *International Scholarly Research Notices Biomaterials*, 2013: 1–14.

Sobieraj, M., Cudak, E., Mrówczyński, W., Nalecz, T.K., Westerski, P. & Wojtalik, M. 2016. Application of the CardioCel bovine pericardial patch - A preliminary report. *Polish Journal of Cardiothoracic Surgery*, 13(3): 210–212.

Tanjore, H. & Kalluri, R. 2006. The role of type IV collagen and basement membranes in cancer progression and metastasis. *American Journal of Pathology*, 168(3): 715–717.

Thubrikar, M.J., Deck, J.D., Aouad, J. & Nolan, S.P. 1983. Role of mechanical stress in calcification of aortic bioprosthetic valves. *The Journal of Thoracic and Cardiovascular Surgery*, 86(1): 115–125.

Tran, H.L.B., Dinh, T.T.H., Nguyen, M.T.N., To, Q.M. & Pham, A.T.T. 2016. Preparation and characterization of acellular porcine pericardium for

cardiovascular surgery. *Turkish Journal of Biology*, 40: 1243–1250.

Umashankar, P.R., Mohanan, P. V & Kumari, T. V. 2012. Glutaraldehyde treatment elicits toxic response compared to decellularization in bovine pericardium. *Toxicology International*, 19(1): 51–58.

Vaideeswar, P., Mishra, P. & Nimbalkar, M. 2011. Infective endocarditis of the Dacron patch-a report of 13 cases at autopsy. *Cardiovascular Pathology*, 20(5): e169–e175.

Vinci, M.C., Tessitore, G., Castiglioni, L., Prandi, F., Soncini, M., Santoro, R., Consolo, F., Colazzo, F., Micheli, B., Sironi, L., Polvani, G. & Pesce, M. 2013. Mechanical compliance and immunological compatibility of fixative-free decellularized/cryopreserved human pericardium. *PLoS One*, 8(5): e64769.

Vyavahare, N., Ogle, M., Schoen, F.J. & Levy, R.J. 1999. Elastin calcification and its prevention with aluminum chloride pretreatment. *American Journal of Pathology*, 155(3): 973–982.

Webb, C.L., Schoen, F.J. & Levy, R.J. 1989. Covalent binding of aminopropanehydroxydiphosphonate to glutaraldehyde residues in pericardial bioprosthetic tissue: Stability and calcification inhibition studies. *Experimental and Molecular Pathology*, 50(3): 291–302.

Wiegner, A.W. & Bing, O.H.L. 1981. Mechanical and structural correlates of canine pericardium. *Circulation Research*, 49(3): 807–814.

Wilgus, T.A. 2012. Growth Factor–Extracellular Matrix interactions regulate wound repair. *Advances in Wound Care*, 1(6): 249–254.

Wong, M.L., Wong, J.L., Vapniarsky, N., Griffiths, L. G. 2016. In vivo xenogeneic scaffold fate is determined by residual antigenicity and extracellular matrix preservation. *Biomaterials*, 92: 1-12.

Yakirevich, V.S., Abdulali, S.A., Abbott, C.R. & Ionescu, M.I. 1984. Reconstruction of the pericardial sac with glutaraldehyde-preserved bovine pericardium. *Texas Heart Institute Journal*, 11(3): 238–242.

Yamamoto, H., Yamamoto, F., Ishibashi, K. & Motokawa, M. 2009. In situ

replacement with equine pericardial roll grafts for ruptured infected aneurysms of the abdominal aorta. *Journal of Vascular Surgery*, 49(4): 1041–1045.

Yi, S., Ding, F., Gong, L., & Gu, X. 2017. Extracellular matrix scaffolds for tissue engineering and regenerative medicine. *Current Stem Cell Research & Therapy*, 12(3): 233–246.

Yue, B. 2014. Biology of the extracellular matrix: an overview. *Journal of Glaucoma,* 23(Suppl 1): S20-S30.

Appendices

A1: Ethical approval letter

UNIVERSITY OF THE FREE STATE
UNIVERSITEIT VAN DIE VRYSTAAT
YUNIVESITHI YA FREISTATA

UFS·UV
HEALTH SCIENCES
GESONDHEIDSWETENSKAPPE

Animal Research Ethics

10-Apr-2018

Dear Mr Johannes Van Den Heever

Student Project Number: UFS-AED2015/0081

Project Title: Evaluation of Processed Pericardial Patches in the Circulatory System of a Juvenile Sheep Model

Department: Cardiothoracic Surgery (Bloemfontein Campus)

You are hereby kindly informed that, at the meeting held on 05-Nov-2015, the Interfaculty Animal Ethics Committee approved the above project.

Kindly take note of the following:

1.
A progress report with regard to the above study has to be submitted Annually and on completion of the project. Reports are submitted by logging in to RIMS and completing the report as described in SOP AEC007: Submission of Protocols, Modifications, Amendments, Reports and Reporting of Adverse Events which is available on the UFS intranet.

2.
Researchers that plan to make use of the Animal Experimentation Unit must ensure to request and receive a quotation from the Head, Mr. Seb Lamprecht.

3.
Fifty (50%) of the quoted amount is payable when you receive the letter of approval.

Yours Sincerely

Mr. Gerhard Johannes van Zyl
Chair: Animal Research Ethics Committee